

**A FINITE ELEMENT APPROACH TO REINFORCED  
CONCRETE SLAB DESIGN**

A Thesis  
Presented to  
The Academic Faculty

by

**James B. Deaton**

In Partial Fulfillment  
of the Requirements for the Degree  
Master of Science

School of Civil and Environmental Engineering  
Georgia Institute of Technology  
August 2005

Copyright © 2005 by James B. Deaton

# A FINITE ELEMENT APPROACH TO REINFORCED CONCRETE SLAB DESIGN

Approved by:

Dr. Kenneth M. Will, Advisor  
School of Civil and Environmental Engineering  
*Georgia Institute of Technology*

Dr. Lawrence F. Kahn  
School of Civil and Environmental Engineering  
*Georgia Institute of Technology*

Dr. Michael H. Swanger  
School of Civil and Environmental Engineering  
*Georgia Institute of Technology*

Date Approved: 18 July 2005

## ACKNOWLEDGEMENTS

I would like to express my sincerest appreciation to my advisor, Dr. Kenneth M. Will, for his guidance, expert instruction, and the investments he has made in me over the past two years, giving me the opportunity to be involved in such interesting research. I would also like to extend sincere thanks to my co-advisor, Dr. Lawrence F. Kahn. I will fondly remember the hours upon hours of conversations with both of them discussing finite elements, reinforced concrete, and many other non-technical topics. I could not have asked for an advisor or co-advisor more approachable or willing to help.

I would like to acknowledge Dr. Michael H. Swanger for pushing me to a greater understanding of my research topic through his comments during the preparation of this thesis. Additionally, I would like to thank Rob Abernathy for his assistance in the early stages of this project.

Many people supported me in ways beyond what I could have asked for during the completion of this project. For this I would like to thank several mentors, including Dr. David Parker, Brian Holland, Chris Dawkins, and David Conner. Also, I would like to thank David Ashley, Adam Walker, Eric Henderson, and Joshua Tarbutton for each finding unique ways to encourage me and help me through the good as well as difficult stages of this project. Additionally, I would like to thank all the members of our small group at First Baptist Church of Duluth for praying for me and for hanging out with my wife when I was studying or writing this thesis.

I would not be where I am today if it weren't for the support and love of my parents, Jimmy and Wanda Deaton – thank you for always helping me be my best. I would also like to thank my family-in-law, the Mooney's, for their encouragement.

Most importantly, I would like to thank my wife, Gina, for her unwavering love and support throughout the completion of this project, from the first time I mentioned graduate school to her to the final days of proofreading this thesis. I lovingly dedicate this to her.

# TABLE OF CONTENTS

<b>ACKNOWLEDGEMENTS</b> . . . . .	<b>iii</b>
<b>LIST OF TABLES</b> . . . . .	<b>vii</b>
<b>LIST OF FIGURES</b> . . . . .	<b>viii</b>
<b>SUMMARY</b> . . . . .	<b>x</b>
<b>I INTRODUCTION</b> . . . . .	<b>1</b>
1.1 Flat Plate Systems . . . . .	1
1.2 Literature Review . . . . .	2
1.2.1 Design Based on Linear Analysis . . . . .	5
1.2.2 Extension to Arbitrary Structures . . . . .	8
1.2.3 Design Based on Non-Linear Analysis . . . . .	10
1.2.4 Additional Applications . . . . .	12
1.3 Motivation . . . . .	13
1.4 Outline of Presentation . . . . .	15
<b>II REVIEW OF CONVENTIONAL REINFORCED CONCRETE FLAT PLATE DESIGN</b> . . . . .	<b>16</b>
2.1 General ACI Requirements for Reinforced Concrete Flat Plate Design . . . . .	16
2.1.1 Analysis Requirements . . . . .	17
2.1.2 Flexural Strength Requirements . . . . .	19
2.1.3 Shear Strength Requirements . . . . .	24
2.1.4 Serviceability Requirements . . . . .	28
2.1.5 Detailing of Reinforcement . . . . .	29
2.2 ACI Direct Design Technique . . . . .	31
2.3 ACI Equivalent Frame Technique . . . . .	33
2.4 Yield Line Method . . . . .	35
2.5 Strip Design Technique . . . . .	38
<b>III APPLICATION OF THE FINITE ELEMENT METHOD TO REINFORCED CONCRETE SLAB DESIGN</b> . . . . .	<b>41</b>
3.1 Modeling of Slabs Using Finite Elements . . . . .	41

3.1.1	General Modeling Requirements . . . . .	41
3.1.2	Assumptions in Reinforced Concrete Flat Plate Finite Element Analysis . . . . .	43
3.1.3	Modeling of Boundary Conditions for Flat Plate Systems . . . . .	44
3.2	Techniques for Flat Plate Design Using FEA Results . . . . .	48
3.2.1	Design Using Average Stress Resultants . . . . .	48
3.2.2	Design Using Element Forces . . . . .	54
<b>IV</b>	<b>IMPLEMENTATION OF PROCEDURE . . . . .</b>	<b>58</b>
4.1	Programming Introduction . . . . .	58
4.1.1	Overview of Algorithm . . . . .	58
4.1.2	Overview of GT STRUDL . . . . .	59
4.1.3	Tools Used . . . . .	60
4.2	Model Requirements . . . . .	60
4.3	Command . . . . .	61
4.3.1	Overview of User Options . . . . .	61
4.3.2	Command Syntax . . . . .	62
4.3.3	Explanation of Command . . . . .	63
4.4	Pre-Processing . . . . .	65
4.4.1	Determination of Cut Definition . . . . .	65
4.4.2	Formulation of Cut Coordinate System . . . . .	67
4.4.3	Element Selection Procedure . . . . .	70
4.4.4	User-Defined Element List . . . . .	73
4.4.5	Contribution from Both Sides of Cut . . . . .	77
4.4.6	Element Type Restrictions . . . . .	77
4.4.7	Further Error Checking . . . . .	78
4.5	Computation of Resultant Forces Along Cut . . . . .	78
4.5.1	The CALCULATE RESULTANT Command . . . . .	78
4.5.2	Computation of Design Forces . . . . .	79
4.5.3	Reduction of Multiple Load Cases to Design Envelope . . . . .	80
4.5.4	Interpretation of Results . . . . .	81
4.6	Design Procedure . . . . .	83

4.6.1	Initial Design Processing . . . . .	84
4.6.2	Check Specified Bar and Spacing . . . . .	88
4.6.3	Design with No User Constraints . . . . .	88
4.6.4	Design with Bar Size Constrained . . . . .	89
4.6.5	Design with Bar Spacing Constrained . . . . .	90
4.6.6	Shear Check . . . . .	90
4.6.7	Final Comments . . . . .	90
<b>V</b>	<b>RESULTS AND NUMERICAL STUDIES . . . . .</b>	<b>92</b>
5.1	Example 1 - Convergence of Area of Steel . . . . .	92
5.2	Example 2 - Comparison with Experimental Data . . . . .	96
5.3	Example 3 - Square Bay Flat Plate Structure . . . . .	105
5.4	Example 4 - Irregular Bay Rectangular Flat Plate Structure . . . . .	117
5.5	Example 5 - Square Flat Plate Fix-Supported on Two Sides . . . . .	136
<b>VI</b>	<b>CONCLUSIONS . . . . .</b>	<b>142</b>
6.1	Summary . . . . .	142
6.2	Future Work . . . . .	144
6.2.1	Recommendations for Research . . . . .	144
6.2.2	Program Enhancements . . . . .	145
<b>APPENDIX A</b>	<b>— COMPRESSION REINFORCEMENT . . . . .</b>	<b>148</b>
<b>APPENDIX B</b>	<b>— MODULE DESCRIPTIONS . . . . .</b>	<b>150</b>
<b>REFERENCES</b>	<b>. . . . .</b>	<b>156</b>

## LIST OF TABLES

5.1	Example 1 - Computed Response Quantities . . . . .	94
5.2	Example 2 - Experimental and Finite Element Bending Moments . . . . .	101
5.3	Example 3 - Interior Region Design Results . . . . .	107
5.4	Example 3 - Exterior Region Design Results . . . . .	108
5.5	Example 3 - Interior Bending Moments for Pattern Loadings . . . . .	112
5.6	Example 3 - Interior Area of Steel Computed for Pattern Loadings . . . . .	113
5.7	Example 3 - Exterior Bending Moments for Pattern Loadings . . . . .	114
5.8	Example 3 - Exterior Area of Steel Computed for Pattern Loadings . . . . .	115
5.9	Example 3 - Ratio of Resultant Torsional Moment to Bending Moment for Pattern Loadings . . . . .	116
5.10	Example 4 - N/S Interior Region Design Results . . . . .	120
5.11	Example 4 - N/S Exterior Region Design Results . . . . .	121
5.12	Example 4 - N/S Interior Bending Moments for Pattern Loadings . . . . .	122
5.13	Example 4 - N/S Interior Area of Steel Computed for Pattern Loadings . . . . .	123
5.14	Example 4 - N/S Exterior Bending Moments for Pattern Loadings . . . . .	124
5.15	Example 4 - N/S Exterior Area of Steel Computed for Pattern Loadings . . . . .	125
5.16	Example 4 - N/S Ratio of Resultant Torsional Moment to Bending Moment for Pattern Loadings . . . . .	126
5.17	Example 4 - E/W Interior Region Design Results . . . . .	127
5.18	Example 4 - E/W Exterior Region Design Results . . . . .	128
5.19	Example 4 - E/W Interior Bending Moments for Pattern Loadings . . . . .	129
5.20	Example 4 - E/W Interior Area of Steel Computed for Pattern Loadings . . . . .	130
5.21	Example 4 - E/W Exterior Bending Moments for Pattern Loadings . . . . .	131
5.22	Example 4 - E/W Exterior Area of Steel Computed for Pattern Loadings . . . . .	132
5.23	Example 4 - E/W Ratio of Resultant Torsional Moment to Bending Moment for Pattern Loadings . . . . .	133
5.24	Effect of Torsion . . . . .	137
A.1	Computation of Depth to Neutral Axis . . . . .	149

## LIST OF FIGURES

1.1 Flat Plate System . . . . .	2
1.2 Flat Plate Reinforced Concrete Residential Structure Under Construction . . . . .	3
2.1 General Flexure at Ultimate Capacity . . . . .	19
2.2 Moment Transfer Shear - Interior, Edge, and Corner Columns [27] . . . . .	26
2.3 Flat Plate Cross-Sectional Detailing Requirements . . . . .	29
2.4 Slab-Beam Layout and Dimensions . . . . .	31
2.5 Elevation Showing Plane Frame Analytical Model for the Equivalent Column Method . . . . .	33
2.6 Equivalent Column with Attached Torsional Member . . . . .	34
2.7 Example Yield Line Patterns . . . . .	37
2.8 Example Strip Design Layout . . . . .	39
3.1 3D Solid Slab-to-Column Connection Detail . . . . .	47
3.2 Master-Slave Slab-to-Column Connection Detail . . . . .	47
3.3 Element Stress Resultants at a Node . . . . .	49
3.4 X-Direction Strip Selection Based on $M_{xx}$ Contour Plot . . . . .	52
3.5 Average Bending Moment Resultants at Each Node Along Cut . . . . .	54
3.6 Element Forces at a Node . . . . .	55
3.7 Element Force Resultant From Nodal Forces Along a Cut . . . . .	56
4.1 Bounded Region Between Start and End Node of Cut . . . . .	66
4.2 Cut Coordinate System: (A) General Case (B) Special Case . . . . .	69
4.3a Element Selection Cases 1-5 (Plan View) . . . . .	74
4.3b Element Selection Cases 6-10 (Plan View) . . . . .	75
4.3c Element Selection Cases 11-15 (Plan View) . . . . .	76
4.4 CALCULATE RESULTANT Command Results . . . . .	80
4.5 “Positive” Bending and Surface Naming Convention . . . . .	83
4.6 Direction of Reinforcing Bars for Non-Orthogonal Cut (Plan) . . . . .	85
4.7 Slab Cross-Section: $d$ —Distance . . . . .	86
5.1 Example 1 - Geometry . . . . .	93
5.2 Example 1 - Finite Element Models . . . . .	93



5.3	Example 1 - Convergence of Key Response Quantities . . . . .	95
5.4	Example 2 - Simplified Model with Edge Beams Neglected and Space Frame Member Columns . . . . .	96
5.5	Example 2 - Detailed Model with Edge Beams and 3D Solid Interior Columns	96
5.6	Example 2 - Test Structure Top Reinforcement (Gamble, [28]) . . . . .	98
5.7	Example 2 - Test Structure Bottom Reinforcement (Gamble, [28]) . . . . .	99
5.8	Example 2 - Moment Components Corresponding to Strain Gage Locations	101
5.9	Example 2 - Moments in Interior Panel . . . . .	102
5.10	Example 2 - Total Moment in Interior Panel . . . . .	103
5.11	Example 3 - Geometry . . . . .	105
5.12	Example 3 - Finite Element Model with Space Frame Member Columns (left) and Finite Element Model of $\frac{1}{4}$ of Structure with 3D Solid Columns (right)	106
5.13	Example 3 - Pattern Live Loadings . . . . .	111
5.14	Example 4 - Dimensions and Finite Element Model . . . . .	118
5.15	Example 5 - Geometry . . . . .	137
5.16	Example 5 - Bending Resultant Contours . . . . .	140
5.17	Example 5 - Principal Bending Vectors - M1 (top) and M2 (bottom) . . . .	141
A.1	Depth to Neutral Axis Divided by Concrete Cover . . . . .	149

## SUMMARY

The objective of this study was the development of a procedure in GT STRUDL to design reinforced concrete flat plate systems based on the results of finite element analysis.

The current state-of-practice of reinforced concrete flat plate design was reviewed, including the ACI direct design and equivalent frame techniques, the yield line method, and the strip design method. The principles of these methods along with a critical evaluation of their applicability and limitations were presented as motivation for a finite element based design procedure. Additionally, the current state-of-the-art of flat plate design based on finite element results was presented, along with various flat plate modeling techniques. Design methodologies studied included the Wood and Armer approach, based on element stress resultants, and the resultant force approach, based on element forces.

A flat plate design procedure based on the element force approach was embodied in the DESIGN SLAB command, which was implemented in GT STRUDL. The DESIGN SLAB command provides the user the ability to design a slab section by specifying a cut definition and several optional design parameters. The procedure determines all nodes and elements along the cut, computes the resultant moment design envelope acting on the cross-section, and designs the slab for flexure in accordance with provisions of ACI 318-02.

Design examples presented include single-panel flat plate systems with various support conditions as well as multi-panel systems with regular and irregular column spacing. These examples allowed for critical comparison with results from experimental studies and currently applied design methods in order to determine the applicability of the implemented procedure. The DESIGN SLAB command was shown to produce design moments in agreement with experimental data as well as conventional design techniques for regular configurations. The examples additionally showed that when cuts were not oriented orthogonally to the directions of principle bending, resulting designs based on element forces could significantly under-reinforce the cross-section due to significant torsional effects.

# CHAPTER I

## INTRODUCTION

The purpose of this study was the implementation and verification of a procedure in GT STRUDL to design reinforced concrete flat plate systems based on the results of finite element analysis.

For many years, researchers have been working toward the successful application of finite element technology to the design of reinforced concrete flat plate systems due to practical restrictions inherent in simplified or approximate design techniques. Despite promising research in this area, only a few practical finite element based design tools have been implemented in standard structural engineering technology. The goal of this study was to develop and validate such a tool.

### 1.1 Flat Plate Systems

The scope of this study was limited to reinforced concrete flat plate systems. Flat plate systems are a subset of the two-way slab family, meaning that the system deforms in two directions. Flat plate systems are reinforced concrete slabs of uniform thickness that transfer loads directly to supporting columns, and are distinguished from other two way systems by the lack of beams, column capitals, and drop panels. A simple representation of a flat plate system is shown in Figure 1.1.

Flat plate systems have several advantages over other slab systems. The absence of beams, capitals, and drop panels allow for economical formwork and simple reinforcement layouts, leading to fast construction. Architecturally, flat plates are advantageous in that smaller overall story heights can be achieved due to the reduced floor structure depth required, and the locations of columns and walls are not restricted by the location of beams. Flat plates can be constructed as thin as 5 inches [2]. In fact, Gamble [27] estimates that in areas where height restrictions are critical, the use of flat plates enable an additional floor

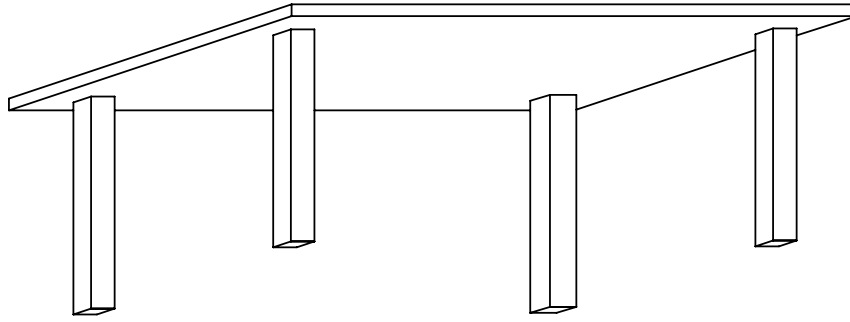


**Figure 1.1:** Flat Plate System

for approximately every 10 floors in a structure, as compared to a general two-way system with the same clear story heights. The savings in height ultimately lead to economic savings in many areas, including mechanical systems, foundations, and non-structural components such as cladding. Another benefit of flat plate systems is good performance under fire conditions, due to the lack of sharp corners susceptible to spalling [51].

Often the limiting factor in the selection of flat plate systems as a design solution is the difficulty in shear and moment transfer at the column connections. Indeed this difficulty often necessitates the inclusion of drop panels or column capitals. As such, the choice to use a flat plate system is often determined based on the span length and loading. According to the Portland Cement Association [58], for live loads of approximately 50 pounds per square foot (psf), a span length of 15 to 30 feet is economical, and for live loads of 100 psf or more, a span length of 15 to 30 feet is economical.

Based on economy of construction as well as the loading limitations described above, flat plate systems are well suited for use in multi-story and high-rise reinforced concrete hotels, apartments, hospitals, and light office spaces, and are perhaps the most commonly used slab system for these types of structures today [51]. Figure 1.2 shows a multi-story flat plate reinforced concrete structure during construction.

## 1.2 Literature Review

Reinforced concrete has long been one of the most widely used materials in construction applications. It has numerous material advantages, but one of its most significant benefits



**Figure 1.2:** Flat Plate Reinforced Concrete Residential Structure Under Construction

is the ability to be cast into a wide variety of shapes. In fact, reinforced concrete is only geometrically limited by the complexities or cost of the construction of formwork. As such, the behavior of concrete structures easily constructed in the field often falls beyond the scope of common frame analysis programs and conventional design methods. This is certainly true for the analysis of reinforced concrete systems where slabs, shear walls, shells, tanks, deep beams, and coupling beams must be modeled. If the structural element contains holes or is subjected to concentrated or otherwise irregular loadings, the analysis is further complicated.

The structural engineering community responded to this challenge with numerous approximate techniques that attempt to simplify the design of these reinforced concrete components. For flat plates, these methods include the direct design, equivalent frame, yield line, and strip design techniques, all of which approximate the results of classical plate theory. These methods have gained wide acceptance among engineers because of their simplicity. However, these approximate techniques have significant limitations. Direct design and equivalent frame methods are both limited to structures with very regular geometry. The application of yield lines or strip design may lead to overly conservative designs as well as to poor serviceability. A detailed explanation of these methods and subsequent limitations is presented in Chapter 2.

As such, the finite element method has been an obvious choice for the modeling and

analysis of reinforced concrete systems for many years. Finite elements have the unique capability to conform to virtually any geometry that could be physically implemented. Thus, the finite element method has gained acceptance as an appropriate tool for the analysis of flat plates, especially those with highly irregular or unusual geometries where the direct design and equivalent frame techniques are not valid. In irregular slabs such as these, the finite element method can be shown to accurately solve for the distribution of stress where numerous approximations and assumptions would be invoked if the yield line or strip design technique were applied.

An additional benefit of a finite element approach to slab design is that engineers no longer need to develop multiple models to design a structure for various types of behavior. By integrating the slab model with the three-dimensional frame, the combined effects of gravity and lateral loading conditions can be assessed together. The interaction of the slab and columns is accurately simulated, providing favorable results to approximations of connection stiffness. An integrated approach to analysis and design thus emerges.

Significant research efforts have been devoted to the application of finite elements in the analysis of reinforced concrete since the emergence of the finite element method in the 1950s. While many achievements have been accomplished in research environments, few of these achievements have been implemented in practical applications for structural engineers in the design office. While much analytical work has been focused on the application of nonlinear constitutive modeling of reinforced concrete, most software packages currently implemented offer only linear elastic finite element capabilities.

The following review details the progression from the conception of finite element based flat plate design to the current state of the art. Much of the work cited deals primarily with the modeling and analysis of flat plate systems by the finite element method, without explicitly discussing reinforcement design. However, the primary purpose of the finite element model is the determination of design forces and moments, and once these quantities have been accurately determined, the resulting design becomes a function of the active design code.

### 1.2.1 Design Based on Linear Analysis

One of the earliest published works concerning the application of the finite element method to reinforced concrete slabs was by Zienkiewicz in 1964 [73]. In this work, Zienkiewicz extended the general finite element method to flat plates and presented the formulation for boundary conditions typical to these systems. The linear elastic isotropic analysis was extended to orthotropic slab systems with variable thickness, and the ease with which a slab can be analytically coupled to frame members or an elastic foundation was presented. Several examples demonstrate excellent agreement between finite element solutions for deflections and moments and those of available exact solutions.

The initial philosophy of flat plate design based on finite element results was formulated by Wood [72], although no explicit mention of the finite element method was made in the original work. Instead, Wood describes the process of designing reinforcement in accordance with a predetermined field of bending moments provided from “analysis by the theory of elasticity ... possible with the use of computer programmes, which can print out a complete field of moments  $M_x$ ,  $M_y$ , and  $M_{xy}$ ” [72]. In addition to presenting the associated mathematical formulation, Wood also argued that design economy of such a method is superior to that of both the yield line and strip design techniques.

Armer [4] generalized the work of Wood for efficient application to both slabs with orthogonal reinforcement as well as skew reinforcement, and as a result, Wood argued that Armer’s formulation should represent the general case. It was because of this collaboration that this technique of design is presently referred to as the *Wood and Armer* technique.

Smith and Faulkes [66] applied the finite element method to analyze a multistory flat plate building, one of the first three-dimensional applications of the method in reinforced concrete, to analytically evaluate the flexural properties of flat plate systems. The analyses conducted used a four-node non-conforming rectangular displacement-based element formulated by Zienkiewicz. A 6 by 6 bay floor with square column spacing was analyzed, and various ratios of column size to bay span were considered. The results of the presented analyses suggest that the flexural behavior of a flat plate varies significantly from that of a beam, and that as a result the equivalent frame technique has limited applicability to the

case where lateral loads are significant.

The work of Gupta and Sen [31] presented alternative methods of reinforcement design based on a predetermined field of bending moments  $M_x$ ,  $M_y$ , and  $M_{xy}$ . The first method was the Principle of Minimum Resistance, and ultimately yielded a formulation identical to the Wood and Armer solution, although derived under different assumptions. The second method applied was the Three Equivalent Moments Method, in which the slab was reinforced according to computed equivalent normal moments in three unique specified directions based on the bending moment field of the element. The second method was shown to provide economy with respect to the total required design capacity, but not with regard to the actual cost of construction. Thus, the general applicability of the Wood and Armer formulation was confirmed.

The work of Gentry [29] confirmed that, in general, linear elastic finite element analysis is applicable to the design of regular reinforced concrete flat plate systems. Various methods of modeling columns and column-to-slab connections were evaluated. Designs based on finite element analysis were critically compared with designs based on the direct design and equivalent frame methods. Finite element designs using working stress design and ultimate strength design, based on element nodal forces as well as element stress resultants, were evaluated. Gentry showed that design using element forces produces results in closer correlation with the equivalent frame technique than element stress resultants, and that the ultimate strength approach is preferable to working stress with respect to performance and economy. Only a rectangular column layout and bay spacing were considered in that study.

The work of Saleh [63] evaluated the applicability of linear elastic finite elements to the analysis and shear design of regular reinforced concrete flat plate systems. In particular, Saleh investigated a finite element determination of moment transfer at slab-column connections, shear stress along the critical column perimeter, and the effect of modeling on shear stress results, showing strong correlation with ACI method results.

Hrabok and Hruđey [35] presented an extensive review of the challenges associated with the application of linear elastic finite element analysis to reinforced concrete flat plate analysis. They cited lack of knowledge of element behavior, lack of experience, and lack of



suitable programs as primary hindrances to widespread application of finite element-based design techniques. A detailed review was presented of several common linear elastic plate bending elements, including the ACM element [1, 52], a selectively reduced bilinear Mindlin element [39], a hybrid stress Kirchoff element [65], the heterosis Mindlin element [38], and a Lagrangian Kirchoff element [34]. The hybrid stress element was recommended for future application to flat plate design problems based on the ease of determination of stiffness matrices for nonrectangular elements as well as the ability to account for the effects of stress singularities within the element.

Davies [21] applied the finite element method to evaluate deflections and moments in a corner supported rectangular slab. Both simple supports and fixed supports were considered. Several loading conditions were considered, and analytical results were compared with scale model tests. Davies demonstrated strong correlation between analytical and experimental studies and showed that actual slab-to-column connections were generally bounded by the simple and fixed support models evaluated.

French [26] derived the stiffness of a single element panel, and implemented a modeling technique based on using single elements for slab panels in the analysis of multistory flat plate structures subjected to lateral loading. The demonstrated technique accurately predicted the distribution of lateral loads among columns as well as story drifts. This method easily handled uneven bay spacings and nonrectangular plans, but provided no information regarding the distribution of moments throughout the floor slab.

Mohr [54] demonstrated the successful application of elastic finite element analysis in the determination of approximate plastic design results. In this research, the flat plate was modeled as a weak core sandwich based on the assumptions that the reinforcement had yielded and the concrete core was cracked. Based on these assumptions, the plastic section modulus was computed and implemented instead of the elastic section modulus. Eight slabs with various boundary conditions were considered, and the analyses showed strong correlation between the finite element results and other well-known plastic design techniques.

Anderheggen [3] presented a method of reinforcement design based on element nodal

forces. In the method proposed, the reinforcement and the concrete were designed, not based on stresses within the element, but based on the forces transmitted from the neighboring elements and acting on the element as applied loads. Element stresses need not be computed. The principles presented were a generalization of a *truss model* for building an equilibrium system of forces and moments on which to base dimensioning.

Raisanen and the CASE Task Group on Finite Element Analysis [60] demonstrated the successful application of linear finite element analyses to the solution of problems with closed-form solutions as well as a powerhouse slab with openings. This work additionally demonstrated the appropriate context of the application of a plate bending element based on the Mindlin formulation, and stressed the significance of boundary conditions and modeling verification.

For many years, researchers sought to optimize the yield line technique using finite element analysis. Borkowski [8], as well as Figueiredo, Foseca, and Azevedo [23], labored toward this end and reached favorable results by applying rigid-plastic modeling techniques, coupled with linear and nonlinear optimization techniques, to compute the associated collapse load of the flat plate. In these techniques, a finite element mesh was assumed and adaptively modified to optimize the locations of yield lines.

The solution for flat slabs on elastic foundations has been another important topic of research associated with the finite element method. Hudson and Stelzer [37], as well as Huang and Wang [36], conducted studies in this area. Results of these implemented procedures compare well with classical theory of thin plates supported on Winkler foundations.

### **1.2.2 Extension to Arbitrary Structures**

The limited applicability of simplified ACI design techniques motivated the application of the finite element method to irregular structures, and research into arbitrary configurations began as the finite element method became widely accepted as an analysis tool.

Davies, Ma, and Cheung [22], under the direction of Zienkiewicz, studied the applicability of the finite element method to the analysis of skew plates under a variety of loading conditions. In this study, finite elements were applied to analyze a square slab, a skew slab

oriented at  $30^\circ$ , and a skew slab oriented at  $45^\circ$ . Applied loading conditions included a uniform loading over the entire slab, a concentrated load at the centroid of the slab, and concentrated loads at the center of two opposite sides. Each slab was also experimentally evaluated, and analytical results were confirmed with experimental data. The finite element models were shown to compute deflections and bending moments in close agreement with the experimental cases.

Cheung, King, and Zienkiewicz [10] presented a general method of analyzing slabs with arbitrary shape and boundary conditions based on the finite element method, accounting for the interaction of plate, beam, and column elements. Particular emphasis was placed on the accuracy of various column-to-slab connection models that account for the finite size of the column at the connection. The ability to compute support reactions using the finite element method was investigated and shown to be in reasonable agreement with experimental data. An actual bridge of arbitrary skewed shape and boundary conditions was analyzed. The authors pointed out that column-to-slab connections may require a three-dimensional analysis to adequately determine the deformation characteristics.

Similarly, Sawko and Cope [64] considered the application of finite elements to the case of skew bridge decks. The benefits of the finite element method with respect to model testing, finite difference methods, and the grillage approach were presented. The application of finite elements to orthotropic skew decks, with longitudinal stiffness greater than transverse stiffness, was detailed and shown to provide accurate results. This work also emphasized the importance of Poisson ratio effects, citing that neglect of Poisson ratio effects can lead to underestimation of maximum longitudinal moments by as much as 6% and transverse moments by as much as 16%.

Law [44] critically evaluated solutions for an arbitrary fix-supported flat plate based on the finite difference technique and the finite element method. The specific application evaluated was an irregular panel resulting from a radial framing concept used in a circular tower core area of a semicircular shaped aircraft hangar. Law demonstrated that for even a generally coarse mesh, results obtained from the finite difference method and finite element method were in close agreement, and that both of these solution techniques were in relative

agreement with ACI approximate techniques for a similar rectangular configuration.

Douglas and Lunniss [24] demonstrated the application of finite elements in the design of a three-dimensionally curved flyover bridge. The study focused on the correct modeling of discrete supports and appropriate column simulation. Douglas and Lunniss concluded that the finite element results for an elastic analysis give valid results, but that further computations of local stresses associated with concentrated forces, such as vehicle loadings, are possibly required. Finite element analysis results were validated with a three-dimensional physical model.

While much work on skew slabs focused on flexure, Cusens and Besser [20] investigated a skew bridge deck with particular focus on the obtuse corners and boundaries in determination of shear forces in the slab. The slab evaluated contained a  $45^\circ$  skew angle, and was modeled as simply supported with one end restrained with semi-infinite rigidity and the other end with several discrete elastic supports. They found that the Kirchoff boundary conditions introduce physically significant corner and edge forces near obtuse corners, distributing a large shear force close to the edge. Also, elastic bearings were recommended in the regions near obtuse corners in order to provide a more even distribution of reaction forces. Significant reversals in bending moment were detected near obtuse corners as well as the largest values of torsional moment.

### **1.2.3 Design Based on Non-Linear Analysis**

As the finite element method was gaining acceptance, researchers were quick to begin re-evaluating the broad range of assumptions invoked when applying a linear elastic homogeneous isotropic analysis to reinforced concrete [9]. The first published works dealing with nonlinear finite element analysis of concrete systems emerged in the late 1960s. These studies focused on various aspects of element formulation, including crack propagation and the bonding of reinforcement.

Jofriet and McNiece [42] conducted some of the earliest research in this area. Their work derived a slab analysis model based on the effects of cracking, capable of representing the orientation of cracking with respect to the slab's coordinate system, the rigidity of the

cracked region when the section has exceeded the cracking moment, and the rigidity of steel with relation to the crack direction. To simulate progressive cracking, the implemented program incorporated a step-based analysis with a bilinear moment curvature relationship for each element. Post-yield behavior of the reinforcement was neglected in their study. This approach is called a *modified stiffness* model.

The work of Lewiński and Wojewódzki [45] demonstrated application of a nonlinear slab model combining the modified stiffness approach and the layered model approach. Nonlinear concrete behavior, such as cracking, and elastic-plastic steel reinforcement deformation were incorporated as well as coupling between extension and flexure. Analyses were based on 10 cracking patterns. Several test analyses were conducted and compared with experimental test data and showed that the proposed method is accurate for evaluation of in-plane and out-of-plane effects in flat plates.

Bashur and Darwin [6] developed a non-layered finite element reinforced concrete model in which a nonlinear variation in material properties could be represented through the depth of the slab. In this study, concrete was modeled as nonlinear in compression and linearly brittle in tension, and steel was treated uniaxially with a bilinear stress-strain curve. Flat plates were modeled as anisotropic plates that were incrementally elastic. Numerical results showed that representation of cracking as a continuous process provides favorable results, and that smaller load increments provide more accurate results after cracking and/or yielding begins. The nonlinear aspects incorporated in this model allow for accurate determination of the load-deflection behavior of the flat plate.

Barzegar and Maddipudi [5] extended many of the common nonlinear finite element reinforced concrete techniques with respect to the simulation of reinforcement in three-dimensional solid elements. Instead of either a smeared or layered approach, a model for spatially embedded reinforcement independent of the finite element nodal coordinates was presented by which an entire reinforcement cage is automatically mapped into a mesh of solid isoparametric concrete elements. This technique was shown to be not only applicable to straight reinforcing bars, but also readily applicable to prestressed systems in which the strand geometry can be approximated using a piecewise linear tendon distribution.

Lourenço and Figueiras [48] extended nonlinear finite element modeling of concrete slabs toward a general element for the design of plates, slabs, and shells in which reinforcement was computed locally at each integration point. The presented method takes into account the biaxial behavior of concrete as well as different moment arms associated with all internal forces, an important point neglected by Gupta and Sen [31]. The method was validated with experimental test data.

More recently, Phuvoravan and Sotelino [57] derived a new finite element for nonlinear finite element analysis of reinforced concrete slab systems. The new element was a combination of the classic four-node Kirchoff shell element with two-node Euler beam elements to simulate the steel reinforcement. Rigid links were applied to couple the reinforcement to the concrete. Prior applications of discrete reinforcement modeling incorporated reinforcement in a mesh of three-dimensional solid elements. Replacing the three-dimensional mesh with a two-dimensional mesh of modified Kirchoff elements allowed for a simple and efficient, yet robust, manner of representing the system per element. The presented element shows better prediction of reinforced concrete flat plate behavior than the general layered shell element, and was verified with experimental data.

The extension to slabs of arbitrary shape was a topic of research in the nonlinear finite element field as well. Famiyesin and Hossain [25] applied a three-dimensional degenerated layered shell reinforced concrete model to determine model parameter values to calibrate the nonlinear analysis of fully restrained slabs, with the goal of extension to arbitrary configurations through parametric sensitivity studies. The resulting parameters were applied to 36 previously tested slabs, with the accuracy of strength determination within a mean value of 2% of experimental data.

#### **1.2.4 Additional Applications**

The ASCE (American Society of Civil Engineers) Task Committee on Finite Element Analysis of Reinforced Concrete Structures has been a driving factor in the development and implementation of finite element modeling of reinforced concrete. This committee has been

responsible for consolidating much research and theory concerning this topic, and published several volumes of conference proceedings. These works contain extensive treatment of constitutive relations and failure theories, modeling of reinforcement and bond, concrete cracking formulations, shear transfer, viscoelastic effects, thermal effects, numerical optimization, and dynamic analysis of reinforced concrete systems from a finite element perspective [55, 53, 71, 40].

Additionally, much research has been conducted concerning the general application of computers to reinforced concrete. Topics studied include the general optimization of design of reinforced concrete systems using computers [32], the general development of programming tools and resources suited to analyze and design reinforced concrete structures [50, 59], and numerical advances in the modeling of multiscale behavior as well as the cyclic and seismic response of reinforced concrete structures [7].

Several commercial software packages offer the capability to design slabs using finite elements. Some of these programs include SAFE, RAM *Concept* (formerly ADAPT Floor), and STAAD. Finite element-based slab design in SAFE, as well as RAM *Concept*, is based on element force results [16, 61], while finite element-based slab design in STAAD is based on element stresses, using the conventional Wood and Armer approach [62]. The exact procedures that these software use to compute design moments are not disclosed in the cited technical reference documentation.

### 1.3 Motivation

Despite the volume of research associated with finite element based flat plate analysis, the finite element method is not without limitations. While finite elements easily handle complexities that restrict simplified design methods, finite elements exhibit several important practical constraints. First of all, the results of finite element analysis are difficult to interpret and are usually unsuitable for direct use [33]. Interpretation of the results involves understanding several sign conventions and coordinate systems. Mistakes are easily made, and errors in interpretation can lead to the placement of steel reinforcement on the wrong face of the member, or in the wrong direction, leading to catastrophic results.

The second limitation pertains to the sheer volume of results produced by finite element analyses. It is not uncommon for a structural model to contain several thousand finite elements and fifty or more loading cases. If each element contains four nodes, each node with six degrees of freedom, the volume of results computed in such an analysis would be difficult for a single engineer to reduce to a simple design. Current practices require the engineer to determine design forces along a cross-section on an element-by-element basis, usually node-by-node per element. All loading conditions must be checked to determine the maximum effect and reduced to a design envelope. This procedure is inefficient and prone to mistakes on the part of the engineer.

Hrabok and Hrudehy described other limitations facing the finite element method. Often engineers are faced with “a perplexing array” of elements from which to choose for the analysis, including various shapes, nodal configurations, and nodal degrees of freedom. General lack of training in the finite element method complicates this further. Additionally, they pointed out that there are few general purpose programs robust enough to model all aspects of flat plate systems. Some of these capabilities include an extensive element library, the ability to model eccentric stiffeners, the ability to model the finite size of connections between the slab and columns, and techniques to evaluate the effects of stress singularities at reentrant corners [35]. It should be noted that GT STRUDL provides capabilities to model the structural characteristics that they listed.

The limitations of the finite element method demonstrate the need for a tool to simplify the design of flat plates using finite elements. This tool must be capable of processing the results of the finite element analysis and reducing the complexities of the sign conventions and coordinate systems to a single rule stating which face of the slab to reinforce. It must also transform the process from an element-by-element approach to one where the user specifies cuts or sections to design, defined by a start and end node, and never individually deals with single element results. This tool must automate the determination of the design envelope such that the engineer deals with final design forces instead of individual loading cases. This tool should also give the user multiple design options, such as the ability to design “from scratch,” design with either the bar size or bar spacing constrained, or check



a user-specified design.

The implementation of such a tool in commercial finite element software would allow engineers to design reinforced concrete flat plates both responsibly and efficiently and would constitute a major reduction in the limitations present in the current practice of finite element based slab design.

## 1.4 Outline of Presentation

The purpose of this study was the implementation and verification of a procedure in GT STRUDL to design reinforced concrete flat plate systems based on the results of finite element analysis. The specific components of the remainder of the study are as follows.

Chapter 2 presents a review of conventional reinforced concrete slab design methodologies. Methodologies reviewed include the American Concrete Institute (ACI) direct design technique, the ACI equivalent frame technique, the yield line technique, and the strip design technique. The principles and limitations of these methods are presented.

Chapter 3 provides an introduction to the application of finite element analysis to reinforced concrete flat plate design. The effects of various modeling techniques are studied and emphasized. Design based on element stresses is contrasted with design using element forces.

Chapter 4 presents the implementation of a flat plate design program in GT STRUDL based on the element force approach. A command was implemented in GT STRUDL, and the resulting preprocessing and design algorithms are explained.

Chapter 5 presents the validation of the implemented design procedure. Test cases are shown in order to determine the applicability of the procedure along with any potential limitations. Finite element design results are compared with results from current approximate techniques as well as experimental studies of both regular and irregular flat plate systems.

Chapter 6 summarizes the significant results of the study and concludes with recommendations for future research.

## CHAPTER II

# REVIEW OF CONVENTIONAL REINFORCED CONCRETE FLAT PLATE DESIGN

The objective of this chapter is to provide an overview of the current state of practice of the design of reinforced concrete flat plate systems. General ACI design requirements are presented, along with a summary of the ACI direct design, ACI equivalent frame, yield line, and strip design techniques. Each procedure as well as its limitations are discussed.

The following discussion is limited to flat plate systems. That is, the design methodologies presented below pertain only to slabs of constant thickness without drop panels, column capitals, or edge beams. In addition, prestressed concrete is not considered.

The methodologies presented in this chapter provide the background for the reinforcement design procedures in the implemented GT STRUDL command as described in Chapter 4.

### 2.1 General ACI Requirements for Reinforced Concrete Flat Plate Design

The proper design and construction of buildings of structural concrete is dictated by “Building Code Requirements for Structural Concrete and Commentary (ACI 318-02)” [2], published by the American Concrete Institute.

According to ACI 318-02, structures and structural members must be designed with a load capacity greater than the required strength as determined by a suitable analysis. The required strength,  $U$ , is computed based on combinations of the loadings required in the general building code. These loads are increased by load factors, depending on the type of load and the specific loading combination. Loads which must be considered include dead loads, live loads, temperature loads, earthquake loads, and loads due to snow, rain, and wind. Loadings considered to be determined less accurately and variable are assigned a

higher load factor. ACI 318 Section 9.2 presents nine loading combinations that must be considered for the design of a reinforced concrete system [2].

The design strength at a location in the system is computed as the nominal capacity, based on mechanics and code assumptions, multiplied by a strength reduction factor,  $\phi$ .  $\phi$ -factors are always less than 1.0 and account for statistical variations in material properties and inaccuracies in design equations.  $\phi$ -factors vary based on the specific response quantity being designed. For flexure,  $\phi$  ranges from 0.65 to 0.9 depending on the strain condition, while for shear and torsion,  $\phi$  is 0.75 [2]. The basic requirements for strength design are expressed as

$$\text{Design Strength} \geq \text{Required Strength}$$

or

$$\phi(\text{Nominal Strength}) \geq U$$

### **2.1.1 Analysis Requirements**

ACI 318 Section 13.5.1 states: “A slab system shall be designed by any procedure satisfying conditions of equilibrium and geometric compatibility, if shown that the design strength at every section is at least equal to the required strength and that all serviceability conditions, including limits on deflections, are met” [2].

Generally a linear elastic analysis is performed to provide the basis for an initial design, although use of a linear elastic analysis is not required. In fact, if inadequate reinforcement is provided in a particular location, the reinforcement will yield locally and the moment will be redistributed internally due to the redundancy of the slab system. Although such behavior may satisfy strength requirements, it can lead to poor serviceability of the slab, evidenced by undesirable cracking. If the slab is reinforced based on the distribution of linear elastic moments, however, serviceability conditions will generally be satisfied [18].

ACI 318 presents two simplified linear elastic analysis techniques which are permitted, providing the structure satisfies various requirements. These two methods are the ACI direct design technique and the ACI equivalent frame technique. Both of these methods are based on analytical studies of moment distributions using elastic theory, strength requirements

from yield line theory, experimental testing of physical models, and previous experience of slabs constructed in the field [27].

Practice has shown that it is acceptable to proportion reinforcement for ultimate limit states as well based on the results of a linear elastic structural analysis. At this limit state, the linear elastic moments do not closely predict the actual moment distribution in the slab, but are acceptable for design provided that equilibrium and compatibility are satisfied. The primary advantage of distributing reinforcement for the ultimate limit state based on a linear elastic analysis is that deflection and cracking requirements are likely to be satisfied, though this is not guaranteed [18].

The actual behavior of the slab at the ultimate limit state is plastic, and it is permitted to apply limit analysis to the design of slabs. Using such a method, the ultimate load is determined, and then the distribution of moments and shears at the ultimate level are determined. Either a *lower bound method* or *upper bound method* may be employed.

A *lower bound method* assumes a distribution of moments at the ultimate condition such that equilibrium is satisfied at all locations in the system, the yield criterion defining the strength of the slab is not exceeded, and all boundary conditions are satisfied. Equilibrium is applied, and with the assumed distribution of moments, the ultimate load can be determined. The lower bound method converges to the correct ultimate load from below the actual value, and never overestimates the ultimate load [27]. The *strip design technique* is a lower bound method.

An *upper bound method* assumes a collapse mechanism at the ultimate condition. In this collapse mechanism, the moments at the plastic hinges are assumed to be less than or equal to the ultimate moment capacity at the hinges, and the collapse mechanism must satisfy the imposed boundary conditions of the structure. The upper bound method converges to the actual ultimate load from above the actual value, and never underestimates this value. As such, it is possible to compute an ultimate load that is too high if an incorrect collapse mechanism is assumed [27]. The *yield line technique* is an upper bound method.

ACI 318 Section 13.5 sets out several other important principles related to the analysis of slabs. For instance, for lateral load analysis, the model of the supporting frame must

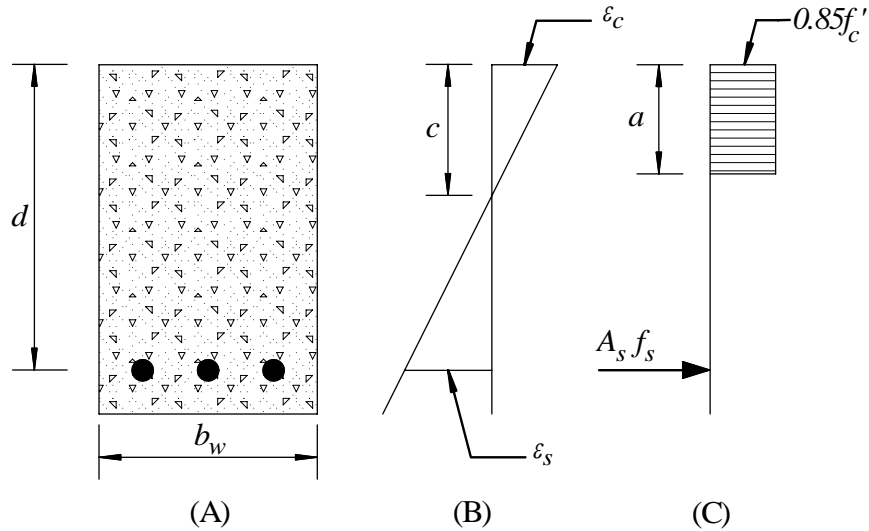


**Figure 2.1:** General Flexure: (A) Cross-Section, (B) Strain Distribution, (C) Stress Distribution

account for the stiffness effects of cracking and reinforcement for frame members. Also, ACI 318 permits the results of gravity load analyses to be superimposed with results of lateral load analyses per Section 13.5.1.3, even though different models may be used to compute each of these structural responses. Displacements under both gravity and lateral loads must remain small for this to remain applicable.

### 2.1.2 Flexural Strength Requirements

One of the significant design limit states considered for flat plate systems is the design of reinforcement to resist flexure. Design for flexure will be the focus of the implemented design procedure described in the following chapters of this study, and as such, will be treated extensively in this section. The general requirements for flexural design are set forth in ACI Chapter 10 [2]. A cross-section in a flat plate system is designed using the same procedure as that in reinforced concrete beam design. The provided ultimate strength of the member,  $\phi M_n$ , must exceed the ultimate factored moment,  $M_u$ , for all locations in a structure.

### 2.1.2.1 Ultimate Flexural Capacity

Figure 2.1-A shows the cross-section of a general reinforced concrete member reinforced for flexure. This figure will be used to develop the equations for the ultimate moment capacity of the section. The concrete compressive strength is  $f'_c$ . The distance  $d$  is the distance from the compression face of the member to the centroid of the layer of reinforcing steel. The width of the beam is given by  $b_w$ . The area of steel reinforcement is given as  $A_s$ , and the steel has a yield strength equal to  $f_y$ .

When the reinforced concrete member is subjected to a loading and a moment is produced, an assumed linear distribution of strain develops through the cross-section, as shown in Figure 2.1-B. In this figure,  $\epsilon_c$  is the strain at the extreme compression fiber of the concrete, and  $\epsilon_s$  is the tensile strain in the steel reinforcement at a distance  $d$  from the compression face of the member. ACI 318 Section 10.2.5 states that the tensile strength of concrete is to be neglected in the calculation of required flexural reinforcement, such that the only tensile component in the system is the steel reinforcement. The neutral axis of the member is located at a distance  $c$  from the compression face.

ACI 318 states that the crushing strain of the concrete,  $\epsilon_{cu}$ , shall not be taken greater than 0.003 [2]. Though experimental results show concrete can achieve compressive strains significantly higher than this value, concrete is assumed to crush when the strain reaches this lower bound for design purposes [49]. In flexure, there are three ways in which the section will fail. First, a section is said to fail at a balanced strain condition when the tension reinforcement strain,  $\epsilon_s$ , reaches the strain corresponding to the specified yield stress,  $f_y$ , at the same time that the extreme compression fiber in the concrete reaches the assumed ultimate strain, 0.003. Second, a section is said to be compression-controlled if the extreme concrete fiber reaches the ultimate compressive strain prior to the tensile strain in the reinforcement reaching  $\epsilon_y$ . (For Grade 60 steel, this value may be taken as 0.002.) In a compression-controlled section, the concrete will crush before any significant yielding of reinforcement occurs, leading to a brittle failure mode with little or no visible warning. Third, a section is said to be tension-controlled if the tensile strain in the steel is equal to or higher than 0.005 when the extreme compression fiber reaches its assumed strain limit

of 0.003 [2]. In a tension-controlled failure, the steel will undergo large strains, and the concrete will experience significant cracking before the compression zone crushes, providing warning of impending failure. Because of this, flexural members are designed to fail in a tension-controlled manner when possible.

Per ACI 318 Section 9.3, the strength reduction factor  $\phi$  is taken to be 0.9 for tension-controlled sections and 0.65 for compression-controlled sections. At failure of the section, if the strain in the steel falls between the limits for compression-controlled and tension-controlled strains, the section is said to fail in the *transition zone*, and the strength reduction factor is to be linearly interpolated between 0.65 and 0.9 based on the value of the strain in the steel [2]. Initially in design,  $\phi$  is assumed to equal 0.9, and after the section is designed, the strain is computed at the ultimate state and verified to be greater than 0.005 in the steel.

Based on the limiting criteria for the strains in both the steel and concrete, the ultimate capacity of the cross-section can be computed. Since a tension-controlled failure is assumed, the strain in the steel at failure is greater than the yield strain. The stress in the steel,  $f_s$ , is therefore set equal to the yield stress,  $f_y$ , producing a tension force,  $T$ , in the section, given by Equation 2.1.

$$T = A_s f_y \tag{2.1}$$

$T$  acts at a distance  $d$  from the compression face of the member and is shown in Figure 2.1-C. The tension force in the section must be resisted by an equal and opposite compression force. Although the distribution of compressive stress in the concrete is nonlinear at the ultimate level, ACI 318 permits the compression zone to be represented by a rectangular distribution of stress of magnitude  $0.85f'_c$ . This uniform stress distribution is also shown in Figure 2.1-C, and extends a depth  $a$  into the section from the compression face. The depth of the rectangular stress block is related to the depth of the neutral axis,  $c$ , by the expression,  $a = \beta_1 c$ , where  $\beta_1$  is 0.85 for concrete strengths less than 4000 psi, 0.65 for concrete strengths greater than 8000, and linearly interpolated between 0.65 and 0.85 for concrete strengths between 4000 and 8000 psi. As such, the compressive force within the

member,  $C$ , is given in Equation 2.2.

$$C = 0.85 f'_c a b_w \quad (2.2)$$

Equating the tension and compression forces in the cross-section, the depth of the rectangular compression block,  $a$ , can be computed using Equation 2.3.

$$a = \frac{A_s f_y}{0.85 f'_c b_w} \quad (2.3)$$

Now that the depth of the compression zone can be explicitly computed, the strain in the steel should be checked to verify that the section is indeed tension-controlled as assumed. The strain in the steel is determined in several steps. First of all, the distance to the neutral axis,  $c$ , is computed as  $c = a/\beta_1$ . Then by assuming  $\epsilon_{cu} = 0.003$ ,  $\epsilon_s$  is computed by applying similar triangles to the strain distribution, shown in Equation 2.4.

$$\epsilon_s = \epsilon_{cu} \left( \frac{d - c}{c} \right) \quad (2.4)$$

If  $\epsilon_s$  is less than 0.005, the value of  $\phi$  must be accordingly computed. Then, the moment capacity of the section,  $\phi M_n$ , is determined by summing the internal moments from the compression stress in the concrete and tension force in the steel, as shown in Equation 2.5.

$$\phi M_n = \phi A_s f_y \left( d - \frac{a}{2} \right) \quad (2.5)$$

### 2.1.2.2 Computation of Required Area of Steel

Now that the ultimate strength of the member has been formulated, the computation can be modified for design application. Equation 2.5 computes the ultimate strength when a known steel reinforcement area is provided. In design, however, the ultimate strength required is known, but not the area of steel. By setting  $M_u = \phi M_n$  and substituting Equation 2.3 into Equation 2.5, a quadratic expression for  $A_s$  as a function of  $M_u$  can be formulated (Eqn. 2.6).

$$M_u = \phi A_s f_y \left( d - \frac{A_s f_y}{1.7 f'_c b_w} \right) \quad (2.6)$$



After several algebraic manipulations, Equation 2.6 can be rewritten using the quadratic equation to explicitly compute the area of steel required (Eqn. 2.7).

$$A_{s,req'd} = \frac{-(\phi f_y d) + \sqrt{(\phi f_y d)^2 - 4 \left( \frac{\phi f_y^2}{1.7 f_c' b_w} \right) (M_u)}}{2 \left( -\frac{\phi f_y^2}{1.7 f_c' b_w} \right)} \quad (2.7)$$

The importance of Equation 2.7 is that all of the arguments are independent, the only exception being the strength reduction factor,  $\phi$ . Thus, once  $A_s$  is computed using Equation 2.7, the strain in the steel must be computed by Equation 2.4, indicating the appropriate  $\phi$ -factor. It may be necessary to iterate on  $\phi$  using these equations until  $A_s$  converges.

Although the case of a rectangular cross-section reinforced only on the tension side is one of the more simple cases for the design of reinforced concrete beams, it provides a sound basis for the design of flat plate sections for several reasons. First of all, flat plate sections are generally rectangular, so the formulation need not be specialized for more complicated geometries. Second, although flat plates may contain reinforcement on both faces, the width of design cross-sections (large with respect to the thickness of the slab) usually produces an  $a$ -depth smaller than the cover between the compression-side bars and the extreme compression face. Thus, compression reinforcement in flat slabs is usually located near the neutral axis and can be neglected since the strain will be very small in comparison to the strain in the tension-face reinforcement [43]. Appendix A presents the results of a study that justifies neglecting the effect of compression reinforcement in flat plate systems.

### 2.1.2.3 Minimum Flexural Reinforcement Requirements

Section 10.5 of ACI 318 dictates that a minimum area of steel is required at all sections of a beam where analysis demonstrates a need for tensile reinforcement. If the amount of reinforcement computed using Equation 2.7 is very small, the computed ultimate moment strength based on a reinforced concrete cracked section analysis can be less than the computed ultimate moment strength of the same unreinforced concrete section computed based on the modulus of rupture [2]. To prevent this, minimum flexural reinforcement must be provided in beams according to Equation 2.8.

$$A_{s,min} = \frac{3\sqrt{f_c'}}{f_y} b_w d \geq \frac{200 b_w d}{f_y} \quad (2.8)$$

### 2.1.3 Shear Strength Requirements

#### 2.1.3.1 General Shear Strength of a Cross-Section in Beam Action

The requirements for shear design of a reinforced concrete system are presented in Chapter 11 of ACI 318. In general, the shear capacity provided must be greater than the required shear strength computed using the factored loading combinations of ACI 318 Section 9.2, as shown in Equation 2.9.

$$\phi V_n \geq V_u \quad (2.9)$$

In this equation,  $V_n$  is the nominal shear capacity of the section and is taken to equal the sum of  $V_c + V_s$  where  $V_c$  is the shear capacity of the concrete and  $V_s$  is the shear strength contributed by shear reinforcement. For flat plate systems, shear reinforcement is seldom provided so it is sufficient to set  $V_n = V_c$ .  $V_c$  is a function of the cross-sectional geometry as well as the compressive strength of the concrete. ACI 318 states that the allowable shear stress for a beam member subjected to only flexure and shear be taken as  $2\sqrt{f'_c}$ . Using this stress, the nominal shear capacity of the concrete can be computed and is given in Equation 2.10 [2].

$$V_c = 2\sqrt{f'_c} b_w d \quad (2.10)$$

For a general cross-section of a flat plate in beam action, the ultimate shear force shall not exceed the value computed by this equation.

If the section fails according to a shear criterion, there are several techniques to increase the shear strength of the system. Drop panels or column capitals could be introduced into the system. Increasing the depth of the slab will increase the shear capacity. The strength of the concrete can be increased. The column dimensions can also be increased. Finally, the section can be reinforced with either stirrups or a stud rail [43]. In fact, stud rails are often the most economical solution to the complications caused by shear in flat plates.

#### 2.1.3.2 Punching Shear with No Moment Transfer

To evaluate the shear strength of flat plate systems in regions near columns (where moment is not transferred in the beam-to-column connection), it is insufficient to assume the slab is behaving according to beam action. Thus the guidelines of the previous section are no

longer valid. For punching shear, the critical section for design is a perimeter  $b_0$  (located around the column) and is at a distance of  $d/2$  from the edges or corners of the column [2]. The shear strength of the concrete is then computed as the minimum of Equations 2.11, 2.12, and 2.13. In Equation 2.11,  $\beta_c$  is the ratio of long side to short side of the column [2]. In Equation 2.12,  $\alpha_s$  is 40 for interior columns, 30 for edge columns, and 20 for corner columns.

$$V_c = \left(2 + \frac{4}{\beta_c}\right) \sqrt{f'_c} b_0 d \quad (2.11)$$

$$V_c = \left(\frac{\alpha_s d}{b_0} + 2\right) \sqrt{f'_c} b_0 d \quad (2.12)$$

$$V_c = 4\sqrt{f'_c} b_0 d \quad (2.13)$$

If the shear capacity provided by these equations is less than that of the required ultimate shear, shear reinforcement can be provided according to the stipulations in ACI 318 Section 11.12.3 [2]. To provide shear reinforcement, the effective depth of the section must be at least 6 inches and not less than 16 times the shear reinforcement bar diameter. Shear reinforcement in the slab must also satisfy development length requirements. Note that if shear reinforcement is added to the section, the shear strength of the concrete must be reduced to  $V_c = 2\sqrt{f'_c} b_0 d$ .

### 2.1.3.3 Moment Transfer Shear

In many slab-to-column connections, an unbalanced moment is transferred in addition to the shear from the slab. The result of this unbalanced moment is non-uniform shear around critical perimeter, as demonstrated in Figure 2.2 [27]. This will generally be the case for exterior or corner columns and sometimes for interior columns depending on the geometry and loading conditions. In these cases, the shear force and unbalanced moment are transferred by a combination of bending, torsion, and shear at the faces of the critical perimeter.

The behavior of moment transfer shear can be analyzed using several techniques, including analysis based on a linear variation in shear stress, analysis based on thin plate theory, beam analogies, or truss analogies. The approach set forth in ACI 318 is to assume that of the unbalanced bending moment  $M_u$ ,  $\gamma_v M_u$  is transferred by torsion and  $\gamma_f M_u$  by

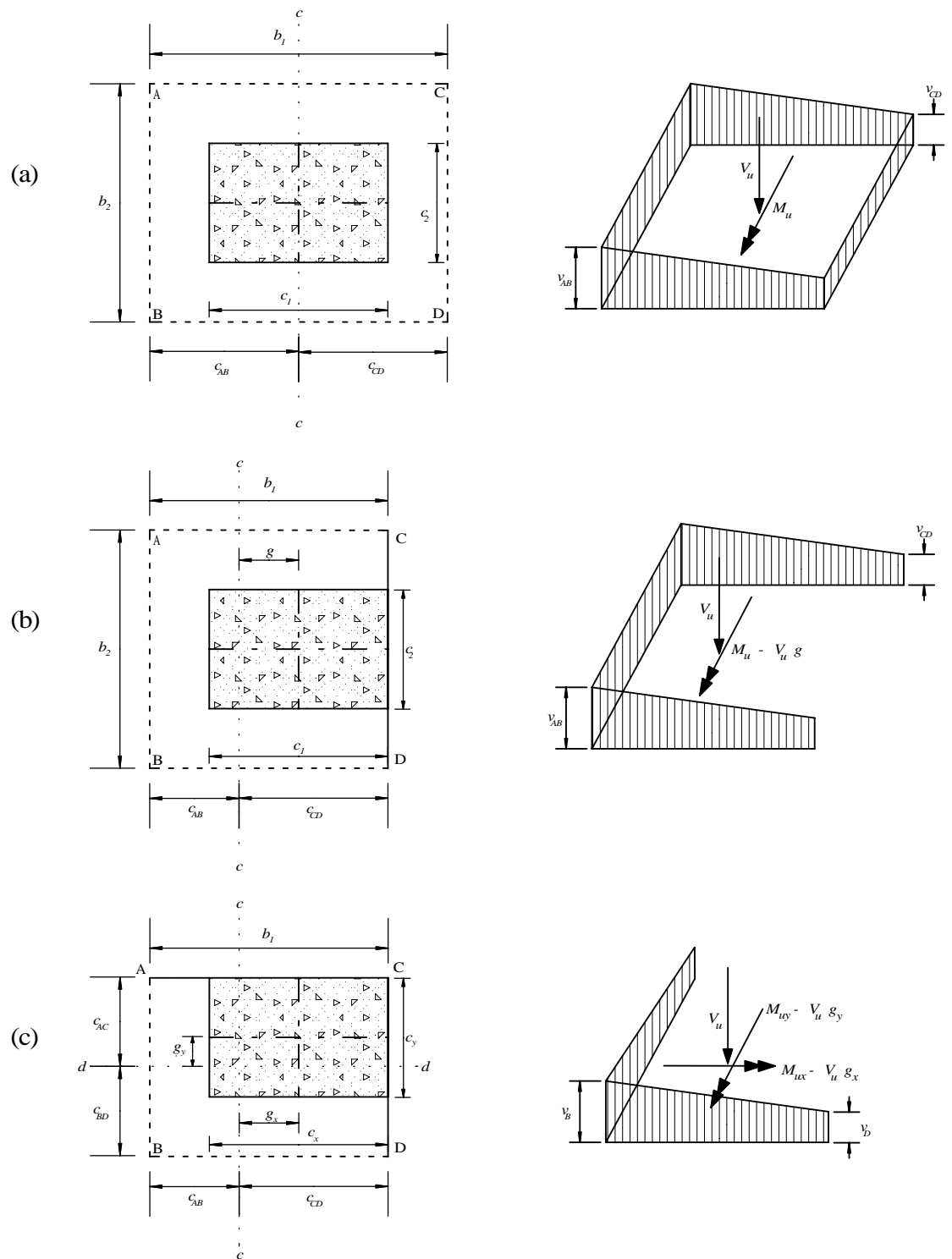


Figure 2.2: Moment Transfer Shear - Interior, Edge, and Corner Columns [27]

flexure, where  $\gamma_f$  is computed using Equation 2.14 [27]. Note that  $\gamma_v + \gamma_f = 1.0$ .

$$\gamma_f = \frac{1}{1 + \frac{2}{3}\sqrt{b_1/b_2}} \quad (2.14)$$

In this equation, the ratio  $b_1/b_2$  is the ratio of the widths of the critical perimeter as labeled in Figure 2.2. For square, interior columns,  $\gamma_f = 0.4$ .

The maximum shear stress on each face of the critical perimeter can then be computed, provided  $M_u$  and  $V_u$  have been computed at the centroid of the column, using Equations 2.16 through 2.20, depending on the nature of the connection. At each face, the moment transfer shear stress is then compared with the nominal shear capacity of the critical perimeter, given by Equation 2.15. If the slab contains no shear reinforcement,  $V_s = 0.0$ .

$$\phi v_n = \frac{\phi(V_c + V_s)}{b_0 d} \quad (2.15)$$

The assumed critical section and shear stress distribution for an interior column connection are shown in Figure 2.2(a). The shear stresses on each face of the critical section are given by Equation 2.16 [27]. In this equation,  $A_c$  refers to the area of concrete enclosed in the critical perimeter,  $J_c$  is the torsional constant of the critical section, and  $c_{AB}$  and  $c_{CD}$  refer to the distance from the column centroid to faces  $AB$  and  $CD$ , respectively [2].

$$v_{u,AB} = \frac{V_u}{A_c} + \frac{\gamma_v M_u c_{AB}}{J_c} \quad v_{u,CD} = \frac{V_u}{A_c} - \frac{\gamma_v M_u c_{CD}}{J_c} \quad (2.16)$$

For an edge column connection, the assumed critical section and shear stress distribution are shown in Figure 2.2(b). The shear stresses on each face of the critical section for this case are given in Equation 2.17 [27]. The distance  $g$  refers to the distance between the centroidal axis of the critical section and the centroidal axis of the column.

$$v_{u,AB} = \frac{V_u}{A_c} + \frac{\gamma_v (M_u - V_u g) c_{AB}}{J_c} \quad v_{u,C} = v_{u,D} = \frac{V_u}{A_c} - \frac{\gamma_v (M_u - V_u g) c_{CD}}{J_c} \quad (2.17)$$

For a corner column connection, the assumed critical section and shear stress distribution are shown in Figure 2.2(c). The shear stresses on each face of the critical section for this case are given in the following equations [27]. The distances  $g_x$  and  $g_y$  refer to the distances in the  $x$ - and  $y$ -directions between the centroidal axes of the critical section and the centroidal

axes of the column.  $M_{ux}$  and  $M_{uy}$  are the unbalanced bending moments in the  $x$ - and  $y$ -directions.  $J_{cx}$  and  $J_{cy}$  refer to the torsional constants about the  $x$ - and  $y$ -axes.

$$v_A = \frac{V_u}{A_c} + \frac{\gamma_{vx}(M_{ux} - V_u g_x)c_{AB}}{J_{cx}} - \frac{\gamma_{vy}(M_{uy} - V_u g_y)c_{AC}}{J_{cy}} \quad (2.18)$$

$$v_B = \frac{V_u}{A_c} + \frac{\gamma_{vx}(M_{ux} - V_u g_x)c_{AB}}{J_{cx}} + \frac{\gamma_{vy}(M_{uy} - V_u g_y)c_{BD}}{J_{cy}} \quad (2.19)$$

$$v_D = \frac{V_u}{A_c} - \frac{\gamma_{vx}(M_{ux} - V_u g_x)c_{CD}}{J_{cx}} + \frac{\gamma_{vy}(M_{uy} - V_u g_y)c_{BD}}{J_{cy}} \quad (2.20)$$

#### 2.1.4 Serviceability Requirements

The performance of a slab at service loads is an important design consideration in addition to strength requirements. Even if strength requirements are fully satisfied, excessive deflections or cracking can interfere with the usefulness of the structure [27]. ACI 318 Section 9.5.1 states that “reinforced concrete members subjected to flexure shall be designed to have adequate stiffness to limit deflections or any deformations that adversely affect strength or serviceability of a structure.” For a slab, the maximum allowable deflections range from  $l/480$  to  $l/240$ , depending on the particular relationship of the slab with respect to the rest of the structure. These criteria are given in Table 9.5(b) of ACI 318 [2].

The primary requirements implemented by ACI 318 to control deflections are the limiting thicknesses for slabs in various applications, unless detailed deflection calculations are made. If deflection calculations are not made and if the flat plate has no edge beams or drop panels, the minimum thickness for exterior panels ranges from  $l_n/30$  for slabs reinforced with 40 ksi bars to  $l_n/28$  for slabs reinforced with 75 ksi bars. The minimum thickness for interior panels ranges from  $l_n/36$  for slabs reinforced with 40 ksi bars to  $l_n/31$  for slabs reinforced with 75 ksi bars. ACI 318 Table 9.5(c) presents these values along with limiting thicknesses for reinforcement of intermediate strengths. Regardless of Table 9.5, ACI 318 limits the thickness of flat plates without drop panels to 5 inches, provided the ratio of long to short span of the panel is less than 2 [2].

By ACI 318 Section 9.5.3.4, a slab can be designed with a thickness less than the minimum requirements described above if it can be shown by computation to satisfy the minimum deflection criteria in ACI 318 Table 9.5(b). Deflection calculations must account

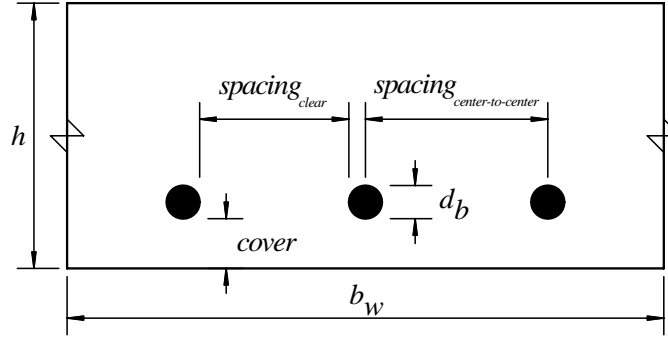


**Figure 2.3:** Flat Plate Cross-Sectional Detailing Requirements

for the size and shape of the panel, conditions of support, and the nature of restraints at the edges of the panel. Additionally, deflection calculations must reasonably agree with the results of comprehensive experimental tests [2].

### 2.1.5 Detailing of Reinforcement

Once an area of reinforcing steel has been determined that satisfies strength and serviceability requirements, this reinforcement must be physically constructed. ACI 318 places many requirements on the actual layout and placement of reinforcing steel. Placement of reinforcing bars must satisfy geometrical constraints, and the bars or welded wire fabric must be of adequate length to fully develop their capacity.

#### 2.1.5.1 Placement of Reinforcing Bars

ACI 318 Section 7.12 dictates that a minimum area of steel must be provided to resist shrinkage and temperature effects. The minimum area of steel required is expressed as the ratio,  $\rho_{min}$ , of reinforcement area to gross concrete area and depends on the yield stress of steel reinforcement used. For Grade 40 or 50 bars,  $\rho_{min} = 0.0020$ . For Grade 60 bars,  $\rho_{min} = 0.0018$ . For steel reinforcement with yield stress in excess of 60 ksi,  $\rho_{min} = (0.0018 \times 60,000)/f_y$ , but not less than 0.0014. The area of steel required as a result of this minimum reinforcement ratio is given in Equation 2.21.

$$A_{s,min} = \rho_{min} b_w h \quad (2.21)$$

Several stipulations apply to the spacing of bars throughout the cross-section. ACI 318 Section 13.3.2 requires that the center-to-center spacing of reinforcement at critical sections,

labeled in Figure 2.3 as  $spacing_{center-to-center}$ , must not exceed two times the thickness of the slab. However, the maximum spacing for temperature and shrinkage steel is limited to 18 inches per Section 7.12.2.2. Thus, Equation 2.22 can be applied to compute the maximum allowable center-to-center spacing of bars.

$$s_{max} = \min(18 \text{ inches}, 2h) \quad (2.22)$$

The minimum allowable clear spacing of bars, labeled in Figure 2.3 as  $spacing_{clear}$ , is governed by ACI 318 Section 7.6.1, which states that the minimum clear spacing between parallel bars is  $d_b$ , also shown in Figure 2.3, but not less than 1 inch [2]. The purpose of this latter stipulation is to allow concrete to flow freely between bars during construction. However, it has been suggested that this value is unconservative and that a minimum clear spacing of 2.5 inches is more appropriate [43].

The vertical location of bars in a layer is generally governed by the cover requirements. Cover refers to the distance from the concrete surface to the face of the bar, and is shown in Figure 2.3. The purpose of cover is to provide adequate embedment of bars to protect from moisture, other corrosive agents, and fire. The minimum applicable cover is a function of the bar size used. ACI 318 Section 7.7.1 states that for slabs not exposed to earth or weather, #14 and #18 bars require a minimum cover of 1.5 inches, and #11 bars and smaller require a minimum cover of 0.75 inches [2].

#### 2.1.5.2 Development Length Requirements

In general, the development lengths of various bar sizes are governed by Chapter 12 of the ACI code. Development of flexural reinforcement is discussed in ACI 318 Section 12.10. The stipulations of ACI 318 Chapter 12 are presented in a simplified form specific to slabs without beams in ACI 318 Table 13.3.8 [2]. This table dictates the minimum extensions for reinforcement in slabs without beams. The development lengths for slab reinforcing bars are then determined without computing the development length individually for each bar size used. In the case that adjacent spans are unequal, extensions of the negative moment reinforcement beyond the face of the support must be based on the minimum development length associated with the longer span.



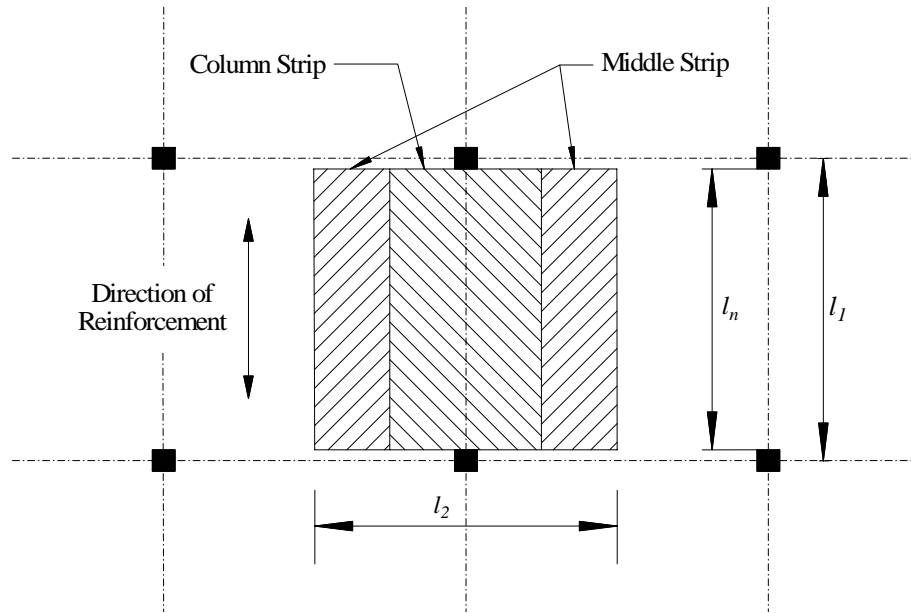


Figure 2.4: Slab-Beam Layout and Dimensions

## 2.2 ACI Direct Design Technique

The ACI Direct Design technique is presented in Section 13.6 of ACI 318.

A flat plate system must meet several requirements for the direct design method to be applicable. First, there must be a minimum of three consecutive spans, or bays, in each direction. Second, panels must be rectangular, and in each panel, the ratio of the longer to the shorter span must be less than 2. Third, successive span lengths must not vary by more than one-third of the longer span in each direction. Fourth, columns must not be offset by a distance greater than 10% of the span length in the direction of the offset between the centerlines of adjacent columns. Finally, the structure must only be loaded with gravity loads, and applied loads must be uniformly distributed over the entire panel. The applied live load must not exceed two times the dead load [2].

The direct design technique reduces the general slab structure to smaller panels within the slab, which are designed independently. In Figure 2.4, a typical slab panel, or *slab-beam*, is shown by the hatched pattern. Several key dimensions are given. The distance  $l_1$  is the spacing between column center lines in the direction parallel to reinforcement to be designed. The distance  $l_2$  is the width of the slab-beam in the direction transverse to the

reinforcement to be designed. The distance  $l_n$  is the clear spacing between columns in the same direction as  $l_1$ , and becomes the effective length of the slab-beam for the distribution of bending moment in the panel.

To compute the design moments at various sections throughout the panel, the distributed load on the panel,  $w$ , must be computed. This load is the ultimate factored gravity load on the slab and is computed using Section 9.2 of ACI 318 [2]. The fundamental calculation for a slab panel in the direct design procedure is the computation of the total static moment,  $M_0$ . For a slab-beam, the total static moment is equal to the average of the negative moments at each end of the member plus the maximum positive moment throughout the member. The formulation for  $M_0$  is shown in Equation 2.23 [27].

$$M_0 = \frac{wl_2l_n^2}{8} \quad (2.23)$$

The total static moment is then distributed throughout the slab panel according to the rules of ACI 318 Sections 13.6.3, 13.6.4 and 13.6.6. Depending on the location of the panel within the structure,  $M_0$  is distributed in different ways. For instance, for an internal slab-beam, 65% of  $M_0$  is distributed to the negative factored moment at the column faces, and 35% of  $M_0$  is distributed to the positive factored moment at the midspan. If the span terminates at an outside edge or at special restraints such as a edge beams, the distribution of  $M_0$  changes according to the table in ACI 318 Section 13.6.3.3.

Once the total static moment has been computed and distributed between the positive and negative moment locations of the slab-beam, these moments must be distributed between column and middle strips. For a general case, the layout of the column and middle strips is shown in Figure 2.4. ACI 318 defines a column strip as “a design strip with a width on each side of a column centerline equal to  $\frac{1}{4}l_2$  or  $\frac{1}{4}l_1$ , whichever is less ... A middle strip is a design strip bounded by two column strips” [2]. The percentages of the total static moment to be distributed to the column and middle strips are presented in tabular form in ACI 318 Sections 13.6.4 and 13.6.6 [2]. Note that the design moment for the middle strip is divided to each side of the column strip, and subsequently added to the design moment in the middle strip from adjacent slab panels, and then the reinforcement is placed in the

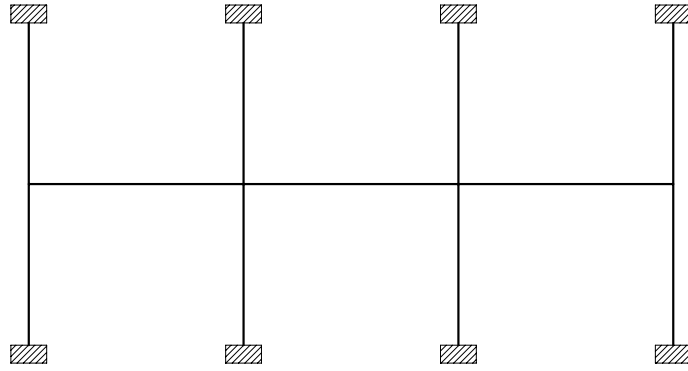


**Figure 2.5:** Elevation Showing Plane Frame Analytical Model for the Equivalent Column Method

middle strip uniformly. The moment distribution factors are based on both experimental and analytical studies of moments in linear elastic slabs, and are intended to “ensure that steel stresses are not excessively high at service load so that crack widths and deflections remain within acceptable bounds” [27].

### 2.3 ACI Equivalent Frame Technique

The ACI equivalent frame method is presented in Section 13.7 of ACI 318. The equivalent frame method refers to two methodologies. The first is called the equivalent column method and is the focus of this section. The second is the equivalent slab method and will be discussed shortly in the conclusion of this section.

The premise of the equivalent column method is that a three-dimensional slab system is represented by a series of adjacent two-dimensional frames. A general plane frame model used in equivalent column design is shown in Figure 2.5. Applied loads act in the plane of the frame. Each frame corresponds to a column line in the structure. Equivalent frames are assumed longitudinally and transversely through the building, and each frame is analyzed independently.

Accurate calculation of the stiffness of the slab-beams and columns is critical in equivalent frame analysis. A slab-beam is a horizontal member in an equivalent frame, and for a flat plate consists only of the slab. A slab-beam in the equivalent column method is the same as that for direct design, as shown in Figure 2.4. The moment of inertia of each slab-beam is computed based on the gross section area of the concrete, and variation in moment

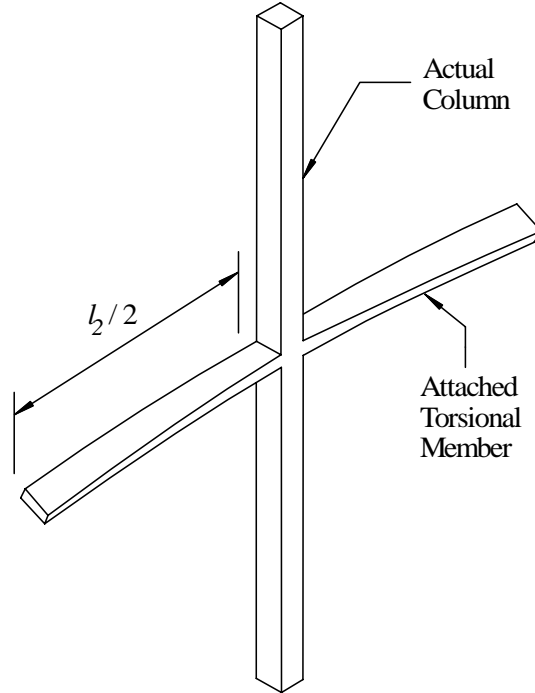


**Figure 2.6:** Equivalent Column with Attached Torsional Member

of inertia along the slab-beam must be taken into account, although there is typically none in a plate. The moment of inertia of columns from the top to bottom of the slab-beam at a connection is assumed to be infinite.

The columns in the slab system will actually be modeled as *equivalent columns*, with geometry as shown in Figure 2.6. An equivalent column consists not only of the physical columns above and below the connection, but it also contains a torsional member attached at the level of the slab. For a flat plate, the torsional member consists of a portion of the slab with a width equal to that of the column in the direction of the span for which moments are being determined [2]. Thus, the stiffness provided by the equivalent column is a combination of the stiffness of the physical columns and of the attached torsional member. The equivalent column stiffness  $K_{ec}$  is given in Equation 2.24 as a function of the column stiffness  $K_c$  and the torsional member stiffness  $K_t$  [19].

$$\frac{1}{K_{ec}} = \frac{1}{\sum K_c} + \frac{1}{K_t} \quad (2.24)$$

Once the stiffness has been determined for the slab-beams and equivalent columns, the structure is analyzed. When the equivalent frame technique was first introduced, the

analysis was conducted using moment distribution, although today this procedure has been largely replaced with frame analysis programs that analyze the system using the direct stiffness procedure.

The results of the frame analysis will provide the distribution of moment and shear throughout the slab-beam. The moments and shears must be determined at the face of the columns, not the centerlines, and at other sections throughout the members to find the critical effects. Once the critical design forces have been determined, the positive and negative moments are distributed between column and middle strips using the same factors as those used in the direct design method. The reinforcement is then designed using the theory and procedures presented earlier in this chapter to resist flexure and shear, to satisfy serviceability criteria, and to provide appropriate detailing of reinforcement.

The methodology presented so far for the equivalent frame technique is limited to gravity load analysis only. However, the equivalent frame technique has been shown to be applicable to analyze unbraced multistory buildings for both lateral loads as well as gravity loads using a modified technique known as the equivalent slab technique [69]. According to ACI 318 Sections 13.5.1.2 and 13.5.1.3, any analysis accounting for lateral loads must take into account the effects of cracking, and it is permissible to combine the results of lateral load analysis with the results of gravity load analysis [2]. Literature pertaining to the lateral load analysis of slab systems indicates that satisfactory deflections and force results can be obtained provided that the technique is limited to parallel planar frames with similar stiffnesses [69].

## **2.4 Yield Line Method**

The yield line method is an upper bound approach to limit analysis of reinforced concrete slab systems. As such, this method should only be applied with sufficient knowledge and experience to assure an accurate design, or else the strength of the slab could be greatly overestimated. Note that that yield line theory is generally applied to slabs with a uniform distribution of reinforcement. The theory has been applied to slabs with non-uniform reinforcement, but this is not treated in this study. In general, the yield line theory is a method

to check the strength of an already reinforced slab system [33]. For design, the distribution of reinforcement is assumed initially and then checked.

The yield line method is particularly applicable to slab systems that cannot be analyzed by either direct design or equivalent frames due to geometric limitations. The yield line method can be used to design slab systems with various shapes, boundary conditions, openings, and complicated loading conditions.

Due to the fact that reinforced concrete slab systems are generally designed to exhibit a tension-controlled failure, most are under-reinforced. As the loading on the slab increases, some of the steel begins yielding locally, and the stiffness of the system (and thus the distribution of moment) redistributes in response to this yielding. The first instance of localized yielding usually occurs at the location of maximum bending moment as determined by elastic theory [27]. Assuming sufficient ductility is present, as this redistribution occurs and subsequent progressive yielding of adjacent zones follows, large changes in curvature occur with increase in loading until a collapse mechanism is exhibited in the form of one or more plastic hinges. *Yield lines* are the narrow zones of localized yielding that occur as a result of this plastic behavior [18].

The basic premise of design based on the yield line method is that the engineer must postulate a collapse mechanism, i.e. the location of yield lines, that satisfies the boundary conditions of the slab. For a given slab layout, multiple collapse mechanisms are often possible, depending on the distribution of reinforcement, so the engineer must examine all possible mechanisms to determine the actual ultimate load. Some examples of possible collapse mechanisms for uniformly loaded slabs with various shapes and boundary conditions are shown in Figure 2.7.

A combination of multiple yield lines in a slab panel is called a *yield pattern*. The behavior of a yield pattern is subject to several principles that engineers may apply in the determination of the collapse mechanism. In a slab panel, the slab segments between yield lines are assumed to behave as a rigid plane and deflect as such after the plastic mechanism is formed. In addition, to act as a plastic *hinge*, a yield line must be straight in order to form an axis of rotation. Plastic hinges will always develop along fixed supports. For instance, a

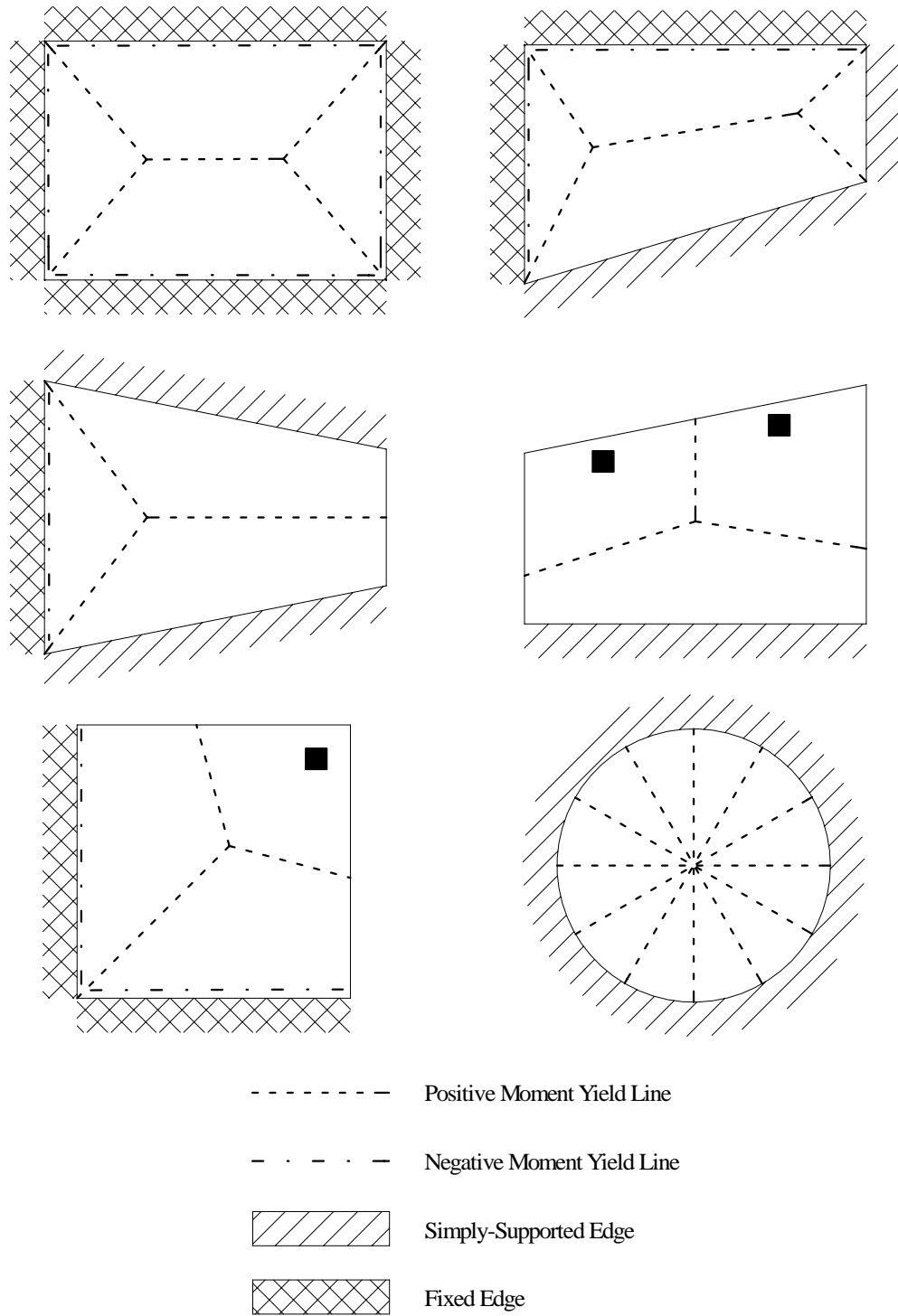


**Figure 2.7:** Example Yield Line Patterns [27]

yield line may form along a fixed edge, and plastic hinges will develop over columns. Also, a yield line must intersect at the axes of rotation of two adjacent slab segments if deflections are to be compatible [27].

Once a yield pattern has been assumed, the system must be analyzed to determine the actual location of the yield lines. The two primary methods employed to solve for the unknown dimensions defining the actual yield pattern are analysis by the *principle of virtual work* or analysis using the equations of equilibrium [27]. Theoretically, both solution techniques should compute the same yield line geometry. Once the unknown yield pattern dimensions are determined, the system can be evaluated to determine the ultimate uniform load required to produce this yield pattern. After the actual collapse mechanism and ultimate load have been determined, the engineer can distribute reinforcement throughout the slab. Here, the engineer assumes the manner of yielding, and details the slab such that this assumed yield pattern occurs.

The serviceability of slabs designed using the yield line method is an important concern. At service loads, the slab system must be checked to determine that deflections and crack widths are within acceptable bounds. Although uniform distribution of steel may satisfy the ultimate states, concentrations of reinforcement may be required in some areas to provide adequate performance at service loads.

## 2.5 Strip Design Technique

The development of the strip design procedure is attributed to Hillerborg [27]. In contrast to the yield line technique, the strip design method is a lower bound approach to limit analysis of reinforced concrete slab systems. Being a lower bound approach, the strip design method will provide a solution for the ultimate load for a slab that is either correct or too low. Thus, the strip design technique is generally conservative when applied appropriately. In fact, if an unsuitable solution is computed, the strength of the slab may be so conservative as to lead to poor economy [33]. Also in contrast to the yield line technique, the strip technique is a pure method of design, not a method for checking a previously designed system. According to Hillerborg, the stated objective of the strip design technique is to “seek a solution to the



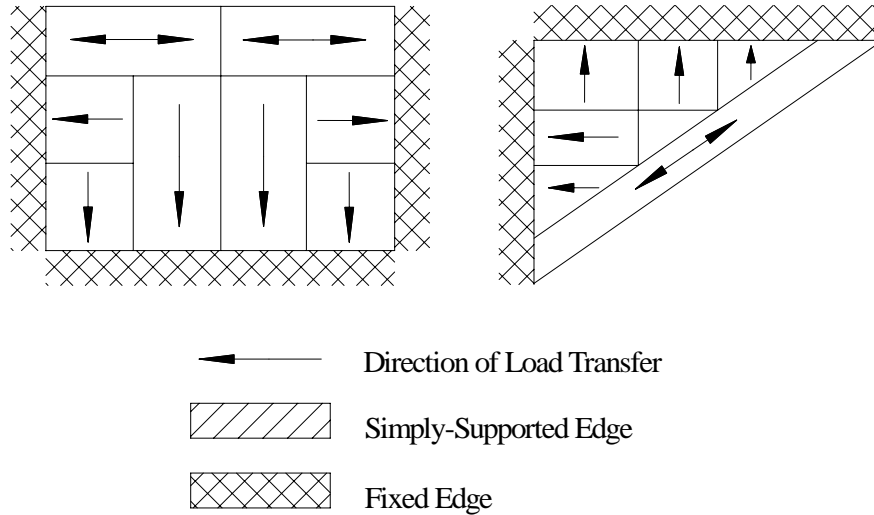


**Figure 2.8:** Example Strip Design Layout [27]

equilibrium equation [and] reinforce the slab for these moments” [33].

Stated by Hillerborg, the general premise of the strip method is that load is assumed to be carried by strips of the slab that are oriented in the directions of reinforcement [33]. Strips are analogous to beams, and as such, this method is only applicable in scenarios where the strips can be suitably approximated as beams with pin or fixed supports. The slab is divided into these strips based on the assumed transfer of load to the supports. Stated by Hillerborg, “The whole load within each part of the slab is assumed to be carried by strips in one reinforcement direction [where] no torsional moments act in these strips” [33]. Distributing the load in this manner generally produces simple and economical designs.

The actual determination of the layout of design strips is subjective and requires a general understanding of the behavior of the system being designed. The goal of design should be to transfer the load to supports in the most economical manner possible. Practically, this means for a rectangular slab with all edges fixed and dimensions  $a$  and  $b$  where  $a > b$ , less reinforcement will be required if the load is assumed to transfer primarily to the supports on the edges of length  $a$ , between which the span is shorter, because the moments in this direction will be less than the moments developed in the long direction, on the edges of length  $b$ . Hillerborg suggests that the portions of the slab loading to be transferred to different supports should be divided based on the location of *lines of zero shear force*, along

which the shear force is assumed to be zero in all directions [33]. Figure 2.8 shows the layout of strips commonly used for some simple slab systems.

Once a field of strips has been determined, each strip is then analyzed independently for the loading assigned to that strip. Top and bottom reinforcement is designed for each strip based on the results of the simple analysis of the strip. Sometimes interaction of strips must be accounted for in the analysis, particularly if one strip is assumed to support others as in the case of a *strong band*, where a concentrated area of steel may be provided.

The primary drawback to the strip design technique is the possibility of poor performance with respect to serviceability. Applied incorrectly, the strip design technique can lead to wide cracking or excessive deflections at the service load level [27]. To avoid this, the distribution of moments should conform reasonably closely to that provided by elastic analysis. Also, additional models may be required beyond those used in design to appropriately evaluate the actual deflections of the slab system.

## CHAPTER III

# APPLICATION OF THE FINITE ELEMENT METHOD TO REINFORCED CONCRETE SLAB DESIGN

### 3.1 Modeling of Slabs Using Finite Elements

If the finite element method is to be a useful tool in the design of reinforced concrete flat plate structures, accurate modeling is a prerequisite. Accurate modeling involves understanding the important relationships between the physical world and the analytical simulation. As Clough states, “Depending on the validity of the assumptions made in reducing the physical problem to a numerical algorithm, the computer output may provide a detailed picture of the true physical behavior or it may not even remotely resemble it” [11]. The following sections attempt to expose the gap between physical and analytical behavior.

#### 3.1.1 General Modeling Requirements

The finite element method is an approximate technique, and as such, results computed using the finite element method must be critically evaluated before relied upon in a design application [46]. This process of critical evaluation involves several steps for any structure being analyzed.

The number of elements used in a model can greatly affect the accuracy of the solution. In general, as the number of elements, or the fineness of the mesh, is increased, the accuracy of the model increases as well. As multiple models are created with an increasingly finer mesh, the results should converge to the correct numerical solution such that a significant increase in the number of elements produces an insignificant change in a particular response quantity.

Not all response quantities will converge at the same rate, however. Displacements will generally be the most accurate response quantity computed and will converge faster than stresses, with the exception of some elements derived with hybrid stress formulations,

in which case the stresses can converge at the same rate or higher than the displacements. Generally, however, convergence of displacements does not guarantee convergence of stresses since stresses are computed as derivatives of the displacement field. Furthermore, it may be necessary to increase the number of elements in areas of the model near either concentrated loads or boundary conditions, where the stress gradient is steeper.

The type of element applied in the analysis also can significantly affect the quality of the results because various finite elements are derived from different assumptions. Since flat plate systems are modeled using plate bending elements, this discussion will be limited to several types of plate bending elements. For instance, Kirchoff plate elements are derived for application to thin plates and only account for flexural deformation. “Thin” generally refers to a plate with thickness much smaller than its in-plane dimensions [47]. Mindlin plate elements are derived for application to moderately thick plates and account for both flexural and shear deformations. Generally, a “thick” plate is one with a thickness greater than one-tenth the span of the plate [47]. If an engineer used a Kirchoff element to analyze a moderately thick plate, the results could deviate significantly from the physical behavior of the real plate, as the Kirchoff element can only represent flexural deformation while the physical structure is exhibiting significant shear deformation, behavior represented by the Mindlin element. There are numerous other examples similar to this one that demonstrate the importance of selecting an element appropriate to the specific application of the analytical model. Elements with higher order shape functions are more accurate than those with lower, and elements with midside nodes are generally more accurate than those without.

Finally, once an engineer is confident that the numerical solution has converged and that the specific element chosen is appropriate for the current application, several other checks are necessary to validate the analysis. The sum of reactions of the model should be verified with hand calculations. The magnitude of global displacements should be checked and verified to be small with respect to the geometry of the structure. The equilibrium of the structure must be verified, as the finite element method does not guarantee that this important condition is satisfied.

Once these criteria have been satisfied, it is important to determine if the results roughly

follow the expected outcome. “The engineer must determine whether or not the results make physical sense” [70]. Contour plots of stresses and the displaced shape of the structure should roughly correspond to the intuitive sense of the engineer. For example, symmetric results must accompany a structure with symmetric geometry and symmetric loading. Any deviation between expected and computed results must be critically investigated.

### **3.1.2 Assumptions in Reinforced Concrete Flat Plate Finite Element Analysis**

Several important assumptions are invoked in the analysis of reinforced concrete flat plates. Understanding these assumptions is critical if accurate design results are to be obtained.

First of all, the type of analysis applied in this study is a linear elastic analysis. This introduces several important factors into the analysis. Reinforced concrete is a highly nonlinear material. Made up of many elastic, brittle materials, the stress-strain curve of concrete indicates some degree of ductility. This is due to the gradual development of micro-cracking, internal to the concrete [49].

Concrete begins cracking at a tensile stress of approximately 8 to 15% of its compressive strength [51]. While ultimately this cracking is indicative of a brittle failure mode, the reinforcing bars within the cross-section will begin yielding and introduce important ductility to the failure of the component. At the ultimate level, ACI 318 states that the maximum allowable strain at the extreme concrete compression fiber shall be assumed equal to 0.003 [2]. This limiting value of compressive strain corresponds to the lower bound of experimental test data [49]. A linear elastic analysis does not account for any of the above nonlinear failure components. Instead, this analysis assumes the gross section is resisting the applied loads at all stress levels, and that the stress-strain relationship is perfectly linear, even if the compressive strain in the concrete exceeds 0.003 or if the tensile stress at the location of the reinforcing bars exceeds the yield stress of the steel.

There are several methods that can be applied to effectively reduce the stiffness of the finite element mesh in areas where cracking and highly nonlinear behavior are expected. One technique is to reduce the thickness of the elements in the areas around columns or supports. Another technique is to reduce the elastic modulus in these areas. While these

methods may produce favorable results from an analysis perspective, they would be invalid in an implemented program procedure where the thickness and elastic modulus are used internally to the program for design calculations. In other words, the section must be designed for the full thickness, not a reduced thickness; likewise for the elastic modulus. As such, these techniques are not investigated in this study.

Another important assumption in finite element analysis is that the material is isotropic and homogeneous. To the contrary, reinforced concrete is a highly composite material. Plain concrete consists of many materials, primarily various aggregates, bound in a matrix of cement. Aggregates range in size from roughly graded gravel to very fine sands. Experimental tests show that plain concrete can be treated as statistically homogeneous. However, the introduction of reinforcing bars disrupts the isotropy of the material, reducing the actual behavior of the material to orthotropic at best, and anisotropic in some cases. As such, the actual constructed concrete component will behave preferentially in some principle direction, and the relative stiffness due to this preferential material orientation will produce a distribution of stress much different from an analysis assuming isotropic conditions.

A third important assumption is that generally both Kirchoff and Mindlin plate bending elements are derived based on the assumptions of small displacements and rotations. The importance of this assumption is that it allows the application of a linear analysis that ignores geometric nonlinearity. The exact meaning of “small” is a matter of interpretation on the part of the engineer. However, in general the deflections are small if they are small in comparison to the thickness of the slab [67]. Nonetheless, the requirement of small deflections will usually be satisfied as a result of ACI 318 Section 9.5, “Control of Deflections” [2].

### **3.1.3 Modeling of Boundary Conditions for Flat Plate Systems**

The importance of accurately modeling boundary conditions should never be underestimated or neglected in the analysis of any structure, particularly reinforced concrete flat plates. Great efforts may be applied to verifying that a model has converged and that the specific element used is appropriate to the behavior required. However, if the boundary

conditions are inaccurate, the results of such an analysis may be worthless. There are several important considerations concerning the appropriateness of various techniques of modeling boundary conditions. The two types of boundary conditions presented in this discussion pertain to support boundary conditions as well as slab-to-column connection boundary conditions.

Two general methods are applied to simulate the boundary conditions of flat plates. In the first method, the columns supporting the slab, as well as the columns above the slab, are modeled using either frame elements or three-dimensional solid elements. This method attempts to isolate a particular elevated floor of the structure, but still account for the flexural effects of the columns framing into the floor. In the second method, the flat plate is modeled as a plane of finite elements, and the flexural and translational stiffnesses physically provided by columns are simplified to “pin” or “fixed” supports applied at the elevation of the plane of the slab. Sometimes these supports are modeled as springs with a finite elastic stiffness to improve the behavior of the model. The work of Gentry investigated which of these connections produce the most favorable results. He found that in general, modeled boundary conditions which account for the actual flexural stiffness of the columns, such as modeling the columns with frame members or three-dimensional solids, are preferable to approximations of the columns with pin or fixed supports at the mid-surface elevation of the slab [29]. Based on Gentry’s work, only frame members or three-dimensional solids will be used for column modeling in this study. The following considerations are important to remember when applying these various boundary condition techniques.

First of all, to re-emphasize the concepts presented in Section 3.1.2, the finite element model assumes that the material behaves in a linear elastic fashion. While this is generally untrue in a physical sense, it is especially untrue for connections in flat plates between the slab and columns [56]. These regions are often susceptible to cracking and subsequent yielding of reinforcement, leading to highly nonlinear behavior. Even if the slab is modeled as being supported on frame members, a fully fixed connection in the model dictates that the angle between the column and the slab remain exactly 90 degrees after deformation. This idealization overestimates the stiffness of this connection. An overestimation of stiffness

leads to a change in the relative stiffness throughout the slab, thus significantly decreasing the accurate representation of the physical distribution of stress in the slab.

Another important consideration involving boundary conditions is the physical size of the connection versus that incorporated in the model. When a frame member is connected to a node in the finite element plane, the connection occurs over an infinitesimal area, even though the physical connection maintains some finite size. This is significant for several reasons. First of all, an infinitesimal connection analytically increases the clear span between adjacent columns by a distance equal to the width of the column. The moments computed across a slab section are a function of the square of the clear span. Thus, application of this technique overestimates the bending moments in the adjacent slab panels. Second, design moments at the column face will be inaccurate because the distance between the centroid of the column and the column face is now flexible, according to the stiffness of the slab, when it should be much stiffer since this area is enclosed within the column. Third, a concentrated boundary condition, such as column connected via a single node, causes the same result that any concentrated effect in a finite element model produces: an unrealistic stress concentration. In fact, the analytical solution will indicate a state of infinite stress at locations such as this.

The finite element model will produce more realistic results if the column-to-slab connection can be distributed over some finite number of nodes instead of concentrating the effect at a single node. The first step in modeling the finite slab-to-column connection is to model the slab with a fine enough mesh that multiple elements cover the cross-section of the attached column. This will usually require a mesh fine enough that the column area is overlaid with either a 2x2 or 3x3 mesh of elements, assuming that the overall model converges with this degree of fineness.

After the flat plate mesh satisfies this requirement, there are several techniques to distribute the connection over the entire area of the column. The most accurate means of accomplishing this connection is to model the columns using three-dimensional solid elements. These elements can easily be connected to the plate bending mesh over the entire area of the column, as shown in Figure 3.1. The primary drawback to this method is



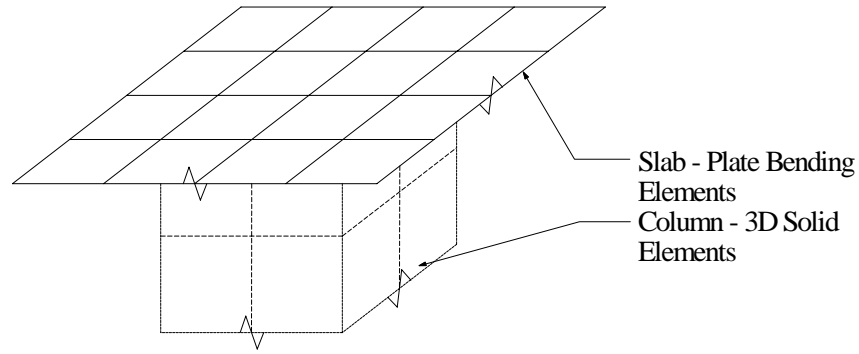


**Figure 3.1:** 3D Solid Slab-to-Column Connection Detail

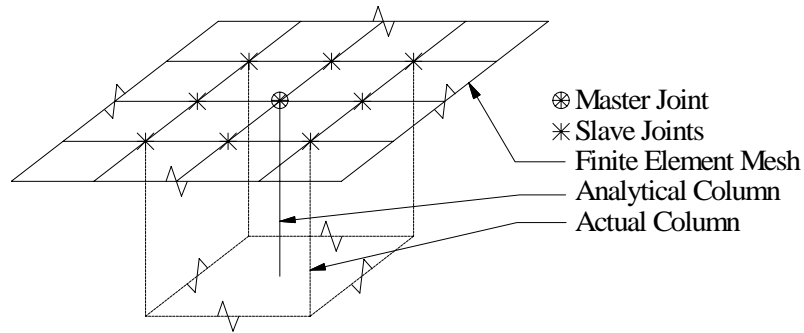


**Figure 3.2:** Master-Slave Slab-to-Column Connection Detail

that the computational and modeling costs of implementing such a large number of three-dimensional solid elements are often uneconomical and impractical.

Another technique is to approximate the finite area of the column using joint constraints. Using this technique, the columns are modeled using three-dimensional frame members, and each frame member is geometrically placed according to the centroid of the column in the physical structure. A rigid solid is then created at the column-to-slab connection to rigidly tie all joints within the area of the column section to the end of the frame member. This technique is otherwise referred to as a master-slave technique, where the end of the frame member column is the master joint, and the joints in the slab within the column area are slaves, as shown in Figure 3.2. This technique offers an advantage over the use of three-dimensional solids with respect to computational efficiency. Numerical studies presented in Chapter 6 will show that this technique is effectively equivalent to the use of three-dimensional solids in terms of the accuracy of computed bending moments.

## 3.2 Techniques for Flat Plate Design Using FEA Results

Assuming that adequate care has been applied in the modeling of the flat plate system, there are two conventional methods for design based on the results of finite element analysis, each of which are presented and evaluated below. These two methods are:

1. Design using average stress resultants
2. Design using element forces

### 3.2.1 Design Using Average Stress Resultants

#### 3.2.1.1 Computation of Element Stress Resultants

Element stress resultants are the computed stress components per unit width located at a node of a finite element. For a plate bending analysis, the primary element stress resultants of interest are the bending stress resultants, which are the bending moments per unit width evaluated at each node of the element, and the shear stress resultants, which are the shear forces per unit width evaluated at each node.

Element stresses can be computed in many locations throughout the element, including the centroid, Gaussian quadrature integration points, and at the nodes. Stresses computed at the integration points are generally considered to be the most accurate [17]. These results are of little use to engineers, however, because the physical locations of the Gauss points are unknown to the user. A common solution to this problem is to extrapolate the stresses to the nodes, a more useful location for the user. Element stresses can also be computed directly at the nodes by evaluating the strain-displacement relation at the nodes instead of the integration points, and then applying the material constitutive relation.

The element stress resultants can be understood as the integration of the stress field over the thickness of the element,  $t$ . The following equations show the theoretical formulation of the element stress resultants at a typical node [17].

$$M_{xx} = \int_{-t/2}^{t/2} \sigma_x z dx \quad M_{yy} = \int_{-t/2}^{t/2} \sigma_y z dx \quad M_{xy} = \int_{-t/2}^{t/2} \tau_{xy} z dx \quad (3.1)$$

$$Q_x = \int_{-t/2}^{t/2} \tau_{zx} dx \quad Q_y = \int_{-t/2}^{t/2} \tau_{yz} dx \quad (3.2)$$

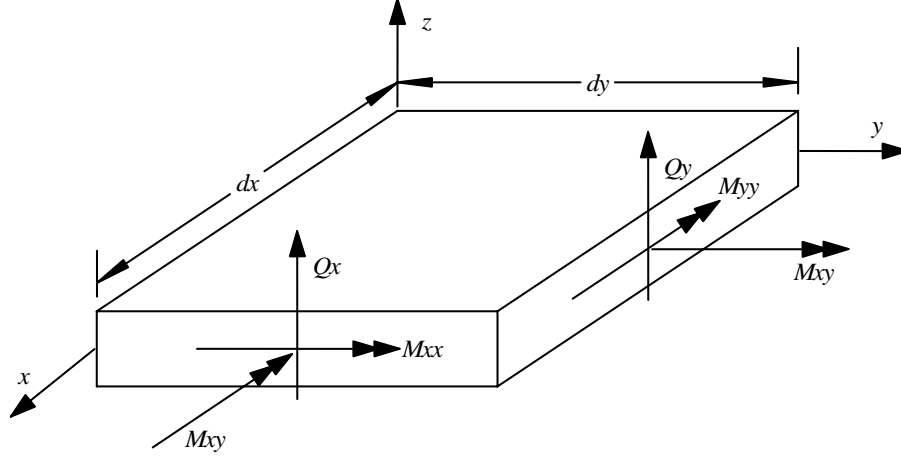


**Figure 3.3:** Element Stress Resultants at a Node

Here, the  $z$ -axis is the direction perpendicular to the plane of the elements. A common point of misinterpretation on the part of the engineer concerns the coordinate system of the results of Equation 3.1.  $M_{xx}$  refers to a bending moment on the  $x$ -face of a small volume of the element  $dV$  at a particular node, due to stress in the  $x$ -direction. Note that  $M_{xx}$  is not a bending moment about the  $x$ -axis.  $M_{yy}$  refers to a bending moment on the  $y$ -face of a small volume of the element  $dV$  at a particular node, due to stress in the  $y$ -direction.  $M_{xy}$  refers to a torsional moment on both the  $x$ - and  $y$ -faces of a small volume of the element  $dV$  at a particular node, due to the shear stress at the particular node. Figure 3.3 presents a visual representation of this concept. The units of each of the bending moment resultants are force-length/length. An easy way to remember the naming convention when applying these results in design is to say that  $M_{xx}$  is used to compute the reinforcing bars required in the  $x$ -direction, and  $M_{yy}$  is used to compute the reinforcing bars required in the  $y$ -direction.

In implemented finite element analysis codes, element stress resultants are seldom computed by integrating the stress field because the moment-curvature relations can be directly applied to the strain field. For a Kirchoff element, the moment resultants can be computed directly using Equation 3.3 [17].

$$\begin{Bmatrix} M_{xx} \\ M_{yy} \\ M_{xy} \end{Bmatrix} = - \begin{bmatrix} D & \nu D & 0 \\ \nu D & D & 0 \\ 0 & 0 & \frac{(1-\nu)D}{2} \end{bmatrix} \begin{Bmatrix} w_{,xx} \\ w_{,yy} \\ 2w_{,xy} \end{Bmatrix} \quad (3.3)$$

In Equation 3.3,  $w$  is the normal displacement,  $\nu$  is Poisson's Ratio, and  $D$  is known as the *flexural rigidity* and is given by Equation 3.4.

$$D = \frac{Et^3}{12(1 - \nu^2)} \quad (3.4)$$

The shear resultants cannot be directly evaluated using the Kirchoff formulation, however. Instead, these results are computed by evaluating the equilibrium of the element. Thus,  $Q_x$  and  $Q_y$  can be computed using Equation 3.5 [67].

$$Q_x = \frac{\partial M_{yx}}{\partial y} + \frac{\partial M_{xx}}{\partial x} \quad Q_y = \frac{\partial M_{yy}}{\partial y} - \frac{\partial M_{xy}}{\partial x} \quad (3.5)$$

For the Kirchoff element, the accuracy of  $Q_x$  and  $Q_y$  will generally be less than that of the bending stress resultants because, as shown in Equation 3.5, an additional derivative is required to compute this response quantity.

For Mindlin elements, the bending moment resultants are computed using the exact formulation as that for the Kirchoff element. However, because the Mindlin element has the ability to represent transverse shear strain through the element thickness, the shear resultants can be computed directly from the strain field. Equation 3.6 shows the formulation of element stress resultants for a Mindlin element [17].

$$\begin{Bmatrix} M_{xx} \\ M_{yy} \\ M_{xy} \\ Q_x \\ Q_y \end{Bmatrix} = - \begin{bmatrix} D & \nu D & 0 & 0 & 0 \\ \nu D & D & 0 & 0 & 0 \\ 0 & 0 & \frac{(1-\nu)D}{2} & 0 & 0 \\ 0 & 0 & 0 & kGt & 0 \\ 0 & 0 & 0 & 0 & kGt \end{bmatrix} \begin{Bmatrix} \psi_{x,x} \\ \psi_{y,y} \\ \psi_{x,y} + \psi_{y,x} \\ \psi_x - w_{,x} \\ \psi_y - w_{,y} \end{Bmatrix} \quad (3.6)$$

In Equation 3.6,  $G$  is the shear modulus,  $\psi_x$  and  $\psi_y$  refer to the rotation of the mid-surface normals at the node, and  $k$  accounts for the parabolic variation of transverse shear stress in the  $z$ -direction. Generally,  $k = 5/6$  for an assumed homogenous plate [17].

Once element stress resultants have been computed at each node of each element in the structure, there is no guarantee that for nodes with multiple elements connected, the element stresses computed at the node from contributing elements will be identical. This is because the finite element method only guarantees compatibility of the displacements and

rotations at the nodes. Thus, if four elements are connected to a single node, it is likely that four different states of stress have been computed at that node from each element. As the finite element solution converges, these results should approach each other, but even in a converged solution, there is no guarantee that these results will all lie within a small tolerance. If these results vary by more than an order of magnitude, further investigation is required as to the source of the discrepancy.

As a solution to the variation in stresses computed at a node, most programs average the stresses computed at a node to effectively smooth the solution of the stress field. Thus, an acceptable convergence criterion is to assess whether the average element stresses have converged. If so, the analyst may proceed with design, understanding that each element contributes a different stress component to each node and that, as such, compatibility of stresses is not satisfied.

Another important consideration in the computation of element stresses is that there is no guarantee that equilibrium is satisfied. Since stresses are only computed at the nodes, if an engineer wishes to consider the equilibrium of a single element, or the entire structure for that matter, the stresses must be interpolated between nodes. The physical distribution of stress will seldom be accurately predicted by such an interpolation procedure. This does not mean that the solution is altogether invalid, but rather that the engineer must understand that the applied technique is an approximate one, and that the resulting design should be critically evaluated, as described in the introduction of this chapter.

### *3.2.1.2 Design Procedure Using Bending Moment Resultants*

Once the average element bending moment resultants have been computed for each node in the structure, the engineer must reduce this information to something useful for design. The first step is to divide the finite element mesh into strips, similar to those in either direct design or the equivalent frame method, which will bound the basic cross-sections, or cuts, to be designed. This is most easily accomplished by generating contour plots of the three bending moment resultants. Contour plots are useful because they provide an overview of the distribution of moment in the slab, making it easy to see not only the areas of high

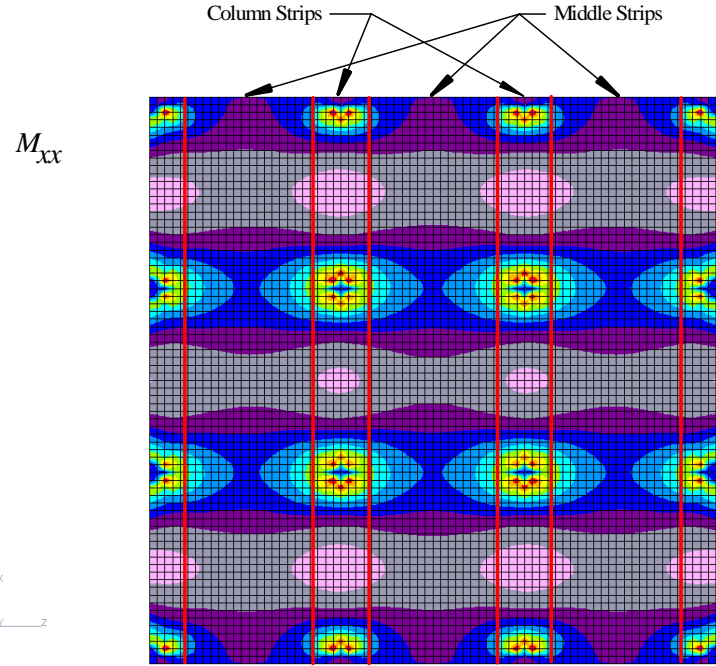


**Figure 3.4:** X-Direction Strip Selection Based on  $M_{xx}$  Contour Plot

concentration, but also the inflection points where the moment changes from positive to negative. An example of selecting strip locations based on a bending resultant contour plot is shown in Figure 3.4. “Narrow” strips should be used in areas with a high stress gradient, whereas “wider” strips can be used in areas with little variation in moment [43]. What constitutes “narrow” or “wide” is subjective and can only be determined with experience and expertise in modeling. One applicable guideline is that the width of a strip should always be narrower than the dimensions of the adjacent bays. Another critical guideline is that a strip should never represent a change in sign of bending moment across a cross-section to be designed. If the moment changes signs across the cross-section, the cross-section is too wide and must be reduced.

Once an adequate layout of strips has been determined, there are two methodologies for determining the design moments for a particular cross-section of a strip, or cut. A cut represents a free body upon which a resultant moment is computed for design. One methodology for computing this design moment is to average the results of each node along the cut. This method assumes it is possible at some locations along the cut that the capacity

provided by the reinforcement will be exceeded, but that when this occurs, these areas will crack and thus the moments will redistribute to areas that were over-reinforced initially. The second methodology is to design a whole cut for the maximum effect present on that cut. In this method, it is likely that more reinforcement will be provided than necessary, leading to an uneconomical design as well as a decrease in ductility of the section. In this study, the first methodology is applied: design based on average results along the cut.

### 3.2.1.3 Computation of Design Moments Using Bending Moment Resultants

The actual computation of design moments using bending moment resultants is attributed to Wood [72] and Armer [4]. At a particular node to be designed, the slab must be reinforced in the  $x$ - and  $y$ -directions to resist bending about both  $x$ - and  $y$ -axes. The capacity to be resisted by bars in the  $x$ -direction is  $M_{rx}$ , and the capacity to be resisted by bars in the  $y$ -direction is  $M_{ry}$ . Initially,  $M_{rx}$  appears to be the same as  $M_{xx}$ , and  $M_{ry}$  the same as  $M_{yy}$ . However, this neglects the effect of the computed torsional resultant  $M_{xy}$ . From Figure 3.3, it is readily apparent that as  $dA$  becomes very small,  $M_{xy}$  acts simultaneously with both  $M_{xx}$  and  $M_{yy}$ . Because the shear stress,  $\tau_{xy}$ , in the slab acts effectively without sign, the effect of  $M_{xy}$  is to always increase the magnitude of moment to be designed.

Based on these concepts, reinforcement at the bottom of the slab in both directions must be designed to provide positive bending moment resistance of

$$M_{rx} = M_{xx} + |M_{xy}| \quad \text{and} \quad M_{ry} = M_{yy} + |M_{xy}| \quad (3.7)$$

If the required positive moment capacity computed using either of these equations is negative, the capacity for that component should be set equal to zero. Subsequently, reinforcement at the top of the slab in both directions must be designed to provide negative bending moment resistance of

$$M_{rx} = M_{xx} - |M_{xy}| \quad \text{and} \quad M_{ry} = M_{yy} - |M_{xy}| \quad (3.8)$$

If the required negative moment capacity computed using either of these equations is positive, the capacity for that component should be set equal to zero [27].

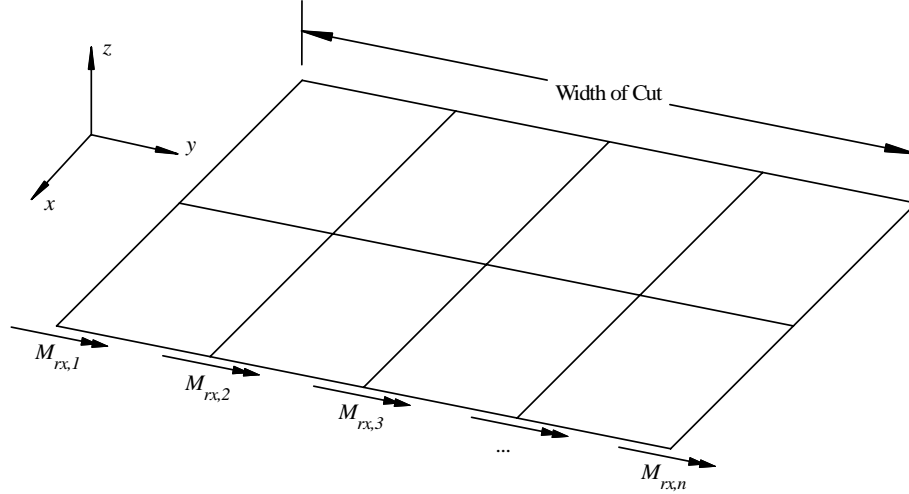


**Figure 3.5:** Average Bending Moment Resultants at Each Node Along Cut

Using the procedure set forth in Section 3.2.1.2 above, the resultant design moment across the section can be determined. An example cut is shown in Figure 3.5 to illustrate computation of the resultant moment for the design of reinforcement in the  $x$ -direction. The average bending resultants at each node,  $M_{rx,1}$  through  $M_{rx,n}$ , are computed using Equations 3.7 and 3.8, where  $n$  refers to the number of nodes along the cross-sectional cut. The total resultant moment acting on the cut,  $M_B$ , is then computed as

$$M_B = \frac{1}{n} \left\{ \sum_{i=1}^n M_{rx,i} \right\} \cdot (\text{Width of Cut}) \quad (3.9)$$

In this equation, the average moment resultants from each node,  $M_{rx,i}$ , are averaged and then multiplied by the width of the cut to compute the entire resultant moment acting on the cross-section [29]. Once the resultant design moment has been computed, flexural reinforcement is designed according to ACI 318 as explained in Section 2.1. The resultant bending moment for the design of reinforcement in the  $y$ -direction is similarly computed using Equation 3.9 by replacing  $M_{rx,i}$  with  $M_{ry,i}$ .

### 3.2.2 Design Using Element Forces

#### 3.2.2.1 Computation of Element Forces

Element forces are computed quite differently from element stresses, and can be computed directly from the displacement field without evaluation of the strain field. Element forces



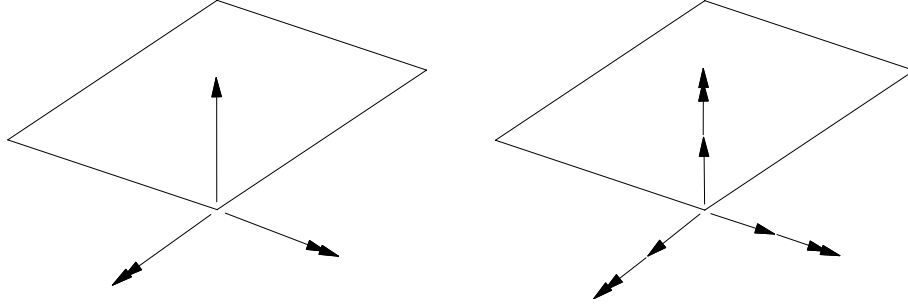


**Figure 3.6:** Element Forces at a Node (a) Plate Bending Element (b) Plate Element  
 (Note: Forces shown with single arrow-head. Moments shown with double arrow-head.)

are computed as the product of the element stiffness matrix with the element displacement vector, which is extracted from the global displacements. The results of this computation are forces and moments computed at each node. For general plate bending elements, this procedure computes three components: one shear force perpendicular to the plane of the elements, and two orthogonal bending moments in the plane of the element. For a general plate element, also known as a stretching and bending element, six orthogonal force components are computed: two in-plane forces, an out-of-plane shear force, a moment perpendicular to the plane of the elements, and two bending moments in the plane of the cut. These components are shown in Figure 3.6.

### 3.2.2.2 Computation of Resultant Design Moment Using Element Forces

Once element forces have been computed at each node for each element, the resultant forces acting along a cross-sectional cut are easily computed. Let a cut be defined by a linear list of joints. Then, the computed element forces at each node along that cut are simply summed. In-plane torsional effects are neglected in the computation of the resultant bending moment. Note that for some nodes along a cut, more than one element contributes to this resultant computation. Thus, the resultant bending moment across the section,  $M_B$ , is computed as

$$M_B = \sum_{i=1}^n \sum_{k=1}^m M_{i,k} \quad (3.10)$$

where  $n$  is the number nodes along the cut,  $m$  is the number of elements contributing force components at node  $n$ , and  $M_{i,k}$  is the moment component contributed at node  $i$  from element  $k$ . This concept is expressed graphically in Figure 3.7.

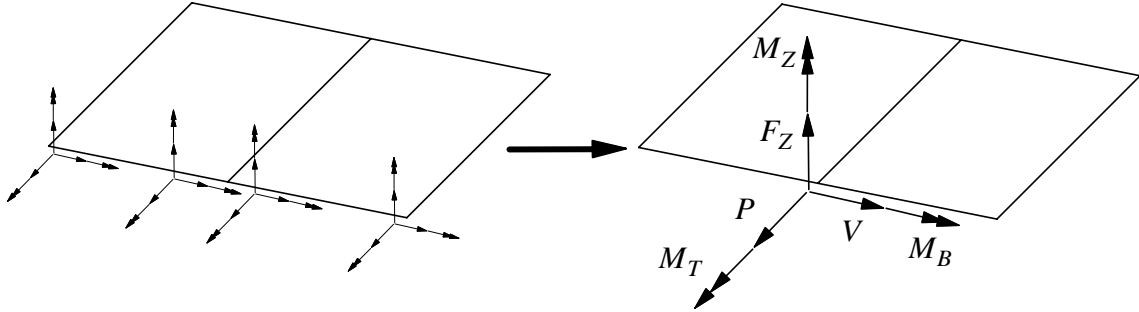


**Figure 3.7:** Element Force Resultant From Nodal Forces Along a Cut

Once the resultant bending moment acting on the cut has been computed, flexural steel reinforcement for the cross section is designed according to ACI 318 as explained in Section 2.1.

### 3.2.2.3 Comments on Design Using Element Forces

Previous work by Gentry indicates that designs using element forces produce areas of reinforcement closely matching those of the equivalent frame technique for interior panels of simple, regular structures. He states, “It would seem that element forces better predict the actual bending moments in the plate ... For total steel placed in the plate, element forces were more accurate than average stress resultants” [29]. The extension for using element forces to design exterior panels is presented in Chapter 5.

One of the most important characteristics of element force results is that equilibrium is preserved because forces are computed directly from element stiffnesses. As stated previously, element stress resultants do not always share this characteristic. Therefore, if an engineer chooses to design based on element forces, he knows that although the finite element technique produces an approximate solution, the computed solution satisfies equilibrium [3].

Another important characteristic of element force based design is that the application of this method is much simpler than that of element stress resultants. With element forces, the computation of the resultant moment along a cross section requires a simple summation. With element stress resultants, the average resultant must be computed from each contributing node, and then this average resultant must be scaled by the width of the cross section, introducing further approximation to an already approximate result. The use of

element forces reduces this interpolative step from the design procedure, requiring less time and reducing the opportunity for mistakes.

## CHAPTER IV

### IMPLEMENTATION OF PROCEDURE

The objective of this chapter is to present in detail the reinforced concrete flat plate design procedure implemented in GT STRUDL. A background of program development in GT STRUDL is presented, and then the algorithm is explained, including the user options and command, information pre-processing, computation of resultant forces, and design procedure.

#### 4.1 Programming Introduction

##### 4.1.1 Overview of Algorithm

The goal of the implemented procedure is to design reinforced concrete flat plate systems using finite elements as a tool for the determination of design moments. The algorithm implemented in this study is intended to simplify the procedure presented in Chapter 3 to design based on element force results.

Instead of dealing with results on an element-by-element basis, the user will be able to design slab systems based on cuts. Here, the term *cut* refers to the cross-section of a strip at a particular location to be designed. A cut is defined by two nodes identifying the start and end of the cut, and by an element in the plane of the cut.

Once the definition of the cut has been determined, the resultant forces along the cut are computed using element force results. The final design moment is determined by computing the resultant moment on each side of the cut for each loading condition, and reducing these moments to a design envelope.

Once the design envelope is computed, the cross-section is designed either “from scratch,” or with certain design parameters, such as bar size or spacing, constrained.

An important distinction is to note that each cut is designed independently from all other cuts. That is, a cut specified in one region is independent with respect to a design in

another region. As such, if the user wishes to use the same bar size over multiple adjacent cuts, this information must be specified for each cut.

Descriptions of each subroutine in the implemented algorithm are given in Appendix B.

#### **4.1.2 Overview of GT STRUDL**

The computational algorithm presented in this chapter is implemented as a sub-program in GT STRUDL. GT STRUDL, which stands for “Georgia Tech Structural Design Language”, is a computer aided structural engineering information processing software system designed to aid engineers in the process of structural analysis and design [13].

GT STRUDL contains both a powerful command-driven environment as well as a user-friendly graphical user interface. The command environment allows the engineer to communicate with the application via conventional structural engineering terminology. Commands may be selected from menus, or they may be typed directly into the interface or input file. The graphical interface allows the user to visually create the structural geometry, member and element topology, properties, boundary conditions, material characteristics, loading conditions, and other important model characteristics [15].

GT STRUDL maintains a broad range of finite element capabilities for solving a variety of two- and three-dimensional linear and non-linear elastic continuum problems, both for static as well as dynamic systems. The extensive element library contains multiple formulations of the commonly applied finite element types, including plane stress, plane strain, plate bending, shell, and three-dimensional solids, and allows for problems containing combinations of these element types. Finite elements may be modeled with isotropic or anisotropic materials, and be subjected to thermal, surface, edge, and body loading conditions. Powerful post-processing options of the finite element results include graphical visualization of the displaced shape, contour plots of stresses, strains, stress resultants, failure/yield criterion, and error estimation, and animation of the displaced shape under various loading conditions [13].

### 4.1.3 Tools Used

The flat plate design procedure was implemented using two tools developed by the GTICES Systems Laboratory: CDL and ICETLAN.

A new user command was developed using “Command Design Language”, or CDL. CDL allows for simple communication of information and control between the user and the application in a format that is logical and intuitive to the engineer, yet robust and capable of transmitting complex data [30].

The primary flat plate design algorithm called as a result of the user command was developed using the ICETLAN language. ICETLAN is an extension to FORTRAN 77 that provides extended array, module, and secondary storage management [30].

The program was developed on a Dell Inspiron 8600 notebook PC, with a 1.6 GHz Intel Pentium M processor and 768 MB of RAM. The WATCOM FORTRAN and C/C++ compilers were used to develop the application.

## 4.2 Model Requirements

Before the user can begin the design of flat plate reinforced concrete systems using the presented application, there are several modeling prerequisites that must be completed. It is assumed that the engineer has created a model that accurately simulates the physical behavior of the system, as described in Chapter 3.

First of all, the user must have specified the elements modeling the slab to be reinforced concrete. This is accomplished simply by the command, MATERIAL REINFORCED CONCRETE [14]. This will allow the user to specify the appropriate compressive strength of the material as well as the yield strength of the steel reinforcement.

Second, a stiffness analysis must be carried out before the slab can be designed. If a stiffness analysis has not occurred, there will be no results with which to design. This analysis is carried out in GT STRUDL via the command, STIFFNESS ANALYSIS.

## 4.3 Command

A user begins design of flat plates by means of typing a command while in the Command Environment of GT STRUDL. The following sections explain the options and syntax of this command.

### 4.3.1 Overview of User Options

The implemented command allows the user to communicate all data necessary for design to the application. The application processes this information and generates a design for the system based on the input. The command is designed to provide varying levels of control for the user so as to make the command as broadly applicable as possible.

The first information the user must communicate to the application is the cut definition. A cut is defined by a start and end node ID, and an element ID in the plane of the cut. The user has the option of giving each cut an alphanumeric name for organizational purposes. The purpose of the required element ID is to determine the appropriate plane to design in the event that multiple planes of finite elements intersect along the cut, as defined by the start and end node. An example where this might occur is the intersection of a slab with a shear wall. In this case, a misleading design could be generated if the slab was designed using the forces in the shear wall. The cut definition constitutes all information required to compute the resultant forces acting along the cut.

Once the cut has been defined, the user may indicate parameters to be used to design the system. The user may constrain the bar size or spacing to a certain value, either for the top face, bottom face, or for both faces. In this case, the final design will utilize the information provided. If the bar size is constrained, the appropriate spacing of bars is determined. If the bar spacing is constrained, the appropriate bar size is determined. In the case that the user supplies a bar size and spacing for the cut, the application will simply check the strength of the cross-section against the computed design envelope according to ACI 318. If the user specifies no design constraints, the application assumes a bar size and designs the section to satisfy ACI 318. As such, the user maintains explicit control over the function of the application.

The user may also specify which layer of bars to be designed and concrete cover. If neither are specified, default values are applied as explained in the following sections. All user-specified constraints, such as concrete compressive strength, yield strength, cover, and spacing are checked against ACI minimum/maximum values. The thickness of the cross-section is determined internally based on the modeled thickness of the user-specified element.

The DESIGN SLAB command is implemented in files DES.cdl and CRSLAB.cdl.

### 4.3.2 Command Syntax

The command implemented in GT STRUDL is of the following form:

$$\begin{aligned} \text{DESIGN SLAB (REINFORCEMENT) (ALONG) (CUT } & \left. \begin{array}{c} \text{'a'} \\ i_1 \end{array} \right) \left\{ \begin{array}{c} \text{JOINTS} \\ \text{NODES} \end{array} \right\} list_1 - \\ & \text{ELEMENT } list_2 \left\{ \begin{array}{c} \text{TOP (FACE) (BARS } i_2 \text{) (SPACING } v_1 \text{)} \\ \text{BOTTOM (FACE) (BARS } i_3 \text{) (SPACING } v_2 \text{)} \\ \text{BOTH (FACES) (BARS } i_4 \text{) (SPACING } v_3 \text{)} \end{array} \right\} - \\ & \left\{ \begin{array}{c} \text{OUTER (LAYER )} \\ \rightarrow \text{INNER (LAYER )} \end{array} \right\} (\text{COVER } v_4) (\text{TOLERANCE } v_5) - \\ & (\text{TORSIONAL (MOMENT) (WARNING) } v_6) \end{aligned}$$

In this command, the input arguments are subject to the following descriptions.

- 'a' or  $i_1$  = optional alphanumeric or integer cut name
- $list_1$  = list of start and end nodes of cut
- $list_2$  = alphanumeric or integer ID of element in plane of cut
- $i_2$  = integer bar size to be used to design top surface
- $i_3$  = integer bar size to be used to design bottom surface
- $i_4$  = integer bar size to be used to design both surfaces
- $v_1$  = bar spacing to be used to design top surface
- $v_2$  = bar spacing to be used to design bottom surface



$v_3$	=	bar spacing to be used to design both surfaces
$v_4$	=	minimum concrete cover
$v_5$	=	linear tolerance for cut definition
$v_6$	=	ratio of torsional moment to bending moment warning threshold
TOP	=	surface with $+Z^{PLANAR}$ coordinate
BOTTOM	=	surface with $-Z^{PLANAR}$ coordinate

### 4.3.3 Explanation of Command

#### 4.3.3.1 Command Description Conventions

In the above commands, the subtleties of the presented syntax are important. Each word given in the command is called a *modifier*. Only the portion of the modifier that is underlined in the command is required to indicate that modifier. As such, to denote the modifier “DESIGN”, the user need only type “DES”. Any modifier given in parentheses, ( ), is optional and is not required for the command to operate correctly. For optional input data, if the modifier is not supplied by the user, the default value will be used. Curved brackets, { }, indicate that only one choice of the command elements within the brackets must be given. As an example in the above commands, the user may type either “JOINTS” or “NODES”, but not both, to indicate the list of nodes. An asterisk before curved brackets, \*{ }, indicates that one, or multiple, choices of the command elements within the brackets can be given. As an example from the above commands, the user may specify data for the top face and then immediately specify data for the bottom face. An arrow ( $\rightarrow$ ) indicates the default choice for an optional command. Thus, if the user does not specify which layer to design, the inner layer is designed as the default option. Input arguments of the form  $i_n$  refer to  $n^{th}$  integer input value, and arguments of the form  $v_n$  refer to the  $n^{th}$  decimal input value [12].

#### 4.3.3.2 Example Commands

The following commands are examples of appropriate syntax conforming to the above rules.

1. “DESIGN SLAB NODES 1 2 ELEMENT 1” – This example indicates that the slab

cross-section starts at node 1, ends at node 2, and element 1 defines the plane of the slab. Default values are applied for all other design parameters, and reinforcement for the cross-section is designed “from scratch”.

2. “DESIGN SLAB REINFORCEMENT ALONG CUT ‘A1’ JOINTS 1 2 ELEMENT 1 BOTH FACES BAR 5 SPACING 12.5 COVER 1.0” – This example indicates that a slab cross-section labeled ‘A1’ is defined to start at node 1, end at node 2, and only elements in the plane of element 1 are to be considered. Top and bottom reinforcement is constrained to #5 bars at a spacing of 12.5 inches, such that the cross-section is checked against the design envelope. A value of 1.0 inches is used for cover, instead of the default 0.75 inches.
3. “DESIGN SLAB REINFORCEMENT NODES 1 2 ELEMENT 1 TOP FACE BAR 5 BOTTOM FACE SPACING 10” – This example gives the same cut definition as the previous example. Top reinforcement is constrained to #5 bars, and bottom reinforcement is constrained to a spacing of 10 inches. As such, spacing is computed for top reinforcement, and a bar size is determined for bottom reinforcement.
4. “DESIGN SLAB REINFORCEMENT NODES 1 2 ELEMENT 1 OUTER LAYER TORSIONAL MOMENT WARNING 0.25” – The cut definition provided is again the same as the previous example. Neither a bar size nor spacing is specified for either face. The user indicates that the reinforcement is to be located at the outer layer, and that a warning should be issued if the resultant torsional moment computed on the cross-section exceeds 25% of the resultant bending moment.
5. “DES SLAB JOI 1 2 ELE 1 BOTH BAR 5 SPA 12.5 COV 1.0” – This example command provides identical functionality as the second example command given above, and is intended to illustrate the abbreviated syntax of the command.

#### *4.3.3.3 Default Values*

Default values are applicable to only the design parameters. If the user provides no bar size to use for design, the program assumes #5 (M16) bars. In this case, no bar spacing

is assumed, but rather the spacing is computed as a function of the bar size. The default reinforcement yield stress,  $f_y$ , is 60,000 psi, and a user-specified yield stress may not exceed 80,000 psi [2]. The default minimum concrete cover is 0.75 inches per ACI 318-02 [2]. The default cut tolerance value is a relative tolerance computed as 0.1% of the length from the start node of the cut to the end node. For example, if the cut is 100 inches from start node to end node, all other joints along with cut must lie within a distance of 0.1 inches from the cut to be considered to lie on the cut. The default torsional moment warning threshold is 10%.

## 4.4 Pre-Processing

After the command has been processed from the user, a pre-processing algorithm uses the input data to build all of the information necessary to compute the resultant forces acting on the cut. The pre-processor was implemented in a general form that is not specific to flat plates with the intention that the process could easily be extended to the design of other reinforced concrete components, such as shear walls or shells, in the future. The components of the pre-processor are described in the following sections.

### 4.4.1 Determination of Cut Definition

The first step in the pre-processor is to fully define the cut. While the user only needs to supply the start and end node of a cut, the application must find all joints lying on a straight line between the start and end node to define the cut. In the implemented procedure, this process is accomplished in the subroutine CRCCGL.ice.

For the following formulation, let  $P_1$  refer to the start node of the cut, and  $P_2$  the end node of the cut. Also, let  $(x_1, y_1, z_1)$  be the global coordinates of  $P_1$  and  $(x_2, y_2, z_2)$  be the global coordinates of  $P_2$ . Let  $P_c$ , located at  $(x_c, y_c, z_c)$ , be a candidate node (hence the subscript  $c$ ) for inclusion in the cut definition.

In order to find the nodes on the line between the start and end node of the cut, the first step is to loop over all nodes in the structure. Only nodes with coordinates bounded by the region between  $P_1$  and  $P_2$  are considered as candidates for nodes on the cut. That is,  $x_c$  must be located between  $x_1$  and  $x_2$ ,  $y_c$  must be located between  $y_1$  and  $y_2$ , and  $z_c$

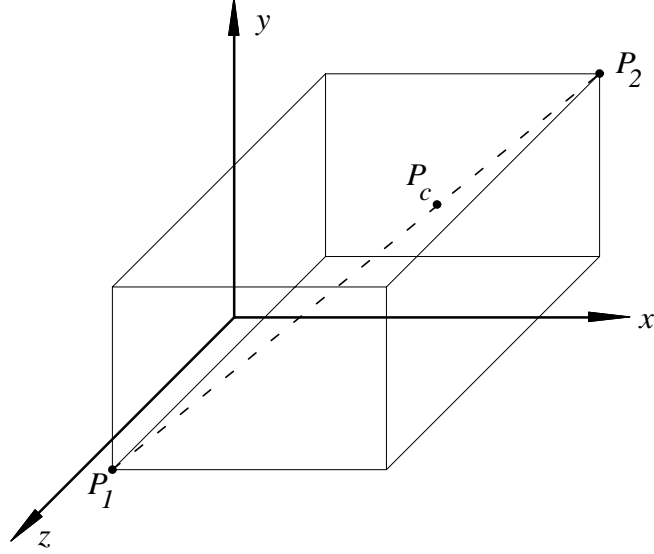


**Figure 4.1:** Bounded Region Between Start and End Node of Cut

must be located between  $z_1$  and  $z_2$ . This concept of the *bounded region* is illustrated in Figure 4.1. This check is imposed to increase the efficiency of the numerical algorithm by reducing the number of operations.

Once the candidate node,  $P_c$ , has been determined to be inside the bounded region, it is checked to determine if it is *collinear* with the start and end nodes of the cut,  $P_1$  and  $P_2$ . A direct way of checking if the three points are collinear is to check if the projections of the lines formed by the three points onto each global plane are collinear. Thus, the projection onto the  $X^G - Y^G$  plane must be collinear, the projection onto the  $Y^G - Z^G$  plane must be collinear, and the projection onto the  $X^G - Z^G$  plane must be collinear. The expression used to verify the collinearity of three points in a plane is given by Equation 4.1 in which case the three coordinates are collinear if the given determinant is equal to zero [74].

$$\begin{vmatrix} x_1 & y_1 & 1 \\ x_2 & y_2 & 1 \\ x_c & y_c & 1 \end{vmatrix} = 0 \quad (4.1)$$

In the form given, Equation 4.1 determines the collinearity of the three points in the  $X^G - Y^G$  plane. The arguments of this equation are easily modified to check the collinearity of the three coordinates in the  $Y^G - Z^G$  and  $X^G - Z^G$  planes. If a set of coordinates satisfies the

collinearity requirements for all three global planes,  $P_c$  is added to the cut definition. All joints in the structure within the bounded region are checked for collinearity with the start and end node of the cut using this procedure.

#### 4.4.2 Formulation of Cut Coordinate System

Once all nodes on the cut have been determined, a new coordinate system can be defined specific to the cut. This system is referred to as the *cut* system, and the axes are denoted  $X^{cut}$ ,  $Y^{cut}$ , and  $Z^{cut}$ . The cut system is important for determining which elements to include in the computation of resultant forces as well as for interpreting the signs of computed results. In the implemented procedure, the transformation to the cut system is computed in the subroutine CRCCTN.ice.

The cut system is a derivative of the planar coordinate system, which must be the same for all elements located in a plane. To understand the formulation of the cut system, the planar system and its determination will be explained. Let the planar coordinate system be denoted  $X^P$ ,  $Y^P$ , and  $Z^P$ . Furthermore, the planar coordinate system is a derivative of the element local coordinate system, denoted  $X^L$ ,  $Y^L$ , and  $Z^L$ , and the global coordinate system, denoted  $X^G$ ,  $Y^G$ , and  $Z^G$ .

Each two-dimensional element in a structural model can have a unique local coordinate system. The  $Z^L$  axis is determined by applying the right hand rule to the order in which the nodes were specified. Thus, the  $Z^L$  axis is always normal to the plane. For an element viewed in plan, if the nodes are specified counterclockwise order, the  $Z^L$  axis is oriented out of the plane, whereas if the nodes are specified in clockwise order, the  $Z^L$  axis is oriented into the plane. The  $X^L$  axis is oriented from the first node to the second node in the element's node list. The  $Y^L$  axis is determined by the cross-product of the  $Z^L$  and  $X^L$  axes, such that  $Y^L = Z^L \times X^L$  [13].

All elements in a common plane share the same planar coordinate system. It is assumed that all elements in a common plane are oriented such that all share the same  $Z^L$  axis. Thus, all elements located in a common plane should be specified consistently with respect to the incidence order of the nodes. If the engineer does not check this, the model may

provide misleading results. The planar coordinate system is determined by the following rules. First of all, the  $Z^P$  axis is parallel to and oriented in the same direction as the  $Z^L$  axis of the elements in the plane. Second, the  $X^P$  axis is located along the line of intersection between the plane of the element and the  $X^G - Y^G$  plane, and is oriented such that its projection on the  $X^G$  axis is in the same direction as  $X^G$ . The  $Y^P$  axis is determined by the cross-product of the  $Z^P$  and  $X^P$  axes, such that  $Y^P = Z^P \times X^P$  [13].

To begin formulation of the cut system for a given cut, the start node of the cut,  $P_1$ , is assumed initially to be the origin of the cut system, and the  $X^{cut}$  axis is located longitudinally along the line connecting  $P_1$  to  $P_2$ .

The  $Z^{cut}$  axis is determined based on the transformation from the global to the planar system for the user-specified element in the command. The  $Z^{cut}$  axis is taken to be the same as the  $Z^P$  axis of the specified element, and is always normal to the plane of elements along the cut.

There are two cases that define the cut system: a general case and a special case. The special case refers to the scenario in which the  $X^{cut}$  axis is parallel to the  $Y^P$  axis. The general case refers to all other cases.

For the general case, the  $X^{cut}$  axis is oriented in the direction of increasing  $X^P$  coordinates. However, for the special case, the  $X^{cut}$  axis is oriented in the direction of decreasing  $Y^P$  coordinates. Figure 4.2 graphically shows the general and special cases of the cut system.

To construct these cases in the application, the first step is to compute the angle between the  $X^{cut}$  and  $Y^P$  axes to determine if the current cut definition is the special case. The angle between two lines in space with direction cosines  $(a_0, b_0, c_0)$  and  $(a_1, b_1, c_1)$  is given in Equation 4.2 [74].

$$\theta = \cos^{-1} \frac{a_0 a_1 + b_0 b_1 + c_0 c_1}{\sqrt{a_0^2 + b_0^2 + c_0^2} \sqrt{a_1^2 + b_1^2 + c_1^2}} \quad (4.2)$$

If the angle  $\theta$ , between  $X^{cut}$  and  $Y^P$ , is equal to either 0 or  $\pi$ , the current cut definition is the special case and  $X^{cut}$  must be oriented in the  $-Y^P$  direction.

If  $\theta \in (0, \pi)$ , the cut definition is the general case, and the  $X^{cut}$  axis is oriented in the

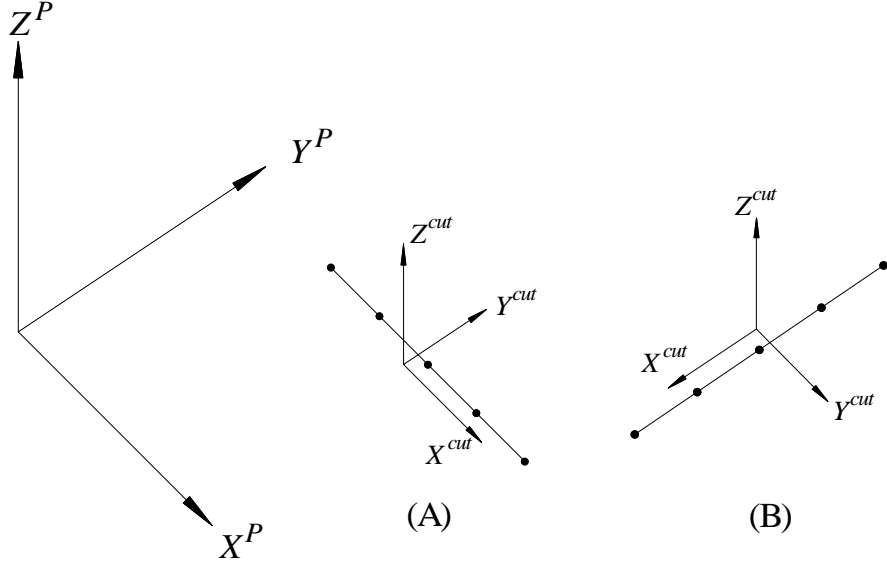


**Figure 4.2:** Cut Coordinate System: (A) General Case (B) Special Case

direction of increasing  $X^P$  coordinates. To check this, the angle between the  $X^{cut}$  and  $X^P$  is computed using Equation 4.2, and if  $\theta \geq \pi/2$ , the direction of  $X^{cut}$  is reversed.

Now that the  $X^{cut}$  and  $Z^{cut}$  axes have been determined, the  $Y^{cut}$  axis is computed using a right hand formulation such that  $Y^{cut} = Z^{cut} \times X^{cut}$ . In the final state,  $X^{cut}$  is collinear with the cut,  $Y^{cut}$  is normal to the cut in the plane of the cut, and  $Z^{cut}$  is normal to the cut out of the plane of the elements along the cut.

The transformation from the global coordinate system to the cut system,  $T_{global \rightarrow cut}$ , is then formed using the normalized direction cosines of the axes of the cut coordinate system. This transformation is given in Equation 4.3, where  $X_1^{cut}$ ,  $X_2^{cut}$ , and  $X_3^{cut}$  are the direction cosines of the  $X^{cut}$  axis, and so on.

$$T_{global \rightarrow cut} = \begin{bmatrix} X_1^{cut} & X_2^{cut} & X_3^{cut} \\ Y_1^{cut} & Y_2^{cut} & Y_3^{cut} \\ Z_1^{cut} & Z_2^{cut} & Z_3^{cut} \end{bmatrix} \quad (4.3)$$

Equation 4.3 is applied to a set of coordinates in the global system to compute the cut

coordinates of a node according to Equation 4.4.

$$\begin{Bmatrix} x^{cut} \\ y^{cut} \\ z^{cut} \end{Bmatrix} = T_{global \rightarrow cut} \begin{Bmatrix} x^G \\ y^G \\ z^G \end{Bmatrix} \quad (4.4)$$

#### 4.4.3 Element Selection Procedure

The design forces for the slab cross-section will eventually be designed based on single element force results that contribute to the forces and moments acting on the cut. In order for these results to be computed, the application must determine which elements should be included in this computation and which should be excluded. In the application, this is accomplished in subroutine CRCCGE.ice. So far, the only information the application has about the topology of the cut are the nodes collinear with the cut, and a single element in the plane of the cut.

The primary goal of the element selection algorithm is that equilibrium be preserved for a given layout of cuts. Another way of saying this is that element forces at one node of an element typically should not contribute to the resultant force for more than one cut. If this occurred, the procedure would account for portions of the loading twice, and thus the total sum forces that the structure was designed to resist will not agree with the global equilibrium of the system. Thus, the resulting design will not always be conservative.

To avoid this overestimation of design force as thoroughly as possible, a hierarchy of element selection rules was developed to determine the optimal configuration of elements to include in the cut definition. The applicability of a given finite element to the computation of resultant force is a function of the behavior of the element as well as geometric constraints related to the cut definition. As will be shown, this overestimation cannot be avoided for all cases, but it can be minimized for many.

The element selection algorithm, as explained in the following paragraphs, can be reduced to fifteen cases, each demonstrated in Figure 4.3. These cases indicate which elements are included in the cut definition.

The first step of the element selection procedure is to build a list of all elements connected



to the nodes forming the cut definition line. Each element in this list is a *candidate* for inclusion in the cut definition. At this point, this list may include truss or frame members, cable members, two-dimensional finite elements, and three-dimensional finite elements. All incident nodes of each attached “element” are assembled into a book-keeping array, and the coordinates of these nodes are transformed into the cut system using Equation 4.4. These coordinates are critical to the element selection algorithm.

Each attached element is then evaluated one by one to determine its applicability to the cut. The first check is to determine if the member is a finite element. If the attached element is a truss or frame member, it is neglected in the resultant computation. If the member is a finite element with two nodes, as in the case of a cable element, it is neglected in the resultant computation. In addition, if the element is three-dimensional, it is also excluded. Elements not eliminated thus far are either triangular or quadrilateral in shape.

Triangular elements are subject to the same selection rules as quadrilateral elements. Candidate elements include 3 node triangles, 6 node triangles, 4 node quadrilaterals, and 8 node quadrilaterals. Midside nodes are ignored in the selection rules such that the inclusion of an element is only a function of its corner nodes. The only restriction concerning midside nodes is that a cut may not originate nor terminate at a midside node. A graphical representation of cuts beginning or ending on a midside is shown in Figure 4.3, Cases 4, 6, and 12. If a cut is detected starting or ending on a midside node, an error message is printed and execution of the “DESIGN SLAB” command is ended.

The primary purpose of the element ID supplied by the user in the command environment is to indicate the plane of finite elements to consider for inclusion on the cut. A practical example of the importance of this is the case of a slab supported on a shear wall. If the specified slab design cut is coincident with the intersection of the slab and shear wall, the specified element indicates which plane corresponds to the slab and which corresponds to the shear wall, information the application cannot intuitively determine. As such, the  $z^{cut}$  coordinate of each node of each candidate element is checked. If an element contains any node where  $|z^{cut}| > 0$ , the element is not co-planar with the user-specified element and is neglected in the element force resultant computation.

After a candidate is determined to be an appropriate element in the plane of the cut, an element's inclusion in the cut definition is a function of the geometry of the corner nodes. The following rules apply to both triangular and quadrilateral elements.

If two corner nodes of a candidate element are co-incident on the cut line, the element is included in the cut definition. An element with two corner nodes on the cut will not be included in the cut definition for an adjacent, collinear cut, thus satisfying the equilibrium requirement explained above. The only stipulation for an element with two corner nodes incident on the cut is that the two corner nodes must be adjacent on the element boundary, i.e., the cut cannot cross over an element surface, but only along its edge. If the application detects a cut definition that traverses an element surface, an error message is printed and the command is aborted.

If a candidate element has only one node co-incident with the cut, the element may or may not be added to the cut definition depending on several stipulations. First of all, if the co-incident node is interior to the cut (i.e. neither the start nor end node of the cut), the element is added to the cut definition and used in the computation of the resultant moment.

If a candidate element with only one node co-incident with the cut is attached at either the start or end node of the cut, a more complicated system of logic is applied. The inclusion of such an element is a function of the geometric location of all nodes of the element with respect to *normals* at each end of the cut. These normals are located at the start and end of the cut, in the plane of the cut, parallel to the  $Y^{cut}$  axis. In Figure 4.3, the normals are indicated by section arrows. The linear tolerance specified by the user applies to the location of nodes with respect to the cut bounds as well. If the user does not specify a linear tolerance, the default value of 0.1% of the length of the cut is used.

If all nodes of the candidate element are located within the normals of the cut, the element is included in the cut definition. If all nodes of the element are located outside the normals of the cut, the element is excluded from the cut definition.

If a candidate element contains a combination of nodes within the bounds of the cut as well as outside the bounds of the cut, the element is included in the cut definition if no more than one node lies outside the bounding normals of the cut. This is most clearly expressed

by comparing the treatment of the quadrilateral element in Cases 14 and 15 of Figure 4.3. This selection rule insures that for quadrilateral elements at the cut boundary incident with only one node, adjacent cuts will not double-count the contribution of the elements on the edge.

This is not true for triangular elements, however, as evidenced by Case 8 of Figure 4.3. Triangular elements that overlap the cut bounds are always included in the cut definition, and when adjacent cuts are designed, the contribution of these elements will be accounted for twice. The magnitude of the effect this introduces to the final design results has not been investigated.

When an element is determined to belong to the cut definition, it is added to one of two arrays corresponding to elements on either the  $+Y^{cut}$  side of the cut or the  $-Y^{cut}$  side of the cut. The purpose of this separation of elements is explained in the following section.

The above discussion can be simplified to several selection rules. In summary, an element is included in the cut definition if:

1. The element is a 2-D *finite element* with more than 2 nodes.
2. The element is located in the plane of the cut.
3. The element only contains nodes on one side of the cut.
4. The element has two corner nodes located on the cut.
5. The element has only one corner node incident on the cut, and this node is not the start or end node of the cut.
6. The element has only one corner node incident on the cut, this node is the start or end node of the cut, and at least all but one of the corner nodes of the element are geometrically located within the normals at the cut bounds.

#### **4.4.4 User-Defined Element List**

In some cases, a user may require more explicit control over which elements are included in the cut definition and which are excluded. To accommodate this, the user is given the option to specify a full node list and full element list in the DESIGN SLAB command.

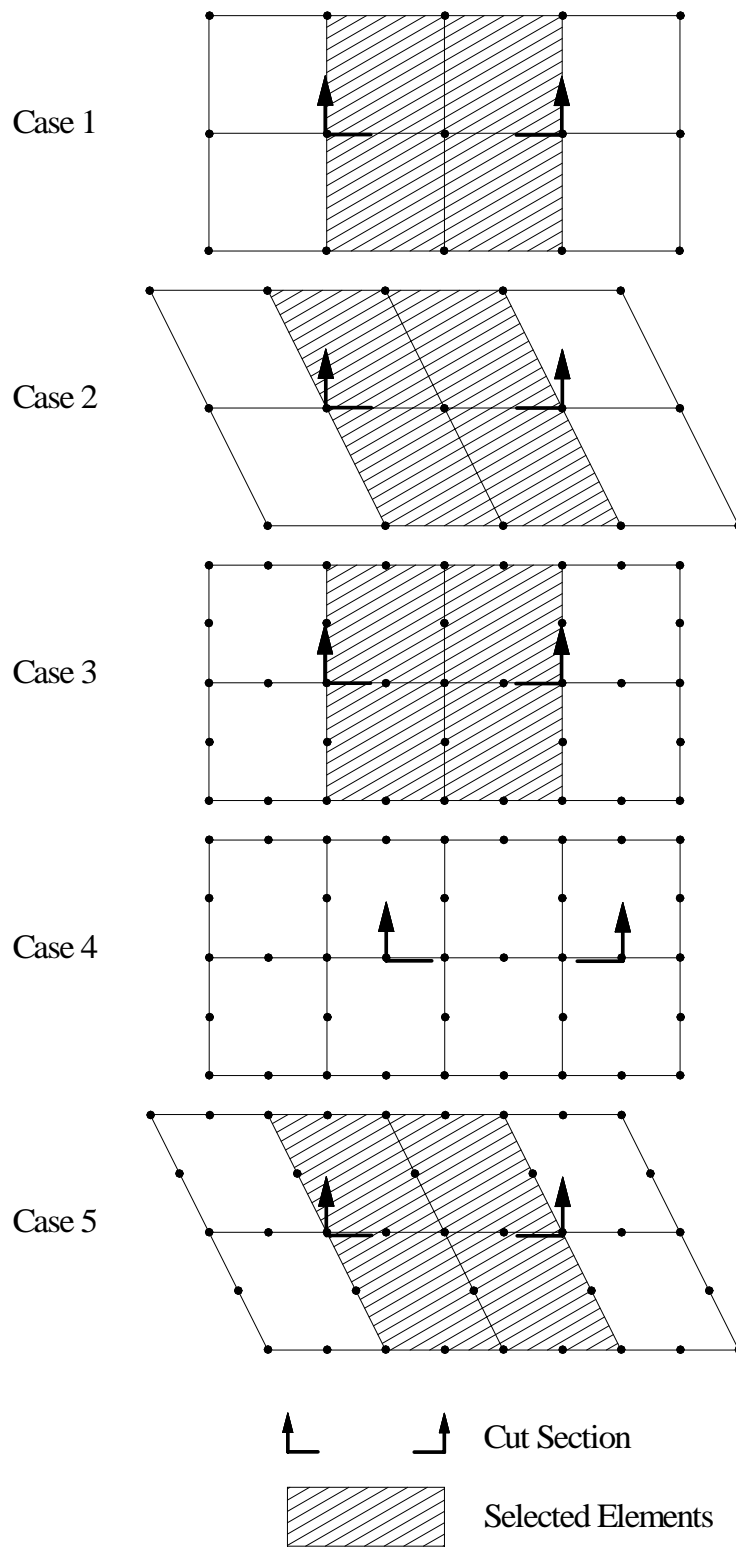


**Figure 4.3a:** Element Selection Cases 1-5 (Plan View)

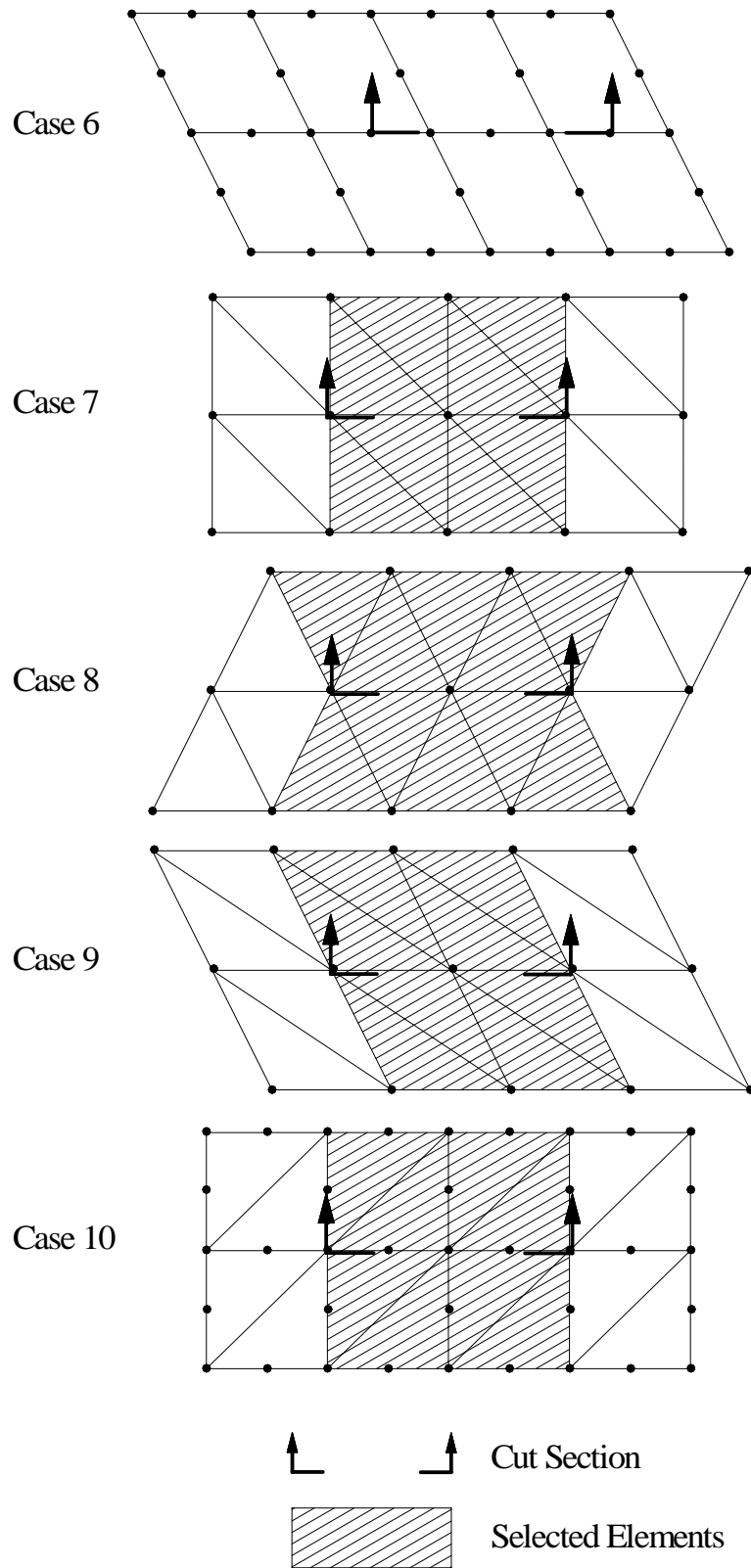


**Figure 4.3b:** Element Selection Cases 6-10 (Plan View)

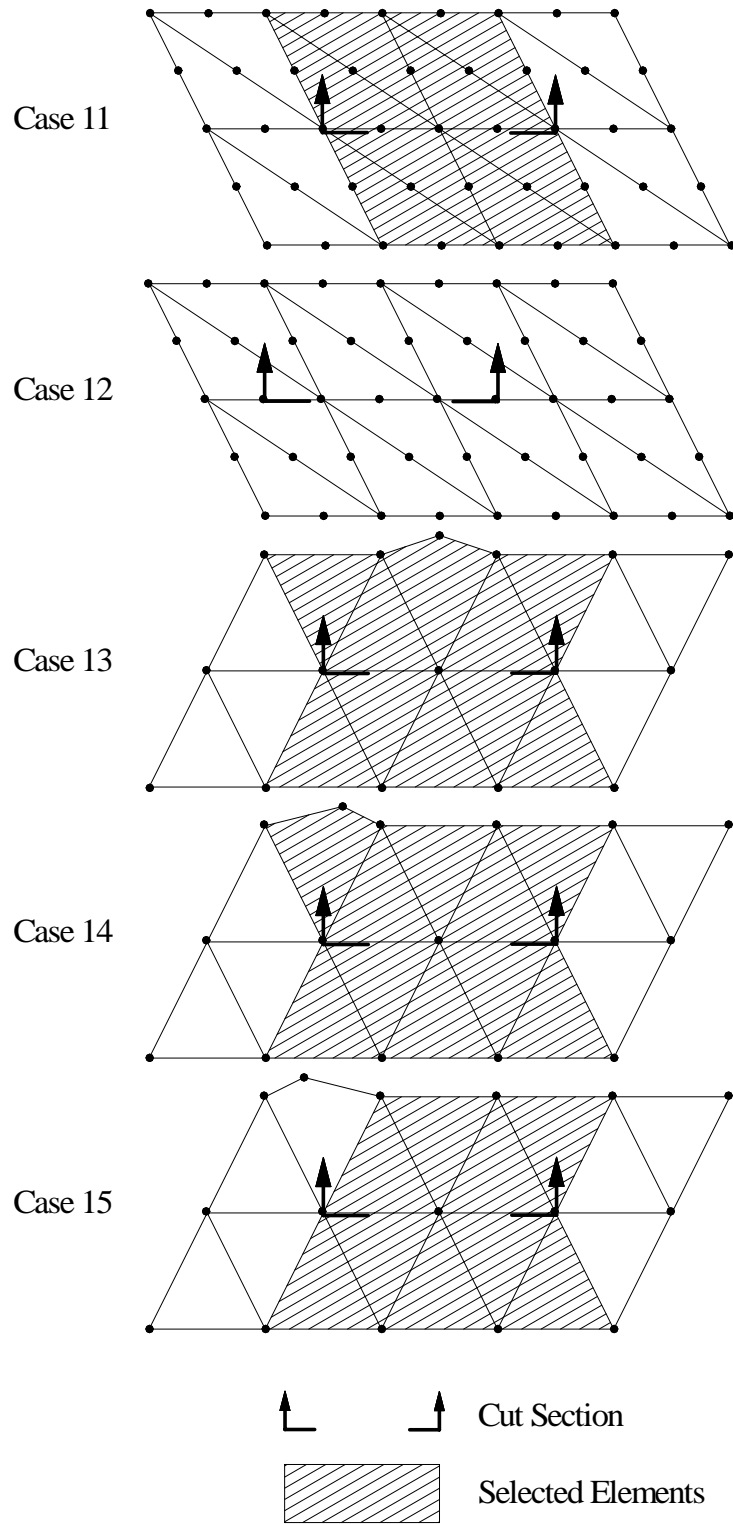


**Figure 4.3c:** Element Selection Cases 11-15 (Plan View)

This option is activated when the user specifies more than two nodes and more than one element in the command input. When the application detects this, the entire element selection procedure is bypassed, and the user-specified list is used. In this method, only the contribution of elements on *one* side of the cut is allowed.

#### **4.4.5 Contribution from Both Sides of Cut**

So far, finite elements have been added to the cut definition located on both sides of the cut. These elements will be used to compute the resultant forces on each side of the cut. This is an important point in the design procedure without which the design forces computed could possibly significantly misrepresent the actual behavior of the system.

The reason for this extra step is the possibility of a concentrated moment effect located along the cut line. The effect of this discontinuity is that the resultant forces computed on each side of the cut need not necessarily be the same. There are several ways this discontinuity could be introduced: an incident frame member such as a column, intersection with a shear wall that provides bending restraint, a transverse force applied at an eccentricity such as in the case of a crane rail, among others. It is possible that the discontinuity could be significant enough that the sign of the bending moment could reverse from one side of the cut to the other.

By computing the resultant forces on each side of the cut, the cross-section of the slab is then designed to resist the maximum effect on each side. In many cases, the effect on both sides will indeed be identical, but the algorithm will confirm, not assume, this to be true.

#### **4.4.6 Element Type Restrictions**

Only elements known to appropriately model the behavior of slab systems are allowed for inclusion in the computation of design forces. For a flat plate system, only plate bending and flat shell elements are used. Thus, if the user models the system using plane stress / plane strain elements, and then issues the “DESIGN SLAB” command, the algorithm recognizes that the modeled elements are not appropriate to the application, the user is warned, and the command is ignored.

Plate bending elements supported in the implemented command include the BPHT, BPR, BPHQ, CPT, and IPBQQ finite elements. General plate elements supported in the implemented command include the SBCT, SBCR, SBHQ, SBHQCSH, SBHT, SBHT6, AND SBHQ6 finite elements [13].

#### 4.4.7 Further Error Checking

A final set of error checking measures are applied to the elements included in the cut definition prior to computation of element force results. First of all, the element list is checked to determine that all elements included are of constant thickness. The slab design algorithm will not design a cross-section with varying thickness. The thickness of all included elements must match the thickness of the user-specified element in the command.

Second, material properties must be the same for all elements along the cut. Neither the modulus of elasticity, nor the concrete compressive strength,  $f'_c$ , may vary from that of the user-specified element in the command.

These error checking measures are implemented in subroutine CRCHEC.ice.

## 4.5 Computation of Resultant Forces Along Cut

The purpose of the pre-processor described in the previous section is to make all necessary preparations to compute resultant forces acting along the user-specified cut. In fact, the entire collection of information in the pre-processor is designed with an existing GT STRUDL command in mind, the *CALCULATE RESULTANT* command. The DESIGN SLAB command makes explicit calls to the subroutines within the *CALCULATE RESULTANT* command to compute the resultant forces in the flat plate system.

### 4.5.1 The *CALCULATE RESULTANT* Command

“The *CALCULATE RESULTANT* command computes resultant forces at the transformed-section geometric centroid of a cut. A ‘cut’ is defined as a combination of straight lines passing through nodes that belong to a series of adjacent, coplanar, PLANE STRESS/STRAIN, PLATE BENDING, or PLATE elements or the faces of TRIDIMENSIONAL finite elements” [13]. As such, the *CALCULATE RESULTANT* command is applicable in a broad



range of applications.

In this command, cuts need not consist of a single straight line. In fact, multiple straight line cuts can be combined to compute the resultant forces acting on a plane. Using this capability, an I- or T-beam could be modeled using finite elements, and the section forces at a given location could be computed over the I or T shape.

The required input for the `CALCULATE RESULTANT` command consists simply of a node list and an element list. The node list must include all nodes incident on the cut that the user wishes to utilize in the computation of forces. The element list must include all elements located on one side of the cut. Each node of the element incident on the cut must be included in the node list. If an element in the element list is not associated with at least one node in the node list, the element is ignored.

The `DESIGN SLAB` pre-processor automates this step by allowing a user to only specify the start/end nodes of the cut as well as an element in the plane, instead of supplying the entire node and element lists manually. As such, it takes no more appreciable time to design a cut across 50 elements than it does to design a cut across 5 elements. This presents a significant increase of efficiency for the handling of finite element analysis results.

#### **4.5.2 Computation of Design Forces**

The computation of resultant forces in the `CALCULATE RESULTANT` command is based on element force results. The procedure of the `CALCULATE RESULTANT` command is similar to that presented in Chapter 3.

The purpose of the node list and element list is to communicate to the application exactly which results should contribute to the resultant forces acting on the cut. Element forces are computed for each element in the element list, at each node in the node list. After the forces at each node along the cut are computed, the equilibrium of the cut is evaluated to compute the resultant forces and moments. Resultant forces are computed simply by summing the force components present at each node. Resultant moments are a function of not only the summation of moment contributions at each node, but also of nodal forces acting at a moment arm as computed from the geometric centroid of the cut.

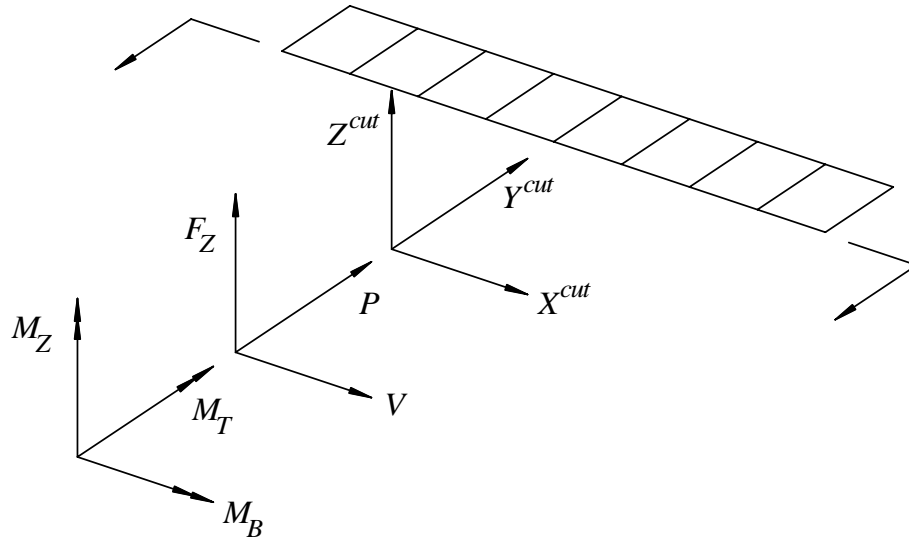


**Figure 4.4:** CALCULATE RESULTANT Command Results

Various resultants are computed based on the type of element used. These results are listed as follows:

- $P$  = in-plane force normal to cut
- $V$  = shear force parallel to cut
- $F_Z$  = transverse (out-of-plane) shear force
- $M_B$  = bending moment vector parallel to the cut
- $M_T$  = torsional in-plane moment perpendicular to cut
- $M_Z$  = rotational moment about out-of-plane axis

For plane stress/strain elements, only  $P$ ,  $V$ , and  $M_Z$  are computed. For plate bending elements, only  $F_z$ ,  $M_B$ , and  $M_T$  are computed. For general plate elements, all six result components are computed. The forces and moments reported act at the transformed section geometric centroid of the cut. Figure 4.4 shows the six resultants acting on a cut section.

### 4.5.3 Reduction of Multiple Load Cases to Design Envelope

In the CALCULATE RESULTANT command, the resultant forces acting on the cross-section are computed for each active loading condition. This includes single loading conditions as well as combinations of multiple loading conditions. The results of each loading

case are simply output to the GT STRUDL Output Window for the user to review.

In design, however, it is impractical to design each loading condition individually. Therefore, when the procedures in the CALCULATE RESULTANT command are called from the DESIGN SLAB command, the results from each loading condition are stored in an array. The application then scans the array to determine the maximum positive and negative bending moments developed from all of the active loading cases. These two bending moments define the *design envelope*. The cross-section is then designed only to resist the design envelope. It is assumed then that all other loading cases will be bounded by the provided design. If the DESIGN SLAB command was extended in the future to design prestressed systems, each load case would have to be considered independently.

Note that this reduction to a design envelope occurs for the element lists on both sides of the cut. The maximum effects from each side are determined and used for design of the section.

A limit of 1000 loading conditions has been placed on the DESIGN SLAB command. If the number of active loading conditions exceeds this value, the command is aborted and the user is instructed to reduce the number of active loading conditions to 1000 or less.

The design envelope is determined in subroutine CRCCEV.ice.

#### **4.5.4 Interpretation of Results**

The interpretation of design results from the CALCULATE RESULTANT command is a critical step in the DESIGN SLAB procedure. If the bending moment is misinterpreted, for instance, the slab will be reinforced on the compression face instead of the tension face, possibly leading to disastrous consequences.

The primary result of interest is the bending moment,  $M_B$ , as this value is used to design flexural reinforcement. The transverse shear,  $F_Z$ , is retained such that a shear check can be performed. The axial force,  $P$ , is retained (provided the element can represent in-plane effects). This value is not used explicitly in design. However, if the cross-section has a significant axial force resultant, it may indicate that the slab is in fact prestressed (perhaps if the user has modeled the system using the balanced load technique) or undergoing significant

membrane action. If either of these is true, the design procedure of the DESIGN SLAB command is not applicable. The application cannot always recognize when this is the case, however, so as a safety measure, the application issues a warning to the user if the cross-section has an axial stress greater than 10% of  $f'_c$  in compression or  $\sqrt{f'_c}$  in tension.

The resultant torsional moment,  $M_T$ , is not directly used in design, either. However, if  $M_T$  is greater than 10% of  $M_B$ , the resultant bending moment may be inappropriate for design, as demonstrated in Examples 4 and 5 of Chapter 5. The user is warned if the computed torsional moment exceeds either the default threshold or the ratio specified in the command. For flat plate design,  $V$  and  $M_Z$  are ignored.

Once the resultant bending moment has been computed, the orientation of this moment must be determined. In order to express the sign of this moment in a manner consistent with standard engineering terminology, a rule for defining the top and bottom of the slab must be introduced. Because the structural model is physically abstract with no knowledge of the orientation of gravity, the terms *up* and *down* are of irrelevance in terms of determining the direction of bending. Therefore, let the *top surface* of the slab refer to the face of the slab with largest positive  $Z^P$  coordinate, and the *bottom surface* refer to the face of the slab with the largest negative  $Z^P$  coordinate. Thus, the top and bottom surfaces are defined without respect to a *gravity* reference frame.

Based on this definition of *top* and *bottom*, the terms *positive bending* and *negative bending* can be defined. In the DESIGN SLAB command, *positive bending* occurs when the top surface is in compression and the bottom surface is in tension. Conversely, *negative bending* occurs when the top surface is in tension and the bottom surface is in compression. Figure 4.5 illustrates the case of *positive bending* for two different orientations of the  $Z^P$  axis. In this graphic, positive bending is defined independently from what a user might intuitively consider to be the top or bottom surface of the slab.

Since the results of the CALCULATE RESULTANT command are reported in the cut coordinate system, *positive* and *negative* bending must be interpreted in this system. As explained previously, the resultant forces and moments are computed on each side of the cut, and because equilibrium of the cut must be conserved, these results may be opposite

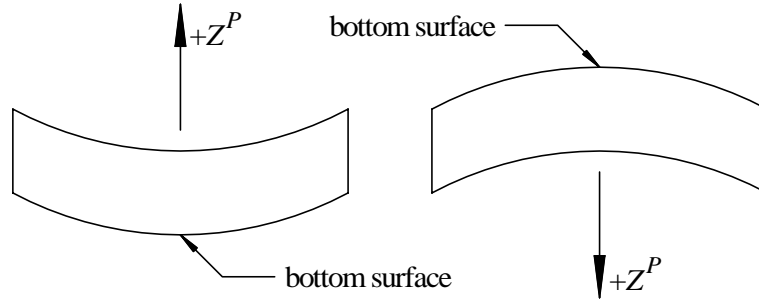


**Figure 4.5:** “Positive” Bending and Surface Naming Convention

in sign across the cut.

The key to the interpretation of CALCULATE RESULTANT results is Figure 4.4, where a general cut is shown, along with the cut coordinate system axes and force resultants. In this figure, the elements shown are located on the  $+Y^{cut}$  side of the cut. To comply with the sign convention presented in Figure 4.5, the sign of  $M_B$  must be reversed in order to produce a *positive* moment in the slab, where the top surface is in compression. However, due to the equilibrium of the forces acting on the cut, the resultant moment due to elements on the  $-Y^{cut}$  need not be reversed. Thus, these two moments, though effectively equal and opposite in the case where no concentrated loads are present, result in the same physical bending behavior although opposite in sign when initially computed.

CALCULATE RESULTANT results are interpreted in subroutine CRCCMN.ice.

## 4.6 Design Procedure

Now that the slab cross-section has been defined and the resultant forces acting on the cut have been computed, steel reinforcement must be designed to resist the design envelope. The cross-section in the flat plate is designed using the same general method as that in reinforced concrete beam design. A procedure to design reinforcement in strict conformity to the ACI requirements presented in Chapter 2 is described in the following sections.

The primary design algorithm is implemented in subroutine CRCSLB.ice.

## 4.6.1 Initial Design Processing

### 4.6.1.1 User Intent

The first step in the design procedure is to determine the design intention of the user. The DESIGN SLAB command was implemented in a manner as to provide the user varying degrees of control, in which case the user can constrain the bar size and spacing, the bar size or spacing, or neither the bar size nor spacing. Based on which input the user specifies, the algorithm determines the appropriate course of action.

For both top and bottom reinforcement, the user can specify any combination of bar sizes and spacing. If the user specifies a bar size or spacing for top and bottom bars separately, and then issues the BOTH FACES modifier followed by a bar size and spacing for both faces, the data specified after the BOTH FACES modifier replaces the data specified by either the TOP or BOTTOM modifiers, and a message reports this to the user.

If the BOTH modifier is not given, top and bottom reinforcement can be designed using different methods. For instance, top reinforcement may be designed with the spacing constrained to 12 inches and bottom reinforcement may be designed with the bar size constrained to #6 (M19) bars.

If the user specifies neither a bar size nor spacing for either face, the algorithm assumes an initial bar size of #5 (M16), and the both faces are designed accordingly.

### 4.6.1.2 Direction of Reinforcement

In the DESIGN SLAB command, reinforcing bars are designed perpendicular ( $\perp$ ) to the cut. In terms of the cut coordinate system, reinforcing bars are placed parallel ( $\parallel$ ) to the  $Y^{cut}$  axis and perpendicular ( $\perp$ ) to the  $X^{cut}$  axis. In the case of a skewed mesh, the reinforcement will often not be orthogonal to the planar axes, as shown in Figure 4.6.

The practical implication of this is that the user must create the finite element model with mesh lines that correspond not only to the locations of the intended cuts, but also perpendicular to the reinforcement direction. A future enhancement to the program may be to design reinforcement at an arbitrary angle with respect to the cut, as has been implemented previously in other studies [68].

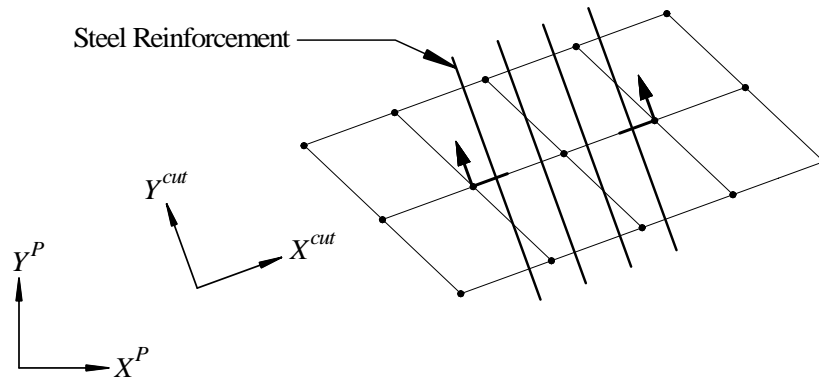


**Figure 4.6:** Direction of Reinforcing Bars for Non-Orthogonal Cut (Plan)

#### 4.6.1.3 Initial Design Calculations

Before the area of steel required can be computed, several parameters must be calculated.

First of all, the yield strain of the steel is computed based on the yield stress. The yield stress can be specified via the `CONSTANTS` command, otherwise the default value of 60,000 psi is used. By Hooke's Law, the yield strain of the steel is given by  $\epsilon_y = f_y/E$ .

The factor,  $\beta_1$ , is computed based on the compressive strength of the concrete,  $f'_c$ , and ranges from 0.65 to 0.85 per Section 2.1.2.1. This factor relates the depth of the assumed rectangular compression zone to the location of the neutral axis.

The depth of steel reinforcement must also be determined prior to the computation of area of steel required. Typically, a slab is reinforced in two orthogonal directions, and two directions of bars cannot occupy the same depth in the cross-section. Instead, these bars are placed on top of each other such that two layers of steel reinforcement are formed. This concept is demonstrated in Figure 4.7.

The user has the option in the `DESIGN SLAB` command to specify whether to design the interior layer or the exterior layer of reinforcement. When the user does not specify a layer, the `DESIGN SLAB` command is not aware of which layer is currently being designed, so it always assumes the distance to the interior layer. This assumption is conservative because the steel will be placed physically in the slab at a distance equal to this assumption or greater, such that the moment arm between this layer of reinforcement and the compression zone is never smaller than assumed. This assumption also assures that the physical strain

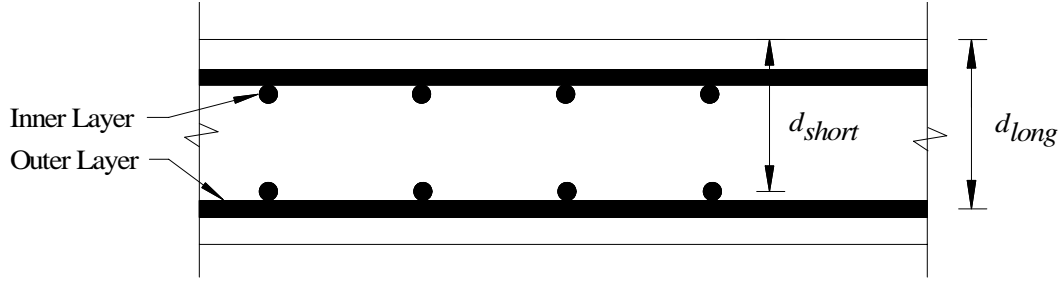


**Figure 4.7:** Slab Cross-Section:  $d$ -Distance

in the steel will be at least equal to the computed value as well.

The depth to the assumed location of the bars is given in Equations 4.5 and 4.6. The depth, either  $d_{short}$  or  $d_{long}$ , is a function of the slab thickness,  $t$ , the cover, the diameter of the bars being used,  $d_b$ , and is labeled in Figure 4.7.

$$d_{short} = t - cover - 1.5 \times d_b \quad (4.5)$$

$$d_{long} = t - cover - 0.5 \times d_b \quad (4.6)$$

If the user specifies to design the interior layer,  $d_{short}$  is used. If the user specifies to design the exterior layer,  $d_{long}$  is used.

The maximum and minimum spacing of reinforcement for the slab must be determined according to the rules presented in Chapter 2. First of all, the maximum center-to-center spacing is computed as the minimum of either 18 inches or two times the slab thickness. The minimum clear spacing between bars is set to 2.5 inches.

#### 4.6.1.4 Scope of Design

A flat plate system will not require reinforcement on both faces at all locations. Interpretation of the design envelope indicates which faces of the slab should be reinforced.

If both the positive ultimate moment and the negative ultimate moment are non-zero, both faces must be designed to resist flexure.

If the set of active loading cases only produces either positive or negative bending, only the face subject to tensile stress during bending must be designed. No reinforcement is required at the opposite face from a flexural perspective. Detailing requirements may



ultimately dictate bars must extend into this region based on continuity and cut-off length requirements, however.

If the envelope suggests that the section is subject neither to positive nor negative bending, the slab is designed with one layer of steel on the bottom surface to satisfy shrinkage and temperature requirements.

#### *4.6.1.5 Required Area of Steel*

In order to design steel reinforcement, the required steel to resist flexure is computed, along with the minimum flexural steel requirements and minimum shrinkage and temperature requirements.

The first computation in determination of the required steel area is the calculation of the area of reinforcement required to resist flexure. The area of flexural steel reinforcement required is computed for the cross-section using Equation 2.7. Here,  $\phi$  is initially assumed to equal 0.9 (for a tension-controlled section), and all other parameters are known. The discriminant of this quadratic equation must be checked to be greater than zero, or else a valid solution for the required steel area does not exist. After computing the area of steel, the depth of the compression block is computed using Equation 2.3. The depth to the neutral axis is computed then such that the strain in the steel can be determined by Equation 2.4. At this point, the assumption that the section is tension-controlled must be verified. If the strain in the steel is less than 0.005,  $\phi$  is decreased based on the strain and the area of steel is recomputed with Equation 2.7 using the new  $\phi$ -factor. This procedure must continue iteratively on  $\phi$  until  $A_s$  converges. In the implemented procedure, if the solution does not converge after 10 iterations, an error is issued to the user and the command is exited.

The minimum area of steel required to resist the effects of temperature and shrinkage is computed using Equation 2.21.

The required area of steel for design is taken as the greatest of these computed values.

#### 4.6.2 Check Specified Bar and Spacing

If a user has specified final bar size and spacing, the capacity of the section must be checked. The same procedure is applied to check a user-specified design via the command, as well as check the results of the DESIGN SLAB-generated designs where either the bar size, spacing, or neither is constrained.

The first step in the ultimate strength check is to compute the area of steel provided. The area of steel provided is simply the area of a single bar divided by the bar spacing to compute the area of steel per unit width, and then scaled by the width of the cross-section.

Next, the distance  $d_{short}$  must be modified to account for the diameter of the actual bar size provided. The depth of the compression block,  $a$ , is computed such that the location of the neutral axis, and thus strain in the steel,  $\epsilon_s$ , can be computed.

Based on the strain condition, the appropriate  $\phi$ -factor is determined, and the ultimate moment capacity is computed using Equation 2.5. The results of the ultimate strength check are reported to the user via the GT STRUDL Output Window.

#### 4.6.3 Design with No User Constraints

If the user specifies neither a bar size nor spacing in the DESIGN SLAB command, the algorithm essentially designs the section “from scratch.”

First of all, the algorithm initially assumes #5 (M16) bars for design. The area of steel per bar as well as the bar diameter are retrieved. Based on this information, the algorithm then determines the minimum number of bars required to collectively supply the computed area of steel required or greater. Based on the number of bars required, the center-to-center spacing of the bars is computed as the width of the slab cross-section divided by the number of bars. From this value, the clear spacing is calculated as the center-to-center spacing minus the width of one bar,  $d_b$ . Both center spacing and clear spacing are reported to the user in 0.5 inch increments, always rounded down. Thus, a computed spacing of 10.79 inches is replaced by the value 10.5 inches.

At this point, the center spacing is compared to the maximum allowable center-to-center spacing. If the center spacing exceeds the maximum, the bar size must be decreased

to generate a smaller spacing. If the clear spacing is smaller than the minimum allowable, the bar size must be increased, thus generating a larger spacing.

After each modification of bar size, the center and clear spacings are computed and checked against the maximum and minimum allowable requirements. If all bar sizes are checked and shown to provide unsatisfactory spacings, the user is issued an error message stating that the required reinforcement cannot be physically constructed due to geometric constraints.

Once a reinforcing solution has been determined, consisting of a bar size, number of bars, and spacing, the ultimate strength of the cross-section must be checked via the procedure described in Section 4.6.2.

#### **4.6.4 Design with Bar Size Constrained**

When the user specifies a bar size constraint but no spacing limitations, the procedure followed is similar to that of Section 4.6.3 with a few modifications.

Based on the specified bar size, both the center-to-center spacing and clear spacing are computed. These values are compared to the minimum and maximum spacing requirements. If the spacing computed satisfies the maximum and minimum requirements, the ultimate strength is checked as described in Section 4.6.2.

If the design spacing exceeds the maximum spacing requirements, the computed spacing is reduced to the maximum allowable spacing. This effectively increases the area of steel provided in the cross-section. At this point, the algorithm does not know if this will be an allowable design. Based on the new spacing, the strain in the steel at ultimate conditions must yield. If this does not occur, this technique will not produce a satisfactory design.

If the minimum spacing requirements are violated with the user-specified bar size, an error message is issued to the user stating that the requested reinforcement cannot be physically constructed due to geometric constraints.

Once a design has been determined, the ultimate strength must be checked using the procedure described above. The final bar size and spacing, along with the area of steel required per unit length, are output to the GT STRUDL Output Window.

#### 4.6.5 Design with Bar Spacing Constrained

Occasionally an engineer will wish to constrain the spacing of reinforcement in the slab. A scenario requiring such a technique may occur if the slab must have special openings for mechanical systems.

In this case, once the required area of steel is computed, the required area is divided by the width of the cross-section, and then scaled by the constrained spacing to determine the minimum area each bar must provide, assuming that the specified spacing satisfies the maximum and minimum spacing requirements described in Chapter 2. The list of available bar sizes are scanned to find the smallest bar satisfying the minimum area requirement. If the required area per bar is greater than that of standard bar sizes, the user is warned that a design using the specified spacing could not be determined.

If a satisfactory bar size is found, the ultimate strength of the provided design is checked using the procedure described in Section 4.6.2.

#### 4.6.6 Shear Check

As implemented, the procedure offers no provisions for the design of shear reinforcement. However, a simple check is provided to indicate the significance of any shear effects acting on the cross-section.

The check performed is the same as that applied to check the shear strength of a reinforced concrete beam without stirrups. The shear capacity is computed using Equation 2.10, and is compared with the ultimate shear, as determined from the CALCULATE RESULTANT command results.

Satisfaction of this check does not guarantee that punching shear and moment transfer shear have been satisfied throughout the system.

#### 4.6.7 Final Comments

The design procedures described are executed for both surfaces of the slab based on the user intent and design envelope. Once both designs have been completed, the results are presented to the user through the screen in *command mode*.

Because the results reported consist simply of a bar size and spacing for the top and bottom surfaces, the engineer must appropriately detail the system based on the full requirements explained in Chapter 2, including development length and continuity requirements.

Another important point is that because the design only accounts for flexural resistance, the engineer must determine independently that serviceability requirements are satisfied for the slab system. The benefit of a finite element-based design procedure is that the engineer will have already created a detailed analytical model of the system that can be used to evaluate deflections. However, these checks are not integrated into the DESIGN SLAB command because only local effects are known for a given cut.

## CHAPTER V

### RESULTS AND NUMERICAL STUDIES

The objective of this chapter is to validate the reinforced concrete flat plate design procedure implemented in GT STRUDL by means of several example problems and numerical studies. Examples presented include single-panel flat plate systems with various support conditions as well as multi-panel flat plate systems with regular and irregular column spacing.

#### 5.1 Example 1 - Convergence of Area of Steel

As stated in Chapter 3, in order for the finite element method to be used for design applications, careful steps must be followed in order to determine that the model accurately represents the physical behavior of the slab. One of the critical components in the validation process is to confirm that the final finite element model has converged, as explained in Section 3.1.1. In general, convergence is confirmed by systematically refining the mesh and tracking the changes in key response quantities. When the model has converged, a significant increase in the number of elements in the model results in an insignificant change in the desired response quantity.

In order to demonstrate the convergence of a flat plate system, a square, fix-supported flat plate was modeled. The geometry of this system is shown in Figure 5.1. The slab was 6 inches thick and was composed of 4000 psi reinforced concrete. The slab was subjected to its own self-weight as well as a 50 psf live load.

The slab was analyzed using four different models, each with an increasing number of finite elements. Each of these models are shown in Figure 5.2. The four meshes contained 16 elements (4x4 mesh), 64 elements (8x8 mesh), 256 elements (16x16 mesh), and 1024 elements (32x32 mesh), respectively. Fixed support conditions were achieved by restraining all translations and rotations for the joints along the boundaries. Each model used the BPR finite element in GT STRUDL, and was then re-analyzed using the BPHQ element [13].

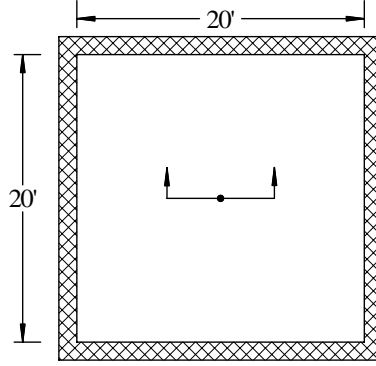


**Figure 5.1:** Example 1 - Geometry

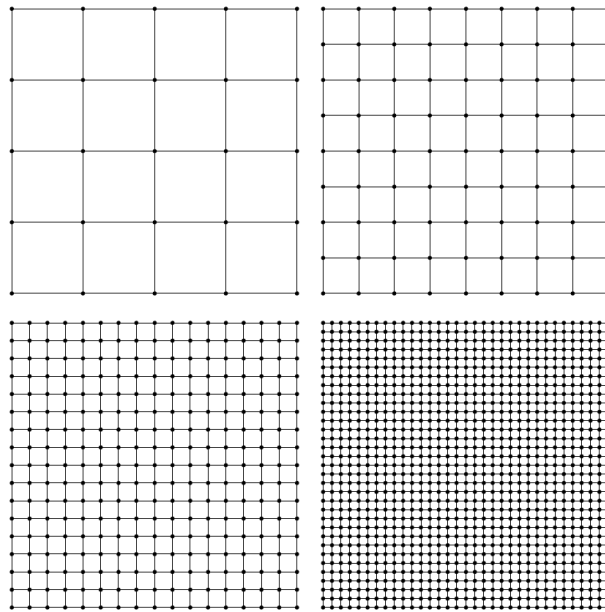


**Figure 5.2:** Example 1 - Finite Element Models

Note that in Example 2, the SBHQ6 finite element was used although the convergence of this element is not explicitly demonstrated in this example. The SBHQ6 is a shell element capable of representing stretching and bending action. In this element, the in-plane and plate bending components are uncoupled, and the plate bending formulation is exactly that of the BPHQ element [13]. As such, the SBHQ6 was not evaluated in this example as bending results obtained from this element would be identical to those obtained by the BPHQ element.

In each model, three key response quantities were examined. First of all, the transverse displacement at the center node; second, the bending moment acting on the cut shown in

**Table 5.1:** Example 1 - Computed Response Quantities

Element	# Elements	Center Displacement (in)	Design Moment (lb-in)	$A_{s,required}$ (in <sup>2</sup> )
BPR	16	-0.1032	146465.60	0.636
	64	-0.0965	172594.40	0.751
	256	-0.0945	178981.40	0.779
	1024	-0.0940	180499.00	0.786
BPHQ	16	-0.0919	148913.98	0.647
	64	-0.0920	170687.77	0.742
	256	-0.0939	178475.89	0.777
	1024	-0.0940	180446.98	0.785

Figure 5.1; and finally, the required area of steel along the cut as computed by the DESIGN SLAB command. The summary of these response quantities is presented in Table 5.1.

Not all of these response quantities converged at the same rate. For the center displacement and the required area of steel, the percent difference between each progressive mesh and the final converged solution were computed. The displacement computed using the 4x4 mesh was within 9.7% of the converged displacement solution computed using the 32x32 mesh. However, the area of steel computed using the 4x4 mesh was 19.1% less than the converged area of steel computed using the 32x32 mesh. Figure 5.3 graphically demonstrates how the center displacement is more rapidly convergent than the required area of steel for both elements used.

Example 1 demonstrated the need to carefully confirm convergence of the actual design response quantity. Although convergence of displacements demonstrates that the model is beginning to accurately simulate the behavior of the slab, it does not guarantee that bending moments have converged. If the mesh is such that the results have not converged, a significant error in the area of steel computed can result. For the structure in Example 1, an inappropriate mesh was shown to produce an error as large as 19% in the area of steel computed.

Based on the small percentage of difference in area of steel obtained between the model with 256 elements and the model with 1024 elements, the analysis results are assumed



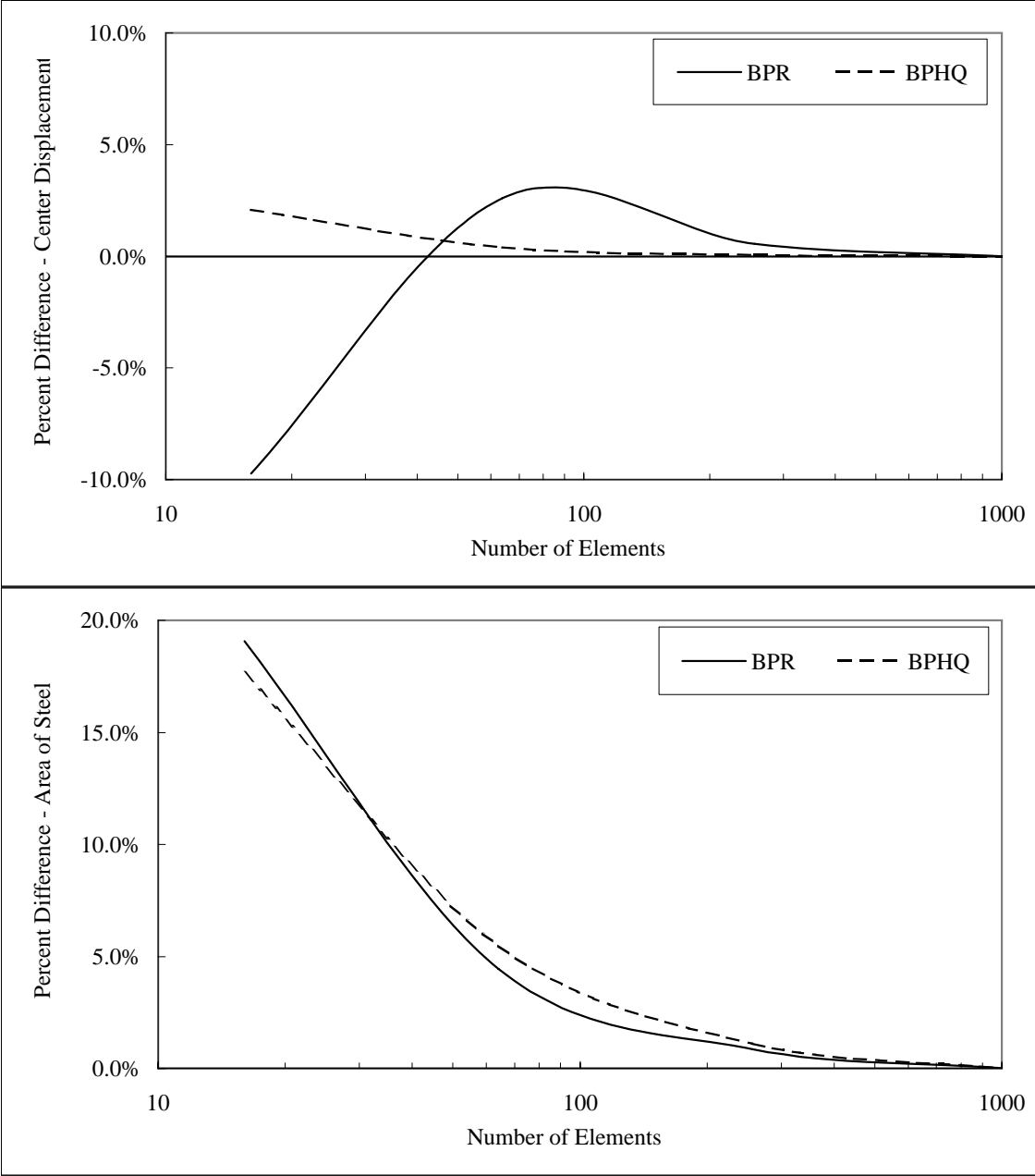


**Figure 5.3:** Example 1 - Convergence of Key Response Quantities

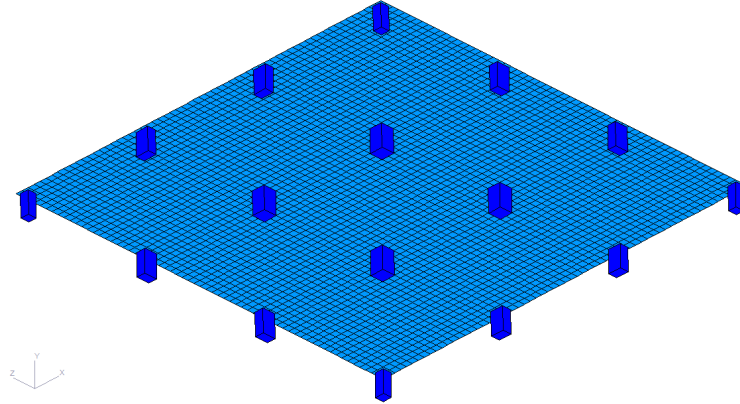


**Figure 5.4:** Example 2 - Simplified Model with Edge Beams Neglected and Space Frame Member Columns

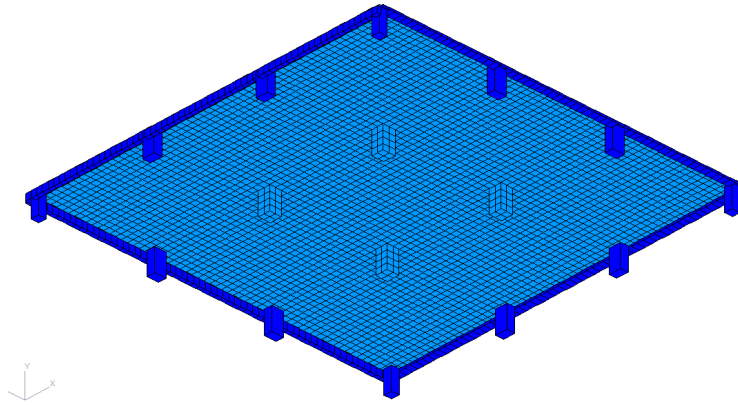


**Figure 5.5:** Example 2 - Detailed Model with Edge Beams and 3D Solid Interior Columns

to converge with the model containing 1024 elements. This dense meshing philosophy is applied to the models in the subsequent examples.

## 5.2 Example 2 - Comparison with Experimental Data

The practice of designing flat plate systems using finite elements cannot be validated solely on the basis of agreement with accepted design techniques. Both ACI direct design as well as the equivalent frame technique are approximate and subject to many limitations. As such, finite element based flat plate analysis must correspond with experimental data as well for purposes of verification.

The particular experimental study used for comparison was conducted by Gamble at the University of Illinois [28]. The test structure consisted of a quarter-scale, nine-panel

reinforced concrete flat plate. The columns were spaced at a distance of 5 ft, and the thickness of the slab was  $1\frac{3}{4}$  in. Edge beams were located around the perimeter of the structure. On two adjacent edges, the edge beams were deep (5 in. deep  $\times$  2 in. wide), and on the other two adjacent edges, the edge beams are shallow ( $2\frac{3}{4}$  in. deep  $\times$  4 in. wide). The structure was progressively loaded from 44 psf to 140 psf. Bending moments were determined throughout the test structure from measured strains in the reinforcement of the structure. The flat plate was supported on  $11\frac{1}{4}$  in. tall, 6 in.  $\times$  6 in. columns. The compressive strength of the concrete was measured as 2510 psi, and the modulus of elasticity was 2800 ksi. The details of reinforcement and arrangement of strips are given in Figures 5.6 and 5.7.

Two finite element models were created to analyze the structure: a simplified model and a more detailed model. The same bending moments were computed and compared for both of these models. The mesh for these models was chosen based on the results of Example 1.

In the simplified model, the flat plate was modeled in GT STRUDL using the SBHQ6 plate element. The columns were modeled using space frame members, and the rigid solid technique was employed to accurately model the slab-to-column connection. In the simplified model, the edge beams were neglected. The base of the columns were pin-supported to simulate the bearing support discussed by Gamble [28]. The simplified GT STRUDL model contained 3985 nodes, 3844 finite elements, and solved in 50.37 seconds. The simplified GT STRUDL model for Example 3 is shown in Figure 5.4.

The detailed finite element model was similar to the simplified model, except with a few modifications. First of all, the interior columns were replaced with 3D solid elements to more accurately represent the interaction of the column and slab. Second, the edge beams were modeled around the exterior of the system using frame members with eccentric connections to translate the centroid to the appropriate depth below the surface of the slab. The detailed GT STRUDL model contained 4125 nodes, 260 members, 3908 elements, and solved in 62.67 seconds. The detailed GT STRUDL model for Example 3 is shown in Figure 5.5.

The interior panels were divided into column and middle strips based on ACI 318. The

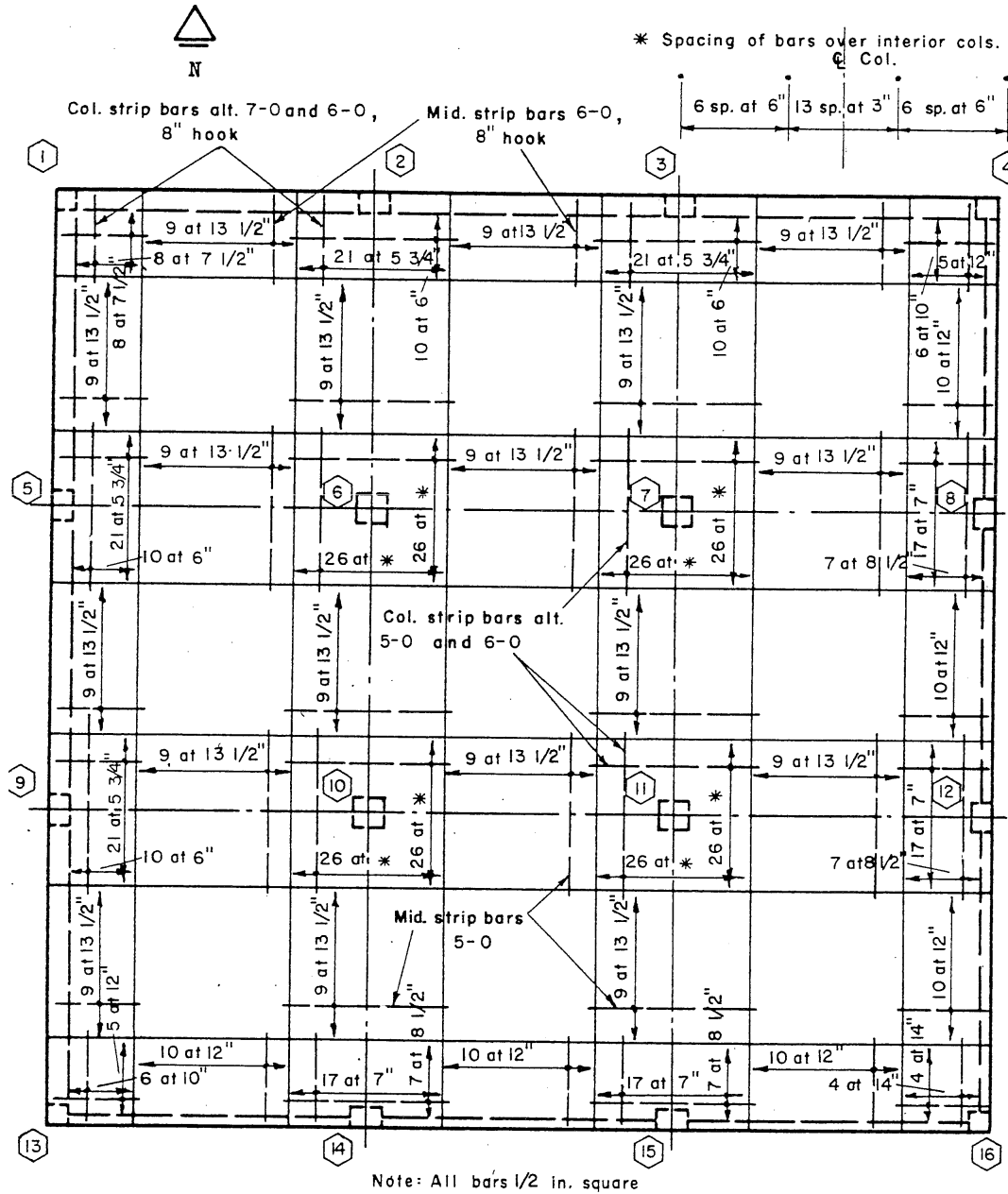


Figure 5.6: Example 2 - Test Structure Top Reinforcement (Gamble, [28])

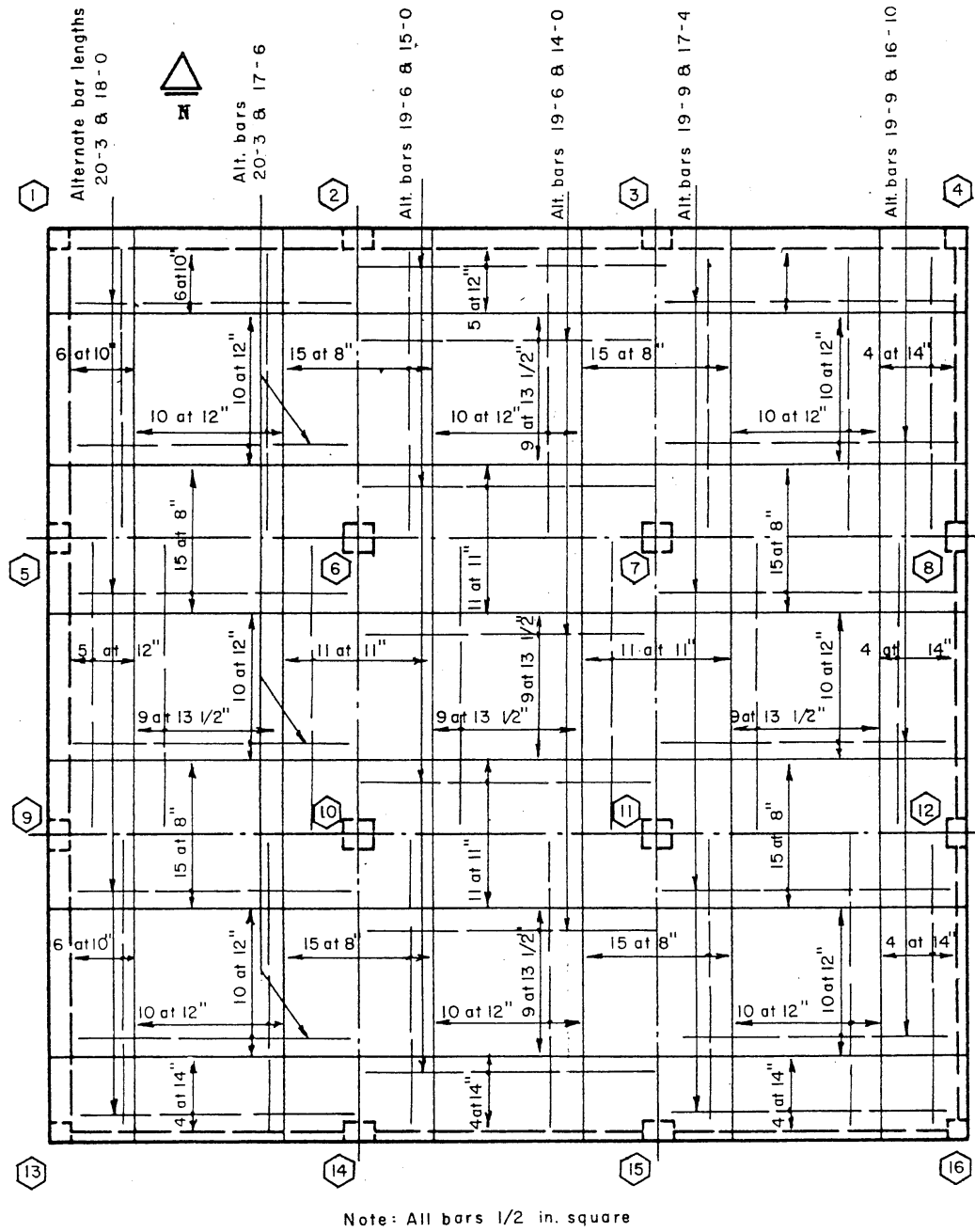
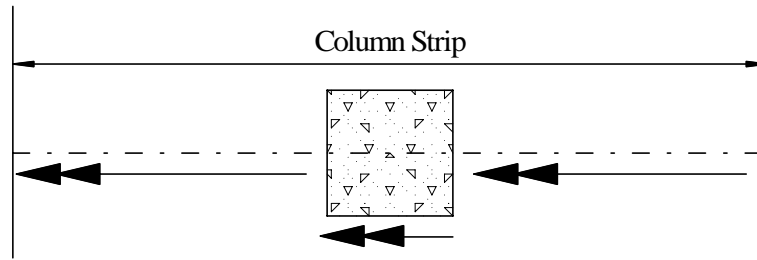


Figure 5.7: Example 2 - Test Structure Bottom Reinforcement (Gamble, [28])

strip dimensions used in the models were the same as those used in the experimental study, shown in Figures 5.6 and 5.7. For the interior panel, bending moments were computed along several sections at each load level, including the negative moment region in the column strip, negative moment region in the middle strip, positive moment region in the column strip, and positive moment region in the middle strip. In addition, the negative moments in the column strip and middle strip were combined to compute the total negative moment in the strip, and the positive moments in the column strip and middle strip were combined to compute the total positive moment in the strip. Finally, the total negative moment was combined with the total positive moment to compute the total static moment, or total variation of moment in the panel. The experimental and finite element results are presented in Table 5.2. Experimental bending moments in the exterior panels were not available and thus not compared.

In the experimental structure, the bending moments were computed based on the strain in the steel as measured at various sections across each region. Based on the details in Gamble's work showing the strain gage locations, it was not completely clear where all of the response quantities were located in the structure. The positive moment regions were located exactly at the center span between columns, and the middle strip negative moment cut was located on the column line. However, what was unclear was whether the column strip negative moment was computed at the face of the column or at the centroid, or even perhaps a piecewise combination. Over the width of the physical column, strain gages were placed at the face of the column. However, in the column strip region beyond the width of the column, the gages appeared to be located at the transverse column line. As such, the column strip negative moment varied depending where it was computed. In the table below, the GT STRUDL values reported (e.g. 10.90 k-in and 10.74 k-in) were located at the column face. Taking the entire cut across the centroid of the column yielded a negative moment equal to 7.14 k-in. If the resultants were computed exactly as detailed (i.e. the resultant across the column width was computed at the column face while the rest of the column strip resultant was computed at the column line, as shown in Figure 5.8), the computed negative moment was equal to 10.67 k-in.



**Figure 5.8:** Example 2 - Moment Components Corresponding to Strain Gage Locations

**Table 5.2:** Example 2 - Experimental and Finite Element Bending Moments

Location	Uniform Applied Load (psf)						
	44	72	84	101	107	118	140
<b>Negative Moment Column Strip</b>							
Experimental (k-in)	2.62	4.46	5.17	6.12	6.67	7.38	8.61
FEA Simplified (k-in)	3.42	5.60	6.54	7.86	8.33	9.18	10.90
FEA Detailed (k-in)	3.38	5.52	6.44	7.75	8.21	9.05	10.74
<b>Negative Moment Middle Strip</b>							
Experimental (k-in)	1.40	2.26	2.90	3.47	3.66	4.08	4.65
FEA Simplified (k-in)	0.89	1.46	1.71	2.05	2.18	2.40	2.85
FEA Detailed (k-in)	1.16	1.89	2.21	2.66	2.81	3.10	3.68
<b>Total Negative Moment</b>							
Experimental (k-in)	4.02	6.72	8.07	9.59	10.33	11.46	13.26
FEA Simplified (k-in)	4.32	7.07	8.25	9.91	10.50	11.58	13.74
FEA Detailed (k-in)	4.53	7.42	8.65	10.40	11.02	12.16	14.42
<b>Positive Moment Column Strip</b>							
Experimental (k-in)	1.42	2.39	2.81	3.47	3.73	4.18	4.87
FEA Simplified (k-in)	1.42	2.32	2.71	3.26	3.45	3.81	4.52
FEA Detailed (k-in)	1.49	2.43	2.84	3.41	3.61	3.98	4.73
<b>Positive Moment Middle Strip</b>							
Experimental (k-in)	1.04	1.69	2.06	2.46	2.63	2.91	3.40
FEA Simplified (k-in)	1.04	1.71	1.99	2.39	2.54	2.80	3.32
FEA Detailed (k-in)	1.02	1.67	1.95	2.34	2.48	2.73	3.24
<b>Total Positive Moment</b>							
Experimental (k-in)	2.46	4.08	4.87	5.93	6.36	7.09	8.27
FEA Simplified (k-in)	2.46	4.03	4.70	5.65	5.99	6.61	7.84
FEA Detailed (k-in)	2.50	4.10	4.78	5.75	6.09	6.72	7.97
<b>Total Static Moment</b>							
Experimental (k-in)	6.48	10.80	12.94	15.52	16.69	18.55	21.53
FEA Simplified (k-in)	6.78	11.10	12.95	15.57	16.49	18.19	21.58
FEA Detailed (k-in)	7.04	11.52	13.43	16.15	17.11	18.87	22.39

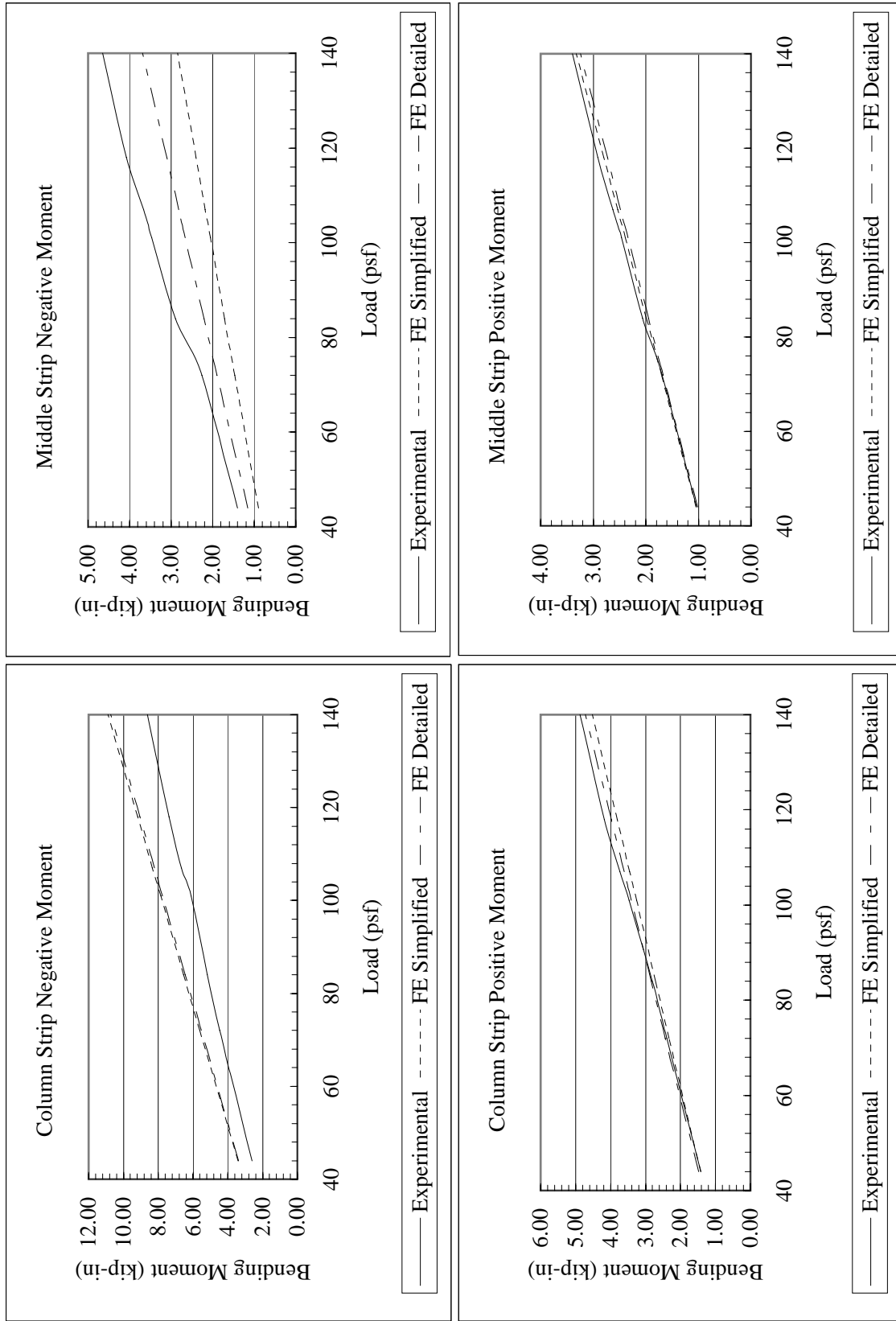
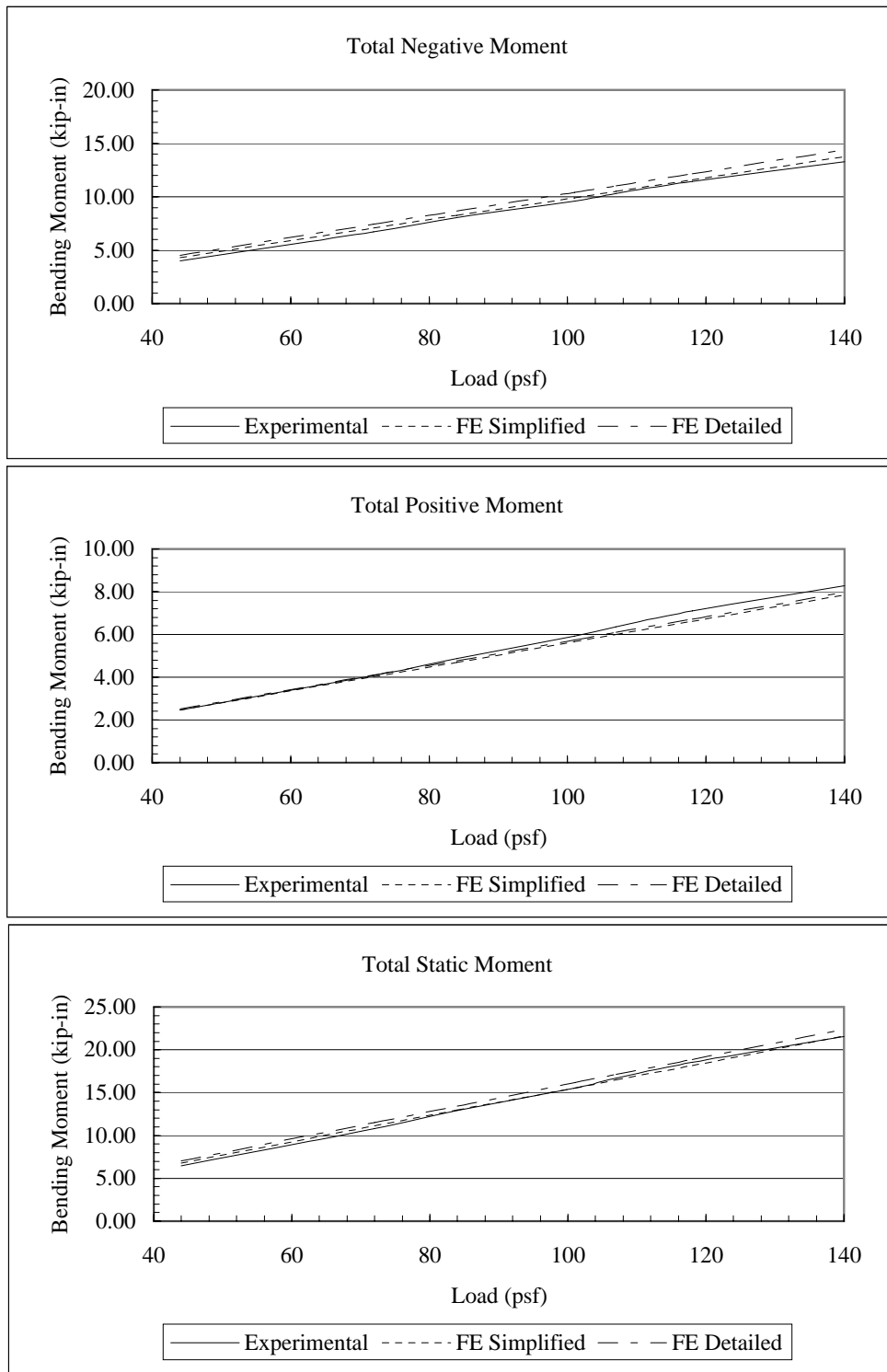


Figure 5.9: Example 2 - Moments in Interior Panel





**Figure 5.10:** Example 2 - Total Moment in Interior Panel

Several important trends are shown in Table 5.2. First of all, for positive bending in both the column strips and the middle strips, the analytical results from the simplified and detailed finite element analyses were in close agreement with experimental data.

However, the negative moments in the column strip and middle strip computed using the finite element models deviated from the experimental results. Graphically, this is shown in Figure 5.9. In the column strip, both finite element solutions overestimated the experimental negative bending moment by approximately identical margins. However, in the middle strip, both finite element solutions underestimated the experimental negative bending moment. The simplified finite element model underestimated this quantity by approximately twice as much as the detailed finite element model. The disagreement between these two models was attributed to the inclusion of exterior edge beams in the detailed model. These edge beams alter the relative stiffness of the system, resulting in a distribution of more moment to the exterior from the interior middle strip negative moment region. These results indicate that the edge beams should be modeled if present in the physical structure.

However, comparing the total negative moment acting on the combined column and middle strips showed that both finite element solutions slightly overestimate the total negative moment in the slab strip. Similarly, both finite element solutions slightly underestimated the total positive moment in the slab strip. As a result, the total static moment in the slab predicted using both finite element models was in close agreement with experimental results. Graphs of these combined moments versus load level are given in Figure 5.10.

The comparison of measured and analytical bending moments in the interior slab panel yielded several important points. First of all, the computed accuracy of the total negative moment, total positive moment, and total static moment confirmed that the application of the finite element method is viable from an equilibrium perspective. If the total static moment computed from the finite element models significantly varied from the experimental results, the applicability of the technique would be suspect.

Further, the fact that more moment was distributed to the column strip in the negative moment regions of the finite element models than in the experimental structure indicated that the finite element models represent a higher stiffness of the column-to-slab connection.

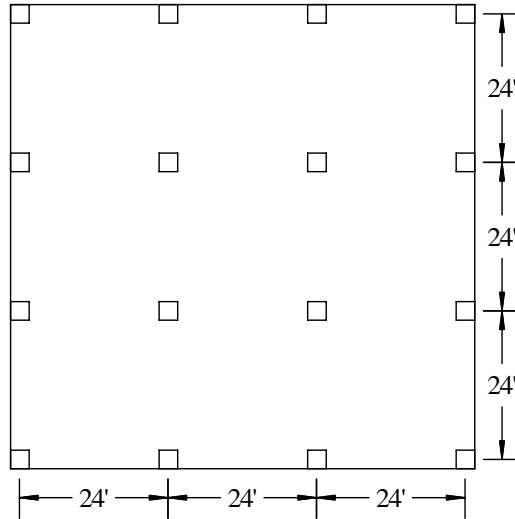


**Figure 5.11:** Example 3 - Geometry

### 5.3 Example 3 - Square Bay Flat Plate Structure

For many years, flat plate structures have been designed using approximate techniques such as ACI direct design or equivalent frame design. Despite the approximations of these techniques, many structures designed using these methods have performed well. In Example 3, the DESIGN SLAB command was used to design a square bay flat plate in order to compare with the results of simplified ACI methods.

The structure modeled consisted of 9 square panels (3 bay  $\times$  3 bay). The plate was 8 inches thick and constructed of 4000 psi concrete. The structure was supported on columns, 2 ft square and 12 ft tall, above and below the slab, and the columns were spaced at 24 feet on center in each direction. The geometry of the structure is shown in Figure 5.11. The structure was loaded with its self-weight, 40 psf superimposed dead load, and 40 psf live load. A load factor of 1.2 was applied to dead loads, and a load factor of 1.6 was applied to live loads. Pattern live loadings were considered for the system, and will be discussed later. Only reinforcement in the East-West direction was designed because of the symmetry of the structure. Column and middle strips were used to define the cut sections, and were determined according to ACI requirements.

Two GT STRUDL finite element models were developed to evaluate the system, and are shown in Figure 5.12. In the first model, the slab was modeled using the BPHQ element

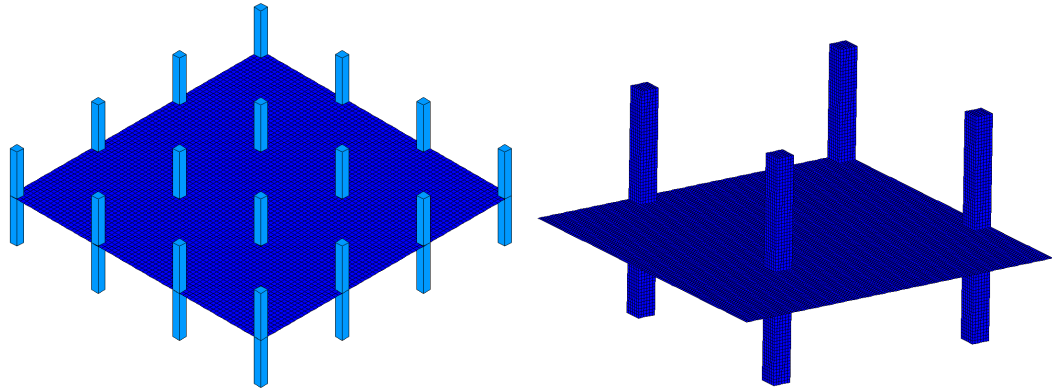


**Figure 5.12:** Example 3 - Finite Element Model with Space Frame Member Columns (left) and Finite Element Model of  $\frac{1}{4}$  of Structure with 3D Solid Columns (right)

[13]. The columns were modeled using space frame members, and the connection between the column and slab was assumed to be fully rigid. The finite size of the column connection was modeled using the rigid solid technique. The columns were fix-supported at the top and bottom. The mesh was chosen for this example based on the results of Example 1. This GT STRUDL model contained 5657 nodes, 5476 elements, 9 independent loading conditions, 8 dependent loading conditions, and solved in 71.69 seconds.

In order to validate the use of the rigid solid technique to model the slab-to-column connection, a second GT STRUDL model was created in which the columns were modeled using 3D solid elements. The example structure was doubly symmetric, so only one fourth of the structure was modeled in order to improve the solution time. This GT STRUDL model consisted of 26,656 nodes, 22,545 elements, 1 loading condition, and solved in 22.15 minutes.

The slab was then designed using direct design, the equivalent column method, the Wood and Armer method, and then the DESIGN SLAB command for both GT STRUDL models. For each method, interior as well as exterior regions were designed. The results of these analyses are given on the following pages. The tabulated bending moments and required area of steel for the interior panel are given in Table 5.3, and the tabulated bending moments and required area of steel for the exterior region are given in Table 5.4. The results in Tables 5.3 and 5.4 corresponded to the case where all loads were applied uniformly over the entire structure.

**Table 5.3:** Example 3 - Interior Region Design Results

Bending Moment Results (kip-ft):

Location	Direct Design	Equiv. Column	Wood & Armer (Rigid Solids)	DESIGN SLAB (Rigid Solids)	DESIGN SLAB (3D Solids)
Column Strip Negative Moment	-164.22	-180.53	-171.89	-174.95	-171.93
Column Strip Positive Moment	70.74	57.72	70.79	70.74	72.34
Middle Strip Negative Moment	-54.74	-60.18	-49.54	-48.67	-47.17
Middle Strip Positive Moment	47.16	38.48	51.29	51.23	51.97

Area of Steel Required (in<sup>2</sup>):

Location	Direct Design	Equiv. Column	Wood & Armer (Rigid Solids)	DESIGN SLAB (Rigid Solids)	DESIGN SLAB (3D Solids)
Column Strip Negative Moment	6.15	6.81	6.21	6.58	6.48
Column Strip Positive Moment	2.55	2.07	2.55	2.55	2.61
Middle Strip Negative Moment	1.96	2.16	1.77	1.74	1.69
Middle Strip Positive Moment	1.69	1.37	1.84	1.84	1.86

**Table 5.4:** Example 3 - Exterior Region Design Results

Bending Moment Results (kip-ft):

Location	Direct Design	Equiv. Column	Wood & Armer (Rigid Solids)	DESIGN SLAB (Rigid Solids)	DESIGN SLAB (3D Solids)
Column Strip Ext. Negative Moment	-87.58	-96.20	-149.12	-155.65	-150.96
Column Strip Positive Moment	105.10	96.18	81.07	81.83	84.58
Column Strip Int. Negative Moment	-176.85	-200.85	-173.34	-189.66	-186.80
Middle Strip Ext. Negative Moment	0.00	0.00	0.00	0.00	0.00
Middle Strip Positive Moment	70.07	64.12	62.57	63.21	65.04
Middle Strip Int. Negative Moment	-58.95	-66.95	-50.44	-46.66	-47.53

Area of Steel Required (in<sup>2</sup>):

Location	Direct Design	Equiv. Column	Wood & Armer (Rigid Solids)	DESIGN SLAB (Rigid Solids)	DESIGN SLAB (3D Solids)
Column Strip Ext. Negative Moment	3.18	3.51	5.76	5.81	5.62
Column Strip Positive Moment	3.84	3.51	2.94	2.97	3.07
Column Strip Int. Negative Moment	6.66	7.64	6.66	7.18	7.06
Middle Strip Ext. Negative Moment	0.00	0.00	0.00	0.00	0.00
Middle Strip Positive Moment	2.53	2.31	2.25	2.28	2.34
Middle Strip Int. Negative Moment	2.12	2.41	1.81	1.67	1.70

Several important comments can be made regarding the results in Tables 5.3 and 5.4. First of all, all three finite element-based design methods produced designs in close agreement with each other. Small variations were expected based on the difference in formulation used in the computation of response quantities. However, the close correlation indicated that modeling the columns using frame members and then distributing the finite size of the column to the slab via the rigid solid technique can be used in place of a more detailed analysis where the columns are modeled as 3D solid elements. The use of 3D solids was uneconomic, and based on the results of these analyses, provided no significant increase in accuracy over the rigid solid technique.

Second, for the interior region, a comparison of bending moments as well as required area of steel showed that the solutions based on finite element analysis deviated only slightly from the simplified ACI methods. For the interior panels, the maximum difference in area of steel computed between the DESIGN SLAB command and all other methods was less than  $0.50 \text{ in}^2$  at each interior location.

However, comparison of finite element-based solutions in the exterior region showed significant deviation from simplified techniques, especially at the exterior column strip negative moment region. In fact, the finite element solutions predicted higher moments at exterior columns by approximately a factor of 2. It is apparent from these values that the assumption of linear elastic behavior (i.e. no cracking), as well as the assumed fully rigid connection, generated a higher stiffness of the slab-to-column connection in these regions. This *stiffening* of the structure caused a redistribution of moment throughout the exterior panel, accounting for further variation between the finite element results and the simplified ACI methods.

It is also possible that, in this example, the larger moments computed at the exterior column faces are associated with the relatively large columns used. Example 4 show that for smaller column sizes, closer agreement with simplified methods was obtained.

This same phenomenon likely occurred at interior column-to-slab connections as well. Column size differences did not produce as much variation in the design results, however, because the continuation of the slab on the opposite side of the column effectively stiffened

the interior panel boundary to a condition of near fixity.

So far the discussion of results has neglected the effects of pattern live loadings. Previous work by Jirsa, Sozen and Siess showed that in flat plates, pattern live loadings may influence bending moment design quantities significantly [41]. In addition to influencing bending moments, pattern live loadings can also develop significant torsional moments in the flat plate.

To evaluate the effect of pattern live loadings on the behavior of the system, the flat plate was subjected to 6 pattern loading cases in addition to the initial case where the live load was applied everywhere simultaneously. The six pattern live loads that were applied are shown in Figure 5.13. These pattern loads were then combined with the self-weight (SW) and superimposed dead load (DL) to create the following ultimate load combinations (PLC stands for *Pattern Load Combination*):

$$\begin{aligned}\text{Uniform} &= 1.2\text{SW} + 1.2\text{DL} + 1.6\text{LL} \\ \text{PLC \#1} &= 1.2\text{SW} + 1.2\text{DL} + 0.75 \cdot 1.6\text{PL1} \\ \text{PLC \#2} &= 1.2\text{SW} + 1.2\text{DL} + 0.75 \cdot 1.6\text{PL2} \\ \text{PLC \#3} &= 1.2\text{SW} + 1.2\text{DL} + 0.75 \cdot 1.6\text{PL3} \\ \text{PLC \#4} &= 1.2\text{SW} + 1.2\text{DL} + 0.75 \cdot 1.6\text{PL4} \\ \text{PLC \#5} &= 1.2\text{SW} + 1.2\text{DL} + 0.75 \cdot 1.6\text{PL5} \\ \text{PLC \#6} &= 1.2\text{SW} + 1.2\text{DL} + 0.75 \cdot 1.6\text{PL6}\end{aligned}$$

For each ultimate pattern load combination, the bending moment at each interior and exterior region was computed and tabulated in comparison to the moments obtained from the original loading case wherein the live load was distributed everywhere (denoted *Uniform* in the list of loading combinations). Each region was designed using the DESIGN SLAB command, the Wood and Armer method, and the Equivalent Column technique. Note that the equivalent column technique is applicable only for pattern load cases 2, 4, and 6 for the design of reinforcement in the East-West direction. For the interior region, the pattern bending moments are given in Table 5.5 and required area of steel in Table 5.6. For the exterior region, the pattern bending moments are given in Table 5.7 and required area



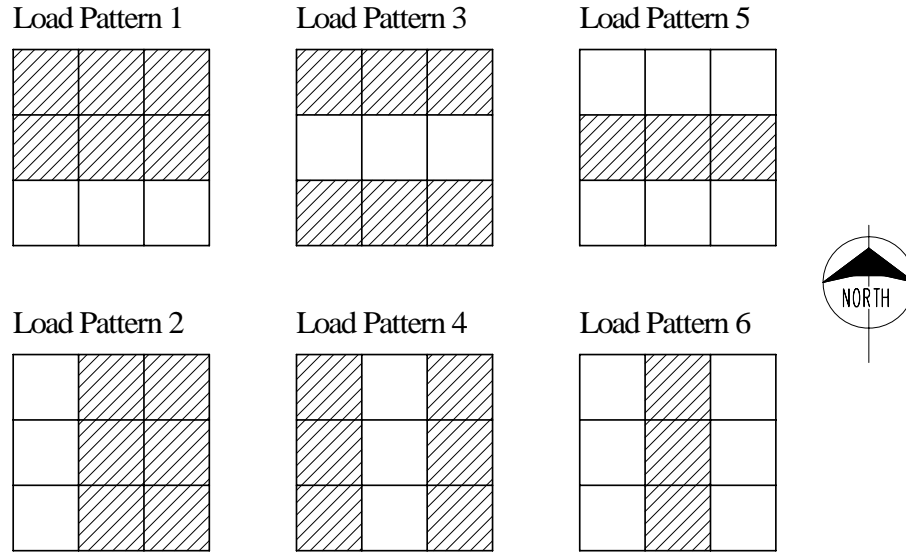


**Figure 5.13:** Example 3 - Pattern Live Loadings

of steel in Table 5.8. In addition, the ratio of torsional moment to bending moment was computed for each pattern load combination. The torsion-to-bending ratios are presented in Table 5.9.

Tables 5.5 through 5.8 show some important trends with respect to the influence of pattern live loads. First of all, for the cases considered, pattern live loads did not significantly increase the bending moments for design in any of the three methods employed. In fact, as shown in Tables 5.6 and 5.8, the increase in area of steel for all cases (both interior and exterior) was smaller than that provided by a #3 bar, indicating that the pattern loads produced insignificant changes in actual design results. Pattern live loadings had such a small effect due to the 0.75 live load reduction factor applied based on ACI 13.7.6 [2].

Perhaps more significantly, pattern live loads created torsional effects that would never be considered if the live load were applied uniformly over the entire structure. Notice in Table 5.9 that under the Uniform loading, the maximum torsional moment ( $M_T$ ) in the interior region was 3.97% of the column strip negative moment ( $M_B$ ). However, this ratio increases to 14.31% under PLC #3. Similarly, the column strip exterior negative  $M_T/M_B$  ratio increased from 3.45% to 16.04% under PLC #3. High torsional moments, such as those developed under the pattern loading conditions, indicated that the principle bending axes were not parallel with the user-selected cut, and as such, must be evaluated with caution.

**Table 5.5:** Example 3 - Interior Bending Moments for Pattern Loadings

Location/Method	Uniform	PLC #1	PLC #2	PLC #3	PLC #4	PLC #5	PLC #6
Column Strip, Negative Moment							
DESIGN SLAB	-174.95	-144.15	-165.09	-144.58	-129.65	-144.95	-159.88
Wood and Armer	-163.10	-134.39	-153.63	-134.90	-125.10	-135.16	-145.69
Equivalent Column	-180.53	-	-174.60	-	-141.98	-	-156.83
Column Strip, Positive Moment							
DESIGN SLAB	70.74	58.37	67.55	58.51	47.88	58.61	69.24
Wood and Armer	70.79	58.40	68.19	58.54	47.91	58.65	69.28
Equivalent Column	57.72	-	58.38	-	32.82	-	62.70
Middle Strip, Negative Moment							
DESIGN SLAB	-48.67	-43.85	-45.84	-38.11	-40.20	-42.40	-40.31
Wood and Armer	-49.54	-44.63	-46.55	-38.85	-42.94	-43.13	-41.51
Equivalent Column	-60.18	-	-58.20	-	-47.33	-	-52.28
Middle Strip, Positive Moment							
DESIGN SLAB	51.23	47.08	50.06	38.39	32.43	46.45	52.42
Wood and Armer	51.29	47.13	50.65	38.42	32.45	46.50	52.47
Equivalent Column	38.48	-	38.92	-	21.88	-	41.80

(All units kip-ft.)

**Table 5.6:** Example 3 - Interior Area of Steel Computed for Pattern Loadings

Location/Method	Uniform	PLC #1	PLC #2	PLC #3	PLC #4	PLC #5	PLC #6
Column Strip, Negative Moment							
DESIGN SLAB	6.579	5.353	6.183	5.370	4.787	5.384	5.975
Wood and Armer	6.209	5.036	5.818	5.062	4.650	5.068	5.515
Equivalent Column	6.805	-	6.565	-	5.267	-	5.853
Column Strip, Positive Moment							
DESIGN SLAB	2.553	2.098	2.436	2.103	1.714	2.106	2.498
Wood and Armer	2.554	2.098	2.457	2.103	1.714	2.107	2.498
Equivalent Column	2.074	-	2.098	-	1.169	-	2.257
Middle Strip, Negative Moment							
DESIGN SLAB	1.743	1.568	1.640	1.360	1.435	1.515	1.439
Wood and Armer	1.774	1.595	1.665	1.386	1.534	1.541	1.482
Equivalent Column	2.164	-	2.091	-	1.694	-	1.874
Middle Strip, Positive Moment							
DESIGN SLAB	1.836	1.685	1.794	1.370	1.154	1.662	1.880
Wood and Armer	1.837	1.685	1.813	1.370	1.155	1.662	1.880
Equivalent Column	1.373	-	1.389	-	0.776	-	1.493

(All units in<sup>2</sup>.)

**Table 5.7:** Example 3 - Exterior Bending Moments for Pattern Loadings

Location/Method	Uniform	PLC #1	PLC #2	PLC #3	PLC #4	PLC #5	PLC #6
<b>Column Strip, Exterior Negative Moment</b>							
DESIGN SLAB	-155.65	-128.37	-144.75	-128.80	-146.99	-128.78	-110.59
Wood and Armer	-149.12	-123.02	-138.68	-123.64	-140.87	-123.29	-105.92
Equivalent Column	-96.20	-	-88.30	-	-95.60	-	-63.70
<b>Column Strip, Positive Moment</b>							
DESIGN SLAB	81.83	67.57	76.09	67.80	77.86	67.68	57.63
Wood and Armer	82.70	68.25	76.90	68.52	78.12	68.38	58.82
Equivalent Column	96.18	-	88.80	-	93.12	-	66.30
<b>Column Strip, Interior Negative Moment</b>							
DESIGN SLAB	-189.66	-156.35	-176.78	-156.90	-171.52	-156.97	-142.34
Wood and Armer	-173.34	-142.89	-161.67	-143.56	-155.21	-143.52	-133.82
Equivalent Column	-200.85	-	-190.35	-	-171.23	-	-161.18
<b>Middle Strip, Exterior Negative Moment</b>							
DESIGN SLAB	0.00	0.00	0.00	0.00	0.00	0.00	0.00
Wood and Armer	0.00	0.00	0.00	0.00	0.00	0.00	0.00
Equivalent Column	0.00	-	0.00	-	0.00	-	0.00
<b>Middle Strip, Positive Moment</b>							
DESIGN SLAB	63.21	57.79	58.73	47.95	61.19	56.72	43.48
Wood and Armer	63.98	58.52	59.45	48.48	61.35	57.44	44.56
Equivalent Column	64.12	-	59.20	-	62.08	-	44.20
<b>Middle Strip, Interior Negative Moment</b>							
DESIGN SLAB	-46.66	-41.98	-43.95	-36.67	-37.73	-40.53	-39.46
Wood and Armer	-50.44	-45.49	-47.59	-39.51	-38.98	-43.96	-44.49
Equivalent Column	-66.95	-	-63.45	-	-57.08	-	-53.73

(All units kip-ft.)

**Table 5.8:** Example 3 - Exterior Area of Steel Computed for Pattern Loadings

Location/Method	Uniform	PLC #1	PLC #2	PLC #3	PLC #4	PLC #5	PLC #6
<b>Column Strip, Exterior Negative Moment</b>							
DESIGN SLAB	5.807	4.737	5.376	4.753	5.465	4.753	4.052
Wood and Armer	5.765	4.666	5.319	4.696	5.410	4.678	3.970
Equivalent Column	3.506	-	3.208	-	3.483	-	2.294
<b>Column Strip, Positive Moment</b>							
DESIGN SLAB	2.966	2.436	2.752	2.445	2.818	2.440	2.070
Wood and Armer	2.996	2.460	2.780	2.470	2.825	2.465	2.113
Equivalent Column	3.505	-	3.227	-	3.390	-	2.389
<b>Column Strip, Interior Negative Moment</b>							
DESIGN SLAB	7.177	5.835	6.653	5.856	6.441	5.859	5.282
Wood and Armer	6.662	5.394	6.168	5.426	5.921	5.420	5.007
Equivalent Column	7.637	-	7.205	-	6.429	-	6.026
<b>Middle Strip, Exterior Negative Moment</b>							
DESIGN SLAB	0.000	0.000	0.000	0.000	0.000	0.000	0.000
Wood and Armer	0.000	0.000	0.000	0.000	0.000	0.000	0.000
Equivalent Column	0.000	-	0.000	-	0.000	-	0.000
<b>Middle Strip, Positive Moment</b>							
DESIGN SLAB	2.276	2.076	2.111	1.717	2.201	2.037	1.554
Wood and Armer	2.301	2.101	2.135	1.734	2.205	2.061	1.592
Equivalent Column	2.309	-	2.128	-	2.234	-	1.580
<b>Middle Strip, Interior Negative Moment</b>							
DESIGN SLAB	1.670	1.500	1.571	1.307	1.346	1.447	1.408
Wood and Armer	1.807	1.627	1.703	1.410	1.391	1.571	1.590
Equivalent Column	2.413	-	2.284	-	2.050	-	1.927

(All units in<sup>2</sup>.)

**Table 5.9:** Example 3 - Ratio of Resultant Torsional Moment to Bending Moment for Pattern Loadings

Location	Uniform	PLC #1	PLC #2	PLC #3	PLC #4	PLC #5	PLC #6
<b>INTERIOR</b>							
Column Strip Negative Moment	3.97%	5.71%	3.76%	14.31%	4.39%	6.34%	3.63%
Column Strip Positive Moment	0.24%	0.24%	0.51%	0.23%	0.29%	0.24%	0.20%
Middle Strip Negative Moment	0.00%	0.00%	0.00%	0.00%	0.00%	0.00%	0.00%
Middle Strip Positive Moment	0.00%	0.00%	0.00%	0.00%	0.00%	0.00%	0.00%
<b>EXTERIOR</b>							
Column Strip Ext. Negative Moment	3.45%	8.91%	3.47%	16.04%	3.21%	9.13%	3.78%
Column Strip Positive Moment	0.62%	0.76%	0.62%	0.72%	0.40%	0.52%	0.93%
Column Strip Int. Negative Moment	3.12%	6.21%	3.14%	12.83%	2.97%	6.59%	3.29%
Middle Strip Ext. Negative Moment	0.00%	0.00%	0.00%	0.00%	0.00%	0.00%	0.00%
Middle Strip Positive Moment	0.00%	1.36%	0.00%	0.00%	0.00%	0.00%	0.00%
Middle Strip Int. Negative Moment	0.00%	2.66%	0.00%	0.00%	0.00%	0.00%	0.00%

For the cases where the torsional moment was greater than 10%, it was important to determine if the Wood and Armer method produced a design moment and area of steel different from the DESIGN SLAB command, since the DESIGN SLAB command did not incorporate the resultant torsional moment. For the interior column strip negative moment region under loading condition PLC #3, the DESIGN SLAB command produced a design moment of -144.58 kip-ft and an area of steel of 5.37 in<sup>2</sup>, while the Wood and Armer technique produced a design moment of -134.90 kip-ft and an area of steel of 5.06 in<sup>2</sup>. For the exterior panel column strip exterior negative moment region under loading condition PLC #3, the DESIGN SLAB command produced a design moment of -128.80 kip-ft and an area of steel of 4.75 in<sup>2</sup>, while the Wood and Armer technique produced a design moment of -123.64 kip-ft and an area of steel of 4.70 in<sup>2</sup>. For the interior panel column strip interior negative moment region under loading condition PLC #3, the DESIGN SLAB command produced a design moment of -156.90 kip-ft and an area of steel of 5.86 in<sup>2</sup>, while the Wood and Armer technique produced a design moment of -143.56 kip-ft and an area of steel of 5.43 in<sup>2</sup>. Note that the equivalent column technique neglected cases producing torsion in the slab, such as loading combinations PLC #3 for East-West reinforcement, and as such was not compared.

The significance of these findings was that in the case of a square flat plate system, for regions where the resultant torsional moment is as large as 16% of the resultant bending moment, the DESIGN SLAB command provides more steel reinforcement than the Wood and Armer technique, which explicitly accounts for  $M_{xy}$  bending stresses.

#### **5.4 Example 4 - Irregular Bay Rectangular Flat Plate Structure**

Up to this point, only structures with square panels have been studied. Few structures in practice conform to such uniform spacing. Because of this, a flat plate system with irregular spacing was designed using the DESIGN SLAB program.

The structure evaluated in this example was similar to that of Example 4. The system had 9 panels, consisting of rectangular 3 × 3 bays. The span lengths are shown in Figure

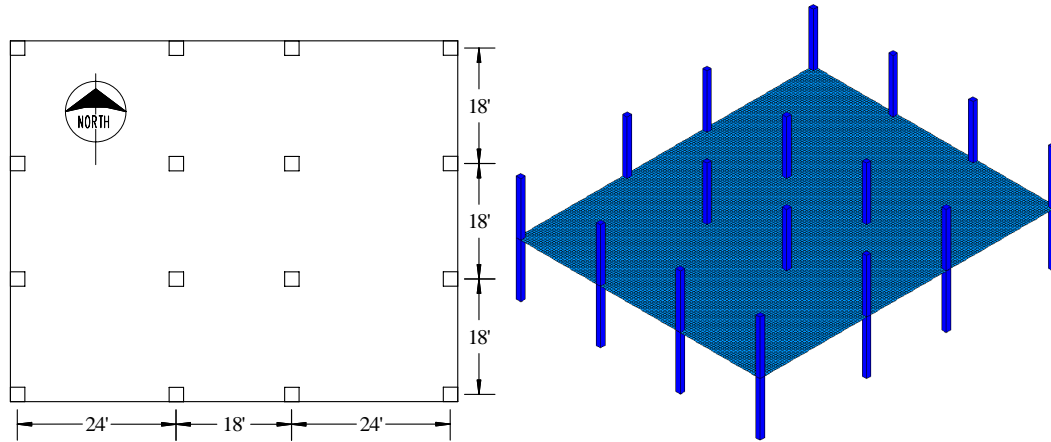


**Figure 5.14:** Example 4 - Dimensions and Finite Element Model

5.14. The columns were 12 feet tall and 12 inches square. The flat plate was 9 inches thick according to ACI deflection criteria. The concrete had a compressive strength of 4000 psi. The slab was loaded with self-weight, 40 psf superimposed dead load, and 40 psf live load. The live load was applied in the same patterns as given for Example 3 in Figure 5.13. Additionally, the same load combinations were used as that of Example 3. For this example, strips oriented in the North-South direction were those reinforced parallel to the North-South direction. Similarly, strips oriented in the East-West direction were those reinforced parallel to the East-West direction. Column and middle strips were used to define the cut sections, and were determined according to ACI requirements.

The structure was modeled in GT STRUDL using the same techniques as Example 3. The flat plate was modeled with BPHQ finite elements [13], the columns were modeled using frame members, and the column-to-slab connection was accomplished using the rigid solid technique. The GT STRUDL model contained 15,017 nodes, 14,740 elements, and solved in 180.24 seconds. A graphic of the GT STRUDL model is shown in Figure 5.14. The mesh size corresponded to elements of size 6 inches  $\times$  6 inches, allowing four elements to cover the cross-section of the column.

Bending moments at critical design locations in the North-South as well as East-West directions were computed using ACI direct design, the ACI equivalent column technique, and the DESIGN SLAB command in GT STRUDL for the ultimate uniform load. Then, the



distribution of bending moment and area of steel were evaluated for each pattern loading, along with the ratio of torsional moment to bending moment. Results in the North-South direction are given in Tables 5.10 through 5.16, and results in the East-West direction are given in Tables 5.17 through 5.23. Several important findings emerged from this example.

For the North/South direction, the bending moments and area of steel computed under uniform factored loads using the DESIGN SLAB command were in close agreement with the Wood and Armer method and the equivalent column technique for the interior panel, as shown in Table 5.10. The maximum difference between area of steel computed using the DESIGN SLAB command and either equivalent frame or Wood and Armer was approximately the area provided by one #5 (M16) bar,  $0.31 \text{ in}^2$ . Direct design results deviated by a difference of as much as  $0.91 \text{ in}^2$ .

For the North/South exterior panel, the bending moments and area of steel computed under uniform factored loads using the DESIGN SLAB command were in close agreement with the equivalent column results and Wood and Armer results in all regions except for the column strip exterior negative moment region, as shown in Table 5.11. At this location, the DESIGN SLAB command calculated a bending moment of  $-34.96 \text{ kip-ft}$ , while the Wood and Armer method computed a bending moment of  $-46.45 \text{ kip-ft}$ , resulting in a difference in computed area of steel of  $0.382 \text{ in}^2$ . At this location, the equivalent column technique design moment was only  $-6.87 \text{ kip-ft}$ . Again, Direct Design produced a distribution of steel throughout the system different from that of the equivalent column method and finite element solutions.

Similar to Example 3, pattern live loadings generated only minor increases in bending moments and area of steel computed in the North/South direction. The results of the pattern live loads are given in Tables 5.12 to 5.15. For instance, pattern load combination PLC #5 increased the interior column strip positive moment from  $35.03 \text{ kip-ft}$  to  $38.25 \text{ kip-ft}$  and increased the middle strip positive moment from  $15.20 \text{ kip-ft}$  to  $20.07 \text{ kip-ft}$ . For North/South strips, pattern live loads did not increase exterior region bending moments.

In the North/South direction, slab strips were unsymmetric because of varied column spacing on each side of the strip. This lack of symmetry resulted in the generation of

**Table 5.10:** Example 4 - N/S Interior Region Design Results

Bending Moment Results (kip-ft):

Location	Direct Design	Equiv. Column	Wood & Armer	DESIGN SLAB
Column Strip, Negative Moment	-91.35	-110.18	-117.31	-119.23
Column Strip, Positive Moment	39.35	24.30	35.04	35.03
Middle Strip, Negative Moment	-30.45	-36.73	-35.60	-34.82
Middle Strip, Positive Moment	26.23	16.20	15.21	15.20

Area of Steel Required (in<sup>2</sup>):

Location	Direct Design	Equiv. Column	Wood & Armer	DESIGN SLAB
Column Strip, Negative Moment	2.854	3.463	3.746	3.759
Column Strip, Positive Moment	1.210	0.744	1.076	1.076
Middle Strip, Negative Moment	0.935	1.130	1.095	1.071
Middle Strip, Positive Moment	0.804	0.495	0.465	0.464

**Table 5.11:** Example 4 - N/S Exterior Region Design Results

Bending Moment Results (kip-ft):

Location	Direct Design	Equiv. Column	Wood & Armer	DESIGN SLAB
Column Strip, Exterior Negative Moment	-48.72	-6.87	-46.45	-34.96
Column Strip, Positive Moment	58.46	69.36	64.08	60.49
Column Strip, Interior Negative Moment	-98.37	-112.73	-122.65	-125.56
Middle Strip, Exterior Negative Moment	0.00	0.00	0.00	0.00
Middle Strip, Positive Moment	38.98	46.24	41.10	40.25
Middle Strip, Interior Negative Moment	-32.79	-37.58	-35.60	-34.83

Area of Steel Required (in<sup>2</sup>):

Location	Direct Design	Equiv. Column	Wood & Armer	DESIGN SLAB
Column Strip, Exterior Negative Moment	1.502	0.209	1.455	1.073
Column Strip, Positive Moment	1.808	2.152	1.985	1.872
Column Strip, Interior Negative Moment	3.080	3.546	3.932	3.966
Middle Strip, Exterior Negative Moment	0.000	0.000	0.000	0.000
Middle Strip, Positive Moment	1.201	1.428	1.266	1.240
Middle Strip, Interior Negative Moment	1.008	1.157	1.095	1.071

**Table 5.12:** Example 4 - N/S Interior Bending Moments for Pattern Loadings

Location/Method	Uniform	PLC #1	PLC #2	PLC #3	PLC #4	PLC #5	PLC #6
Column Strip, Negative Moment							
DESIGN SLAB	-119.23	-113.39	-113.60	-98.39	-101.88	-101.44	-97.96
Wood and Armer	-117.31	-111.58	-111.76	-98.07	-100.40	-98.76	-96.23
Equivalent Column	-110.18	-106.73	-	-92.18	-	-92.48	-
Column Strip, Positive Moment							
DESIGN SLAB	35.03	35.50	33.49	20.48	29.70	38.25	29.02
Wood and Armer	35.04	34.02	33.50	20.48	29.71	38.26	29.03
Equivalent Column	24.30	27.06	-	9.60	-	31.14	-
Middle Strip, Negative Moment							
DESIGN SLAB	-34.82	-33.48	-30.18	-29.21	-30.56	-29.16	-27.80
Wood and Armer	-35.60	-34.03	-30.88	-30.07	-31.27	-29.59	-28.40
Equivalent Column	-36.73	-30.49	-	-26.34	-	-26.42	-
Middle Strip, Positive Moment							
DESIGN SLAB	15.20	17.14	14.44	5.42	10.81	20.07	14.67
Wood and Armer	15.21	17.42	14.45	5.42	10.82	20.08	14.68
Equivalent Column	16.20	15.46	-	5.49	-	17.79	-

(All units kip-ft.)

**Table 5.13:** Example 4 - N/S Interior Area of Steel Computed for Pattern Loadings

Location/Method	Uniform	PLC #1	PLC #2	PLC #3	PLC #4	PLC #5	PLC #6
Column Strip, Negative Moment							
DESIGN SLAB	3.759	3.568	3.575	3.081	3.194	3.180	3.067
Wood and Armer	3.746	3.553	3.559	3.100	3.182	3.130	3.042
Equivalent Column	3.463	3.351	—	2.881	—	2.890	—
Column Strip, Positive Moment							
DESIGN SLAB	1.076	1.090	1.028	0.626	0.910	1.176	0.890
Wood and Armer	1.076	1.044	1.028	0.626	0.911	1.176	0.890
Equivalent Column	0.744	0.829	—	0.293	—	0.955	—
Middle Strip, Negative Moment							
DESIGN SLAB	1.071	1.029	0.927	0.897	0.939	0.895	0.853
Wood and Armer	1.095	1.046	0.948	0.923	0.960	0.908	0.871
Equivalent Column	1.130	0.936	—	0.808	—	0.810	—
Middle Strip, Positive Moment							
DESIGN SLAB	0.464	0.524	0.441	0.165	0.330	0.614	0.448
Wood and Armer	0.465	0.533	0.441	0.165	0.330	0.614	0.448
Equivalent Column	0.495	0.472	—	0.167	—	0.544	—

(All units in<sup>2</sup>.)

**Table 5.14:** Example 4 - N/S Exterior Bending Moments for Pattern Loadings

Location/Method	Uniform	PLC #1	PLC #2	PLC #3	PLC #4	PLC #5	PLC #6
<b>Column Strip, Exterior Negative Moment</b>							
DESIGN SLAB	-34.96	-32.52	-33.15	-33.60	-29.88	-24.99	-28.71
Wood and Armer	-46.45	-43.28	-44.40	-44.10	-39.91	-33.38	-37.94
Equivalent Column	-6.87	-6.12	-	-7.41	-	-4.10	-
<b>Column Strip, Positive Moment</b>							
DESIGN SLAB	60.49	56.23	56.86	59.01	51.57	42.39	49.83
Wood and Armer	64.08	59.54	60.19	63.98	54.88	46.34	52.56
Equivalent Column	69.36	63.90	-	68.22	-	48.18	-
<b>Column Strip, Interior Negative Moment</b>							
DESIGN SLAB	-125.56	-118.72	-119.42	-107.15	-107.30	-103.29	-103.14
Wood and Armer	-122.65	-115.76	-116.71	-103.84	-105.01	-102.01	-100.57
Equivalent Column	-112.73	-108.83	-	-94.28	-	-94.73	-
<b>Middle Strip, Exterior Negative Moment</b>							
DESIGN SLAB	0.00	0.00	0.00	0.00	0.00	0.00	0.00
Wood and Armer	0.00	0.00	0.00	0.00	0.00	0.00	0.00
Equivalent Column	0.00	0.00	-	0.00	-	0.00	-
<b>Middle Strip, Positive Moment</b>							
DESIGN SLAB	40.25	37.17	36.45	40.32	32.21	27.15	35.26
Wood and Armer	41.10	38.06	37.29	40.82	32.83	28.06	36.06
Equivalent Column	46.24	36.51	-	38.98	-	27.53	-
<b>Middle Strip, Interior Negative Moment</b>							
DESIGN SLAB	-34.83	-33.48	-30.18	-29.21	-30.56	-29.16	-27.80
Wood and Armer	-35.60	-34.03	-30.88	-30.07	-31.27	-29.59	-28.40
Equivalent Column	-37.58	-31.09	-	-26.94	-	-27.06	-

(All units kip-ft.)

**Table 5.15:** Example 4 - N/S Exterior Area of Steel Computed for Pattern Loadings

Location/Method	Uniform	PLC #1	PLC #2	PLC #3	PLC #4	PLC #5	PLC #6
<b>Column Strip, Exterior Negative Moment</b>							
DESIGN SLAB	1.073	0.998	1.017	1.031	0.916	0.765	0.880
Wood and Armer	1.455	1.353	1.388	1.379	1.247	1.037	1.180
Equivalent Column	0.209	0.186	-	0.226	-	0.125	-
<b>Column Strip, Positive Moment</b>							
DESIGN SLAB	1.872	1.738	1.758	1.825	1.591	1.305	1.537
Wood and Armer	1.985	1.841	1.862	1.984	1.695	1.428	1.622
Equivalent Column	2.152	1.979	-	2.116	-	1.485	-
<b>Column Strip, Interior Negative Moment</b>							
DESIGN SLAB	3.966	3.742	3.765	3.365	3.369	3.239	3.235
Wood and Armer	3.932	3.698	3.730	3.303	3.339	3.234	3.189
Equivalent Column	3.546	3.419	-	2.948	-	2.963	-
<b>Middle Strip, Exterior Negative Moment</b>							
DESIGN SLAB	0.00	0.00	0.00	0.00	0.00	0.00	0.00
Wood and Armer	0.00	0.00	0.00	0.00	0.00	0.00	0.00
Equivalent Column	0.00	0.00	-	0.00	-	0.00	-
<b>Middle Strip, Positive Moment</b>							
DESIGN SLAB	1.240	1.144	1.122	1.243	0.990	0.833	1.085
Wood and Armer	1.266	1.171	1.148	1.258	1.009	0.861	1.109
Equivalent Column	1.428	1.124	-	1.201	-	0.845	-
<b>Middle Strip, Interior Negative Moment</b>							
DESIGN SLAB	1.071	1.029	0.927	0.897	0.939	0.895	0.853
Wood and Armer	1.095	1.046	0.948	0.923	0.960	0.908	0.871
Equivalent Column	1.157	0.955	-	0.826	-	0.830	-

(All units in<sup>2</sup>.)

**Table 5.16:** Example 4 - N/S Ratio of Resultant Torsional Moment to Bending Moment for Pattern Loadings

Location	Uniform	PLC #1	PLC #2	PLC #3	PLC #4	PLC #5	PLC #6
<b>INTERIOR</b>							
Column Strip, Negative Moment	10.53%	12.45%	12.00%	10.77%	6.76%	10.31%	14.46%
Column Strip, Positive Moment	0.79%	9.02%	0.80%	1.20%	1.12%	0.56%	0.44%
Middle Strip, Negative Moment	0.00%	0.00%	3.12%	0.00%	0.00%	0.00%	0.00%
Middle Strip, Positive Moment	0.00%	0.00%	1.59%	0.00%	0.00%	0.00%	0.00%
<b>EXTERIOR</b>							
Column Strip, Exterior Negative Moment	33.47%	33.64%	33.35%	39.40%	16.83%	25.50%	50.79%
Column Strip, Positive Moment	12.78%	12.38%	11.84%	8.06%	14.34%	19.36%	11.16%
Column Strip, Interior Negative Moment	18.89%	17.93%	19.14%	17.90%	15.68%	19.91%	22.22%
Middle Strip, Exterior Negative Moment	0.00%	0.00%	0.00%	0.00%	0.00%	0.00%	0.00%
Middle Strip, Positive Moment	0.00%	0.00%	2.10%	0.00%	0.00%	0.00%	0.00%
Middle Strip, Interior Negative Moment	0.00%	0.00%	3.12%	0.00%	0.00%	0.00%	0.00%



**Table 5.17:** Example 4 - E/W Interior Region Design Results

Bending Moment Results (kip-ft):

Location	Direct Design	Equiv. Column	Wood & Armer	DESIGN SLAB
Column Strip, Negative Moment	-78.30	-132.83	-117.65	-118.99
Column Strip, Positive Moment	33.73	-9.90	8.31	8.30
Middle Strip, Negative Moment	-26.10	-44.28	-55.20	-51.46
Middle Strip, Positive Moment	22.49	-6.60	-4.39	-4.40

Area of Steel Required (in<sup>2</sup>):

Location	Direct Design	Equiv. Column	Wood & Armer	DESIGN SLAB
Column Strip, Negative Moment	2.446	4.237	3.753	3.775
Column Strip, Positive Moment	1.037	0.302	0.253	0.253
Middle Strip, Negative Moment	0.800	1.366	1.710	1.592
Middle Strip, Positive Moment	.689	0.201	0.136	0.134

**Table 5.18:** Example 4 - E/W Exterior Region Design Results

Bending Moment Results (kip-ft):

Location	Direct Design	Equiv. Column	Wood & Armer	DESIGN SLAB
Column Strip, Exterior Negative Moment	-76.44	-39.10	-66.94	-66.08
Column Strip, Positive Moment	91.73	108.66	89.49	88.27
Column Strip, Interior Negative Moment	-154.35	-148.13	-139.75	-148.64
Middle Strip, Exterior Negative Moment	0.00	0.00	0.00	0.00
Middle Strip, Positive Moment	61.15	72.44	77.91	82.47
Middle Strip, Interior Negative Moment	-51.45	-49.38	-49.93	-49.72

Area of Steel Required (in<sup>2</sup>):

Location	Direct Design	Equiv. Column	Wood & Armer	DESIGN SLAB
Column Strip, Exterior Negative Moment	2.387	1.204	2.136	2.055
Column Strip, Positive Moment	2.880	3.434	2.805	2.768
Column Strip, Interior Negative Moment	4.966	4.754	4.549	4.771
Middle Strip, Exterior Negative Moment	0.000	0.000	0.000	0.000
Middle Strip, Positive Moment	1.899	2.258	2.436	2.581
Middle Strip, Interior Negative Moment	1.592	1.527	1.543	1.537

**Table 5.19:** Example 4 - E/W Interior Bending Moments for Pattern Loadings

Location/Method	Uniform	PLC #1	PLC #2	PLC #3	PLC #4	PLC #5	PLC #6
<b>Column Strip, Negative Moment</b>							
DESIGN SLAB	-118.99	-112.26	-115.05	-99.83	-100.58	-99.59	-98.84
Wood and Armer	-117.65	-110.81	-113.31	-98.85	-100.65	-98.34	-96.54
Equivalent Column	-132.83	-	-129.75	-	-115.58	-	-107.03
<b>Column Strip, Positive Moment</b>							
DESIGN SLAB	8.30	8.72	12.17	6.45	-2.65	7.47	16.58
Wood and Armer	8.31	8.73	12.98	6.46	-2.65	7.48	16.59
Equivalent Column	-9.90	-	-2.02	-	-21.06	-	4.49
<b>Middle Strip, Negative Moment</b>							
DESIGN SLAB	-51.46	-45.26	-49.45	-43.84	-46.52	-42.39	-39.72
Wood and Armer	-55.20	-48.69	-52.90	-46.88	-50.13	-45.64	-42.39
Equivalent Column	-44.28	-	-43.25	-	-38.53	-	-35.68
<b>Middle Strip, Positive Moment</b>							
DESIGN SLAB	-4.40	-3.00	0.97	-5.49	-13.44	-1.88	6.07
Wood and Armer	-4.39	-2.99	-0.41	-5.49	-13.43	-1.87	6.07
Equivalent Column	-6.60	-	-1.34	-	-14.04	-	3.00

(All units kip-ft.)

**Table 5.20:** Example 4 - E/W Interior Area of Steel Computed for Pattern Loadings

Location/Method	Uniform	PLC #1	PLC #2	PLC #3	PLC #4	PLC #5	PLC #6
Column Strip, Negative Moment							
DESIGN SLAB	3.775	3.531	3.645	3.127	3.169	3.120	3.112
Wood and Armer	3.753	3.525	3.608	3.127	3.183	3.110	3.054
Equivalent Column	4.237	-	4.134	-	3.662	-	3.380
Column Strip, Positive Moment							
DESIGN SLAB	0.253	0.266	0.371	0.196	0.081	0.228	0.507
Wood and Armer	0.253	0.266	0.396	0.199	0.083	0.228	0.507
Equivalent Column	0.302	-	0.061	-	0.645	-	0.137
Middle Strip, Negative Moment							
DESIGN SLAB	1.592	1.397	1.529	1.353	1.437	1.307	1.224
Wood and Armer	1.710	1.505	1.637	1.447	1.550	1.409	1.307
Equivalent Column	1.366	-	1.334	-	1.186	-	1.098
Middle Strip, Positive Moment							
DESIGN SLAB	0.134	0.091	0.030	0.167	0.410	0.057	0.185
Wood and Armer	0.136	0.098	0.048	0.167	0.410	0.072	0.185
Equivalent Column	0.201	-	0.041	-	0.429	-	0.091

(All units in<sup>2</sup>.)

**Table 5.21:** Example 4 - E/W Exterior Bending Moments for Pattern Loadings

Location/Method	Uniform	PLC #1	PLC #2	PLC #3	PLC #4	PLC #5	PLC #6
<b>Column Strip, Exterior Negative Moment</b>							
DESIGN SLAB	-66.08	-61.56	-61.34	-55.78	-62.92	-54.97	-47.83
Wood and Armer	-66.94	-62.51	-62.18	-56.27	-63.68	-55.96	-48.53
Equivalent Column	-39.10	-	-35.80	-	-37.90	-	-27.60
<b>Column Strip, Positive Moment</b>							
DESIGN SLAB	88.27	81.84	81.88	74.74	84.32	73.22	63.64
Wood and Armer	89.49	82.88	83.03	75.84	85.26	74.16	64.76
Equivalent Column	108.66	-	100.32	-	103.98	-	78.12
<b>Column Strip, Interior Negative Moment</b>							
DESIGN SLAB	-148.64	-139.48	-141.27	-125.09	-131.59	-124.03	-117.54
Wood and Armer	-139.75	-131.03	-132.72	-117.55	-124.00	-116.70	-110.64
Equivalent Column	-148.13	-	-143.03	-	-130.35	-	-117.90
<b>Middle Strip, Exterior Negative Moment</b>							
DESIGN SLAB	0.00	0.00	0.00	0.00	0.00	0.00	0.00
Wood and Armer	0.00	0.00	0.00	0.00	0.00	0.00	0.00
Equivalent Column	0.00	-	0.00	-	0.00	-	0.00
<b>Middle Strip, Positive Moment</b>							
DESIGN SLAB	82.47	73.77	76.38	67.82	79.14	70.41	59.09
Wood and Armer	77.91	69.75	72.19	64.01	74.64	66.57	55.94
Equivalent Column	72.44	-	66.88	-	69.32	-	52.08
<b>Middle Strip, Interior Negative Moment</b>							
DESIGN SLAB	-49.72	-43.74	-48.06	-42.36	-43.57	-40.97	-39.76
Wood and Armer	-49.93	-44.94	-48.41	-42.59	-43.79	-41.10	-40.36
Equivalent Column	-49.38	-	-47.68	-	-43.45	-	-39.30

(All units kip-ft.)

**Table 5.22:** Example 4 - E/W Exterior Area of Steel Computed for Pattern Loadings

Location/Method	Uniform	PLC #1	PLC #2	PLC #3	PLC #4	PLC #5	PLC #6
<b>Column Strip, Exterior Negative Moment</b>							
DESIGN SLAB	2.055	1.906	1.905	1.724	1.955	1.698	1.478
Wood and Armer	2.136	1.987	1.976	1.782	2.026	1.769	1.526
Equivalent Column	1.204	-	1.101	-	1.167	-	0.847
<b>Column Strip, Positive Moment</b>							
DESIGN SLAB	2.768	2.549	2.562	2.323	2.640	2.275	1.978
Wood and Armer	2.805	2.592	2.597	2.366	2.669	2.312	2.012
Equivalent Column	3.434	-	3.160	-	3.280	-	2.441
<b>Column Strip, Interior Negative Moment</b>							
DESIGN SLAB	4.771	4.426	4.522	3.951	4.195	3.916	3.727
Wood and Armer	4.549	4.244	4.301	3.779	4.003	3.750	3.541
Equivalent Column	4.754	-	4.581	-	4.154	-	3.739
<b>Middle Strip, Exterior Negative Moment</b>							
DESIGN SLAB	0.00	0.00	0.00	0.00	0.00	0.00	0.00
Wood and Armer	0.00	0.00	0.00	0.00	0.00	0.00	0.00
Equivalent Column	0.00	-	0.00	-	0.00	-	0.00
<b>Middle Strip, Positive Moment</b>							
DESIGN SLAB	2.581	2.301	2.385	2.111	2.473	2.194	1.833
Wood and Armer	2.436	2.174	2.252	1.991	2.331	2.072	1.735
Equivalent Column	2.258	-	2.081	-	2.159	-	1.612
<b>Middle Strip, Interior Negative Moment</b>							
DESIGN SLAB	1.537	1.349	1.485	1.306	1.344	1.263	1.225
Wood and Armer	1.543	1.387	1.496	1.313	1.351	1.267	1.243
Equivalent Column	1.527	-	1.473	-	1.340	-	1.211

(All units in<sup>2</sup>.)

**Table 5.23:** Example 4 - E/W Ratio of Resultant Torsional Moment to Bending Moment for Pattern Loadings

Location	Uniform	PLC #1	PLC #2	PLC #3	PLC #4	PLC #5	PLC #6
<b>INTERIOR</b>							
Column Strip, Negative Moment	5.84%	4.36%	5.10%	7.63%	6.17%	4.04%	5.50%
Column Strip, Positive Moment	1.17%	0.76%	6.14%	0.12%	3.52%	2.28%	0.42%
Middle Strip, Negative Moment	0.00%	3.36%	0.00%	0.00%	0.00%	0.00%	0.00%
Middle Strip, Positive Moment	0.00%	4.63%	0.00%	0.00%	0.00%	0.00%	0.00%
<b>EXTERIOR</b>							
Column Strip, Exterior Negative Moment	3.34%	0.04%	3.27%	5.49%	3.71%	12.31%	2.86%
Column Strip, Positive Moment	3.13%	2.53%	3.16%	3.35%	2.62%	2.91%	3.81%
Column Strip, Interior Negative Moment	0.76%	0.12%	0.46%	2.00%	0.93%	3.55%	0.58%
Middle Strip, Exterior Negative Moment	0.00%	0.00%	0.00%	0.00%	0.00%	0.00%	0.00%
Middle Strip, Positive Moment	0.00%	1.36%	0.00%	0.00%	0.00%	0.00%	0.00%
Middle Strip, Interior Negative Moment	0.00%	6.87%	0.00%	0.00%	0.00%	0.00%	0.00%

significant torsional effects for cuts oriented in this direction. Table 5.16 gives the ratio of resultant torsional moment,  $M_T$ , to resultant bending moment,  $M_B$ , as a percentage at each design location for all loading conditions. For instance, in the exterior region at the column strip exterior negative moment location, a torsional moment equal to 33.47% of the bending moment was computed. Under loading condition PLC #6, this percentage was as large as 50.79%. It was under conditions such as these, where significant torsional effects occurred, that the results of the DESIGN SLAB command deviated the most from the Wood and Armer results. In the exterior region at the column strip exterior negative moment location, under the uniform loading condition the DESIGN SLAB command calculated a bending moment of -34.96 kip-ft, while the Wood and Armer method computed a bending moment of -46.45 kip-ft. At the same location under loading condition PLC #6, the DESIGN SLAB command calculated a bending moment of -28.71 kip-ft, while the Wood and Armer method computed a bending moment of -37.94 kip-ft. Both cases demonstrated a difference in design moment of approximately 10 kip-ft, and the Wood and Armer method produced the higher value in both cases. At numerous other locations with a large percentage of torsional moment, the Wood and Armer technique predicted a higher moment than the DESIGN SLAB command, indicating that the DESIGN SLAB command does not produce an appropriate bending moment for design in areas of high torsional moment ( $> 30\%$ ).

In the East/West direction, comparison of direct design results and equivalent column results in Tables 5.17 and 5.18 show substantial disagreement in terms of bending moments computed. This was particularly evident in the interior column strip negative moment region as well as the exterior column strip negative moment region. The reason for this discrepancy is an important limitation of the direct design method. While the equivalent column method explicitly accounts for the size of the column in the computation of the equivalent column stiffness, direct design only accounts for the size of the column in terms of the clear distance between the columns in the strip. As such, under direct design, the column strip negative moment in a system with 12 inch square columns *could* be the same as that of a system with 24 inch square columns, provided the clear distance was the same. Obviously, the latter case should generate more negative moment because of the increased



column stiffness. In this example, the column size used (12 inches square) was relatively small, so deviation between the direct design and equivalent column techniques in the regions adjacent to the columns was expected. Further comparison of design moments and area of steel in the East/West direction shows that the DESIGN SLAB command produced design moments and subsequent reinforcement in close agreement with the Wood and Armer technique.

Unlike Example 3, the DESIGN SLAB command appeared to more accurately compute the values of bending moment in both the exterior and interior East/West strips at the column face, in comparison with the equivalent column technique and direct design results. Because the columns were more flexible (due to a much smaller column size than Example 3), the finite element method appeared to more accurately represent the stiffness of the connection. This suggests agreement with the equivalent column method may only be applicable for a range of column sizes, and must be further investigated.

In Table 5.17, an interesting trend emerged relating to the positive moment regions in the East/West interior panel. Because the exterior spans in the East/West direction were longer than the interior span, the equivalent column method resulted in the entire interior panel exhibiting negative bending, such that a positive bending moment was never developed at the middle of the panel under uniform loading. Direct design does not account for this case, as evidenced by the large positive moments computed. The DESIGN SLAB command, however, showed that the entire interior panel was not in negative bending. Instead, the moment in the column strip positive moment region was in fact positive, while the moment in the middle strip positive moment region was in fact negative. The equivalent column method is incapable of generating a distribution of bending moments such as this – both strips are limited to the same sign. This demonstrated that the DESIGN SLAB command is preferable to both simplified techniques because it created a more detailed representation of the three-dimensional plate behavior of the system, instead of reducing the system to a simplified two-dimensional approximation.

In general, pattern live loadings had little effect in terms of increasing bending moments in the East/West direction. The two primary locations that experienced an increase in

bending moment were the interior positive moment regions in the column strip and middle strip. In both of these areas, the magnitude of the design moment was not only increased, but the pattern loadings created a full moment sign reversal. A reversal such as this indicates the need for reinforcement on both faces.

Table 5.23 shows the torsional moment percentages for the East/West strips. Note that since the slab-beam was symmetric, only small torsional effects were developed. The maximum torsional percentage was 12.31%, developed at the column strip exterior negative moment region under loading condition PLC #5. At this location and loading condition, the DESIGN SLAB command computed a design moment of -54.97 kip-ft, while the Wood and Armer method computed a design moment of -55.96 kip-ft. The close agreement between the DESIGN SLAB command and Wood and Armer suggests that at the maximum torsional moment of 12.31% the bending moment, the DESIGN SLAB command can be used even though it does not explicitly account for the torsional effects.

## **5.5 Example 5 - Square Flat Plate Fix-Supported on Two Sides**

Example 5 demonstrated a critical example of the role that torsional moments can play in the distribution of reinforcement in a slab system.

The geometry of Example 5 is given in Figure 5.15. The structure was a 30 ft by 30 ft flat plate. The slab was fix-supported on two adjacent sides, and the other two adjacent sides were free. The slab was 12 inches thick and constructed with 4000 psi concrete. The slab was loaded with self-weight along with 50 psf live load.

The system was modeled in GT STRUDL. The flat plate was modeled using triangular BPHT elements [13]. Triangular elements were used so as to orient the mesh lines for diagonal cuts. For the fixed edges, all degrees of freedom were restrained at each node. The model contained 961 nodes, 1800 elements, and solved in 0.86 seconds.

Four design cuts, labeled 1-4 in Figure 5.15, were evaluated and designed. Cuts 1 and 2 were orthogonal with respect to the edges of the structure, and cuts 3 and 4 were diagonal (oriented at  $45^\circ$ ) with respect to the edges of the structure. The computed bending moment

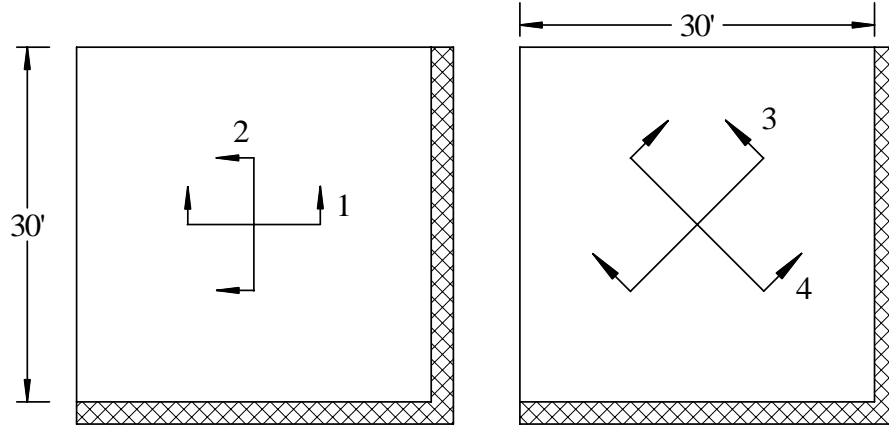


**Figure 5.15:** Example 5 - Geometry

**Table 5.24:** Effect of Torsion

Cut #	Bending Moment (k-ft)	Torsional Moment (k-ft)	$A_{s,required}$ (in <sup>2</sup> )	Surface
1	6.51	240.09	0.1405	Bottom
2	6.51	-240.09	0.1405	Bottom
3	-176.10	0.00	3.8703	Top
4	172.85	5.87	3.7974	Bottom

as well as required area of steel computed for each cut are presented in Table 5.24.

The result of this example was that for the given conditions, the reinforcement provided in both directions by cuts 1 and 2 was insufficient to resist the bending moments computed about cuts 3 and 4. For the required bending moment from cut 3 to be resisted by the combined reinforcement from cuts 1 and 2, cuts 1 and 2 must have each provided  $176.10/\sqrt{2} = 124.52$  kip-ft of resistance via top bars. For the required bending moment from cut 4 to be resisted by the combined reinforcement from cuts 1 and 2, cuts 1 and 2 must have each provide  $172.85/\sqrt{2} = 122.22$  kip-ft of resistance via bottom bars.

Instead, cuts 1 and 2 only provided steel on the bottom face, and the area of steel provided was dangerously insufficient to resist the principal bending moments in the system. For bottom reinforcement, each direction was designed for 6.51 kip-ft when it should have been designed for 122.22 kip-ft.

To investigate this deviation, cuts 1 and 2 were designed using the Wood and Armer

method. The result of these computations were that the Wood and Armer technique provided reinforcement for both top and bottom for both cuts 1 and 2 that was close to that required to resist the principal bending moments computed using element forces along cuts 3 and 4. When transformed to the principal directions, the Wood and Armer method provided 3.85 in<sup>2</sup> of steel in the top (compared to 3.87 in<sup>2</sup> required), and 3.42 in<sup>2</sup> of steel in the bottom (compared to 3.79 in<sup>2</sup> required).

The reason for the large variation in design between these various cuts and methodologies is that, at the present time, design using element forces does not incorporate the torsional moment acting on the cross-section into the design bending moment. For cuts 1 and 2, the resultant torsional moment was much larger than the resultant bending moment, indicating that that cuts 1 and 2 were not oriented orthogonally to the directions of principal bending. Figure 5.16 shows the  $M_{xx}$ ,  $M_{xy}$ , and  $M_{yy}$  bending resultant contours, confirming that the design cuts were located at the region of highest  $M_{xy}$  bending stresses in the system. In such a region, the resultant torsional moment cannot simply be added to the bending moment, analogous to the Wood and Armer method. First of all, this example problem showed that adding  $M_T$  to  $M_B$  would be prohibitively inefficient – each direction would be designed for a capacity of 246.60 kip-ft (over twice the required value). Second, whereas in the Wood and Armer method  $M_{xy}$  acts in the same direction as both  $M_{xx}$  and  $M_{yy}$ , in the DESIGN SLAB method the resultant torsional moment from element forces acts orthogonally to the resultant bending moment. As such, the direct combination of the  $M_B$  and  $M_T$  acting on a cross-section is not justified.

This does not mean that the proposed methodology cannot appropriately design the given structure in this example. Instead, cuts must be oriented so as to roughly correspond orthogonally to the principal bending directions. If the cut lies at a skew to the principal axes, a large torsional moment will be present. In GT STRUDL, vectors showing the directions of principal bending can be generated graphically and are useful for determining the appropriate orientation of strips. For the structure in Example 5, the principal bending vectors M1 and M2 are shown in Figure 5.17. A tool such as this allows the user to efficiently understand the behavior of the system in order to select appropriate cuts. Based on these

principal bending vectors, the user would know to design using cuts 3 and 4 from Figure 5.15 instead of cuts 1 and 2.

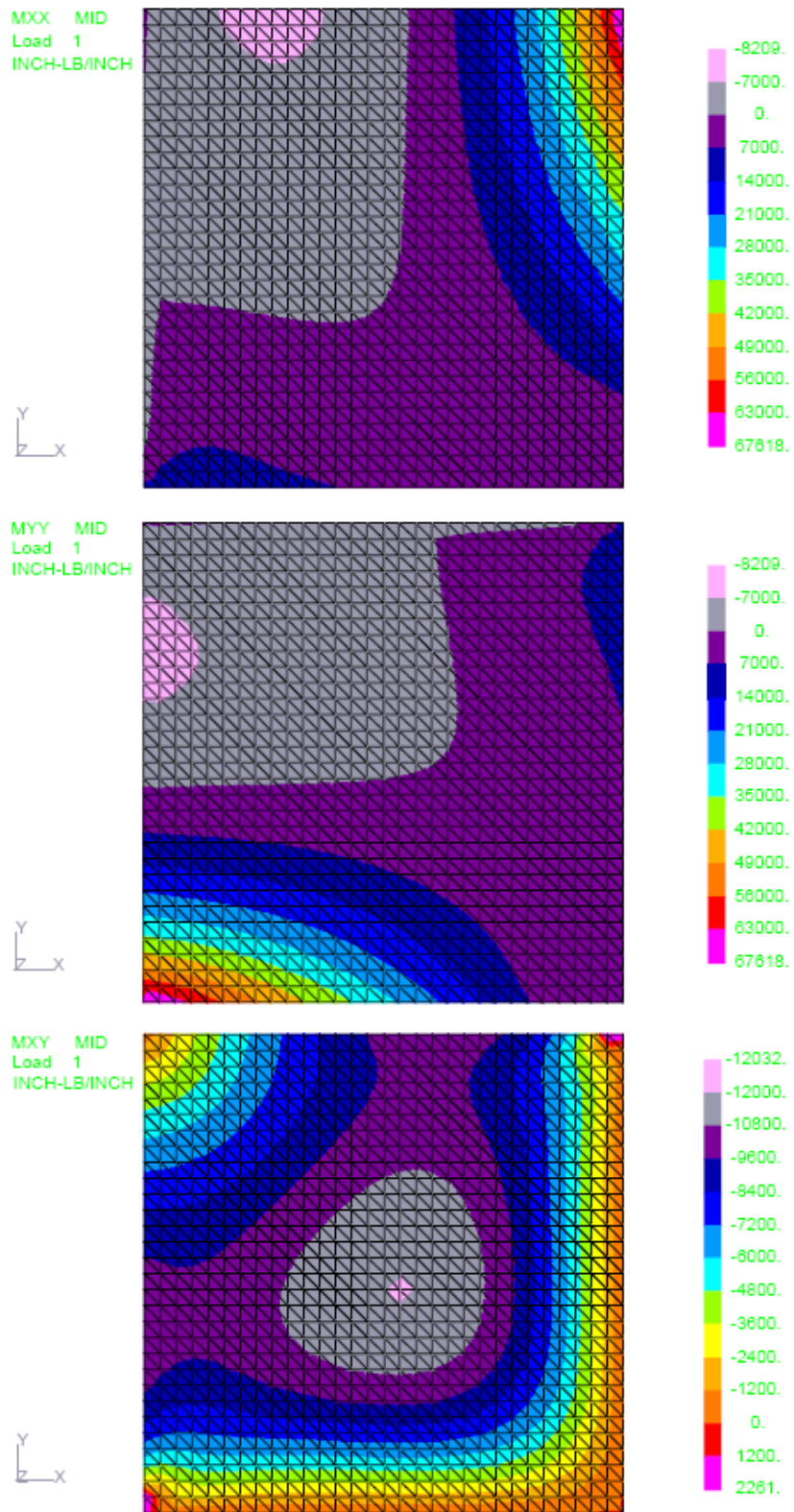


**Figure 5.16:** Example 5 - Bending Resultant Contours

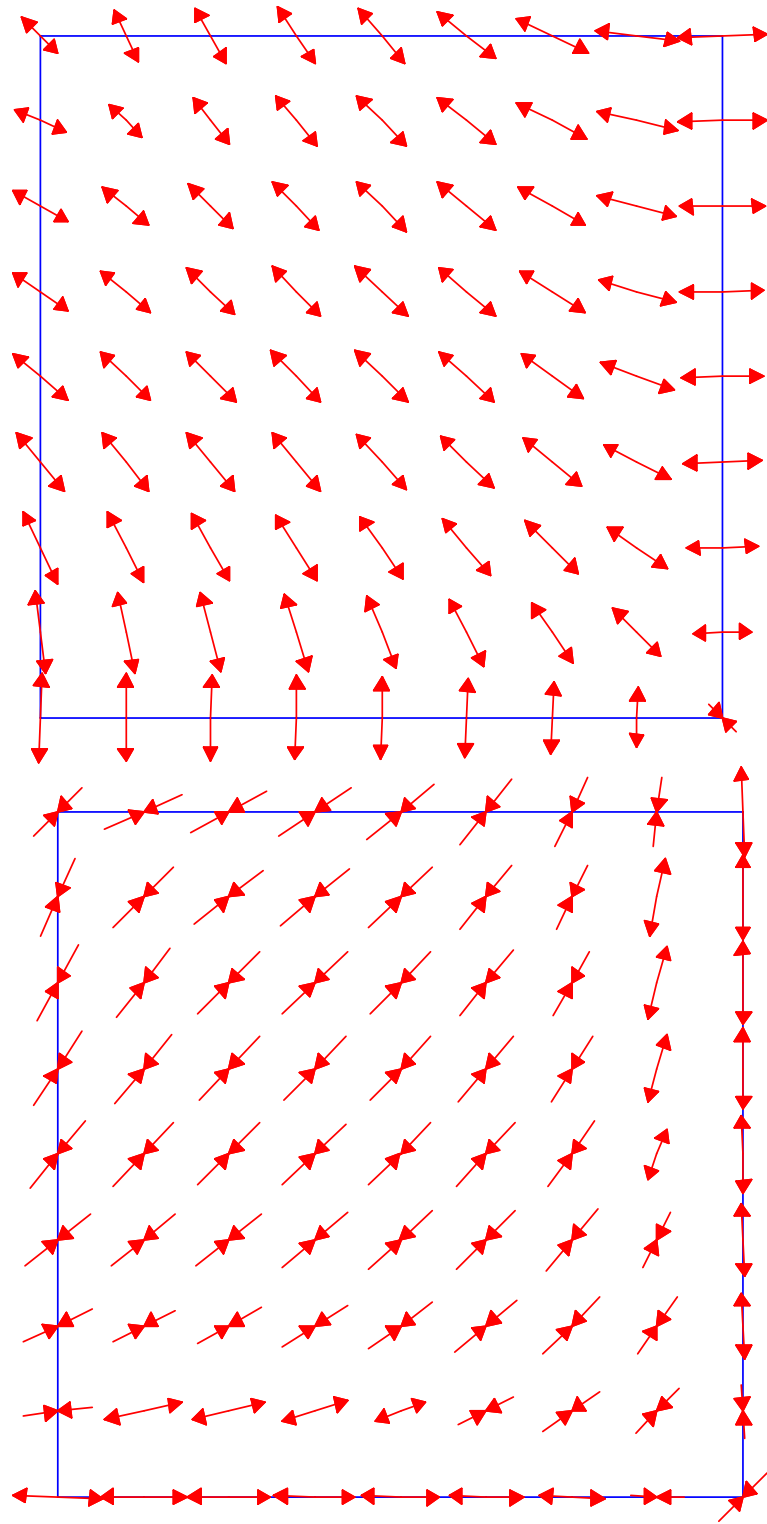


**Figure 5.17:** Example 5 - Principal Bending Vectors - M1 (top) and M2 (bottom)

## CHAPTER VI

### CONCLUSIONS

#### 6.1 Summary

In this study, a procedure was developed in GT STRUDL to design reinforced concrete flat plate systems based on the results of finite element analysis.

The current state-of-practice of reinforced concrete flat plate design was reviewed, including the ACI direct design and equivalent frame techniques, the yield line method, and the strip design method. The principles of these methods along with a critical evaluation of their applicability and limitations were presented as motivation for a finite element based design procedure.

The current state-of-the-art of flat plate design based on finite element results was presented. Various flat plate modeling techniques were evaluated. Design methods studied included the Wood and Armer approach, based on element stress resultants, and the resultant force approach, based on element forces.

A flat plate design procedure based on the element force approach, the DESIGN SLAB command, was implemented in GT STRUDL. The DESIGN SLAB command provides the user the ability to specify a design cross-section simply by a start and end node, an element in the plane of the cut, and several optional design parameters. The procedure then determines all nodes and elements along the cut, computes the resultant forces and moments acting on the cut, and designs according to ACI 318 and any input parameters, such as bar size and spacing, specified by the user.

Several realistic flat plate systems were modeled and designed using the implemented procedure. These examples allowed for critical comparison with results from experimental studies and currently applied design methods to determine the applicability of the implemented procedure. The DESIGN SLAB command was shown to produce design moments for regular flat plate systems in agreement with experimental data as well as conventional



design techniques. ACI column and middle strips were used to define the cut sections for the DESIGN SLAB command.

In the given examples, a technique for modeling slab-to-column connections using joint constraints was shown to appropriately simulate the transfer of moment over a finite area. The results obtained employing this technique did not differ significantly from those obtained by modeling the columns with 3D solid elements. The rigid solid technique is much more efficient than use of 3D solids, both in terms of modeling time as well as computational cost, and as such is recommended for the modeling of slab-to-column connections.

Example 1 of Chapter 5 demonstrated that an appropriate mesh size must be used for the computation of accurate design results. An inappropriate mesh size can lead to a significant error in the area of steel computed. For the structure in Example 1, the percent change in area of steel computed between the most coarse mesh containing 16 elements and the finest mesh containing 1024 elements was 19%.

In Example 2 of Chapter 5, the DESIGN SLAB command was shown to accurately represent the total static moment in the interior panel of a square, 3-bay flat plate system. This example showed that the finite element model was generally stiffer at column connections than the experimental structure. As such, the DESIGN SLAB solution distributed more moment to the column strip negative moment region and less to the middle strip negative moment region than the experimental structure. The distribution of interior positive moment was accurately predicted using the DESIGN SLAB command. A comparison of a simplified model neglecting edge beams and a detailed model including edge beams showed that modeling edge beams when present significantly affects the distribution of moment in the system.

In Examples 3 and 4 of Chapter 5, the DESIGN SLAB command was used to design interior and exterior panels of two 3-bay flat plate structures subjected to pattern loadings. Example 3 had uniform column spacing in both directions, while Example 4 contained varied column spacing. The DESIGN SLAB results for the interior panels agreed with both Wood and Armer design results as well as results of the direct design and equivalent column techniques. The DESIGN SLAB and Wood and Armer techniques showed agreement in the

exterior regions, although both finite element techniques produced moment distributions different from the results of the direct design and equivalent column techniques, particularly at the exterior column strip negative moment region.

For cross-sections in a flat plate system where a large resultant torsional moment is present, designing reinforcement based on bending moments computed from element forces may be inappropriate. For Examples 3 and 4, the ratio of resultant torsional moment to resultant bending moment was computed at each design cross-section under pattern loading conditions. When this ratio was less than 15%, the DESIGN SLAB command was generally shown to provide more reinforcement than the Wood and Armer method. However, when the torsional moment ratio exceeded 15%, the DESIGN SLAB command was shown to provide significantly less reinforcement than the Wood and Armer technique. As a result of these studies, a warning was implemented in the program to notify the user if the torsional moment exceeds 10% of the bending moment for a cross-section.

Example 5 of Chapter 5 showed that when cuts were not defined orthogonally to the directions of principle bending, resulting designs could significantly under-reinforce the cross-section. As such, cuts are recommended to be oriented orthogonally to the directions of principle bending. If taking such a cut is prohibitive due to the element mesh geometry, the Wood and Armer technique is recommended.

## **6.2 Future Work**

### **6.2.1 Recommendations for Research**

One of the most significant questions raised by this study pertained to the correct processing of the resultant torsional moment acting on a cross-section,  $M_T$ . At the present time, no proposed method for including this component as a part of the design envelope was developed.

Future research must be conducted to further define the scenarios in which significant torsional moments are developed, and to define acceptable torsional moment bounds for application of resultant force-based design. Furthermore, research must be conducted into why for some cases of moderate torsional moment the DESIGN SLAB command was shown

to provide more reinforcement than the Wood and Armer method, which directly accounts for torsional effects. The effect of mesh sensitivity must be evaluated in such cases.

The ultimate goal of this study was to develop a framework for the eventual extension of the proposed methods to highly irregular structures. Highly irregular structures include those with openings, non-orthogonal boundaries and reinforcement, non-orthogonal column lines, radial reinforcement, and plate/shear wall interaction. Such structures were not evaluated in this study, and the implemented procedure cannot be assumed to be applicable to such structures. Instead, it must be validated with analytical and/or experimental studies of irregular structures of a variety of classifications.

Further research must be applied toward the development of methodologies for modeling nonlinearity in reinforced concrete flat plates. Implementation of such a methodology will allow for a distribution of reinforcement corresponding to the distribution of bending moments at the ultimate condition. Once this tool has been developed, the distribution of reinforcement based on nonlinear analysis must be studied and contrasted with that of linear elastic analysis to determine the method most appropriate for design practice.

The capability to analyze and reinforce for direct punching shear and moment transfer shear at column-to-slab connections was not implemented. Instead, for each cross-section, the resultant shear is checked against the shear strength computed based on beam shear design. A procedure to account for direct punching shear and moment transfer shear using finite elements must be developed. This is especially significant for flat plates because shear at slab-to-column connections controls the design in many applications [58].

Only gravity loading conditions were considered in this study. Before the proposed methodology can be applied in the design of structures subjected to lateral loads, it must be validated by comparison with analytical solutions and experimental studies of laterally loaded flat plate structures.

### **6.2.2 Program Enhancements**

In the current implementation of the DESIGN SLAB command, a user must specify the input data via the GT STRUDL Command Window. In order to input this information,

the user must have previously gathered the cut data from the graphical user interface, GT Menu. In GT Menu, the user must determine which joints form the beginning and end of the cut, and also determine an element in the plane of the cut.

If, instead, the user could graphically select the start node, end node, and in-plane element defining the cut, productivity would be greatly enhanced. By implementing this change in GT Menu, the step of transferring the cut information from GT Menu to the Command Window would be bypassed, possibly reducing the amount of time required to design a cut by a factor of two.

Also, in the current implementation, all strips must be defined individually by the user. Automation of the strip selection procedure would greatly enhance the productivity of the user. The primary point of concern related to automation of strip selection is related to the responsibility of the engineer in the design process. The manner in which the command is currently implemented places the responsibility on the user to select appropriate cuts and fully understand the consequences of the cuts they select. Automating this procedure may allow the user to think less during design and blindly accept the generated design without critically evaluating the relevance of the computer output. The extent of this point of concern cannot be evaluated until possible automation algorithms are developed and evaluated.

If the strip selection procedure were automated, the possibility would be opened for development of an adaptive algorithm to optimize the layout of strips and reinforcement with regard to various performance measures, such as reinforcement economy, deflections, etc.

Axial force was neglected in the design procedures implemented as described in this study. Axial forces, however, may become significant in some cases, and as such, the procedure must be extended to account for these effects. Incorporating axial forces would significantly change the manner in which the design forces are computed. The technique implemented in this study for determining the design envelope simply extracted the maximum positive and negative bending moments for each active loading condition. Once axial forces are considered, each loading case must be considered independently so that axial

forces remain coupled with the associated bending moments.

The DESIGN SLAB command was implemented with the future extension to other reinforced concrete systems in mind. By including axial force, several additional structural types could be analyzed. As such, the procedure could be extended to design shear walls, foundation structures, shells, tanks, and slabs with beams, drop panels, and column capitals. In addition, this would allow for the extension to prestressed slab systems.

## APPENDIX A

### COMPRESSION REINFORCEMENT

The purpose of this Appendix is to confirm the applicability of the assumption presented in Chapter 2 which stated that compression reinforcement can be neglected in the computation of ultimate moment strength. The greater aim of this Appendix was to show that for a range of geometric and loading configurations, “compression” reinforcement was not actually within the compression zone, but rather was very near the neutral axis and in tension.

A parametric study was conducted where the negative moment in an interior panel column strip was computed under a variety of conditions. The problem studied was as follows:

- Rectangular Bay Layout
- Longitudinal column spacing 1.5 times transverse column spacing
- Loading: Self-Weight + 50 psf live load
- $f'_c = 4000$  psi
- $f_y = 60000$  psi
- Longitudinal Column Spacing varies from 15 feet to 35 feet
- Thickness computed based on ACI ratio  $\frac{l}{33}$

Based on these parameters, the critical moment was computed for each case. Only the column strip negative moment was considered in this study in order to design the location of highest moment in the slab. The width was computed based on the ratio of longitudinal column spacing to transverse column spacing. Using this critical moment, the required area of steel was computed using Equation 2.7. The depth of the compression block was computed using Equation 2.3, and the depth to the neutral axis was computed as  $c = a/\beta_1$ .

**Table A.1:** Computation of Depth to Neutral Axis

Span (ft)	Thickness (in)	Moment (lb-in)	$A_{s,required}$ (in <sup>2</sup> )	Cover (in)	Neutral Axis Depth, $c$ (in)
15	5.45	266241	1.35	0.75	0.23
20	7.27	737455	2.51	0.75	0.33
25	9.09	1648082	4.24	0.75	0.44
30	10.91	3206864	6.62	0.75	0.57
35	12.73	5662423	9.78	0.75	0.73

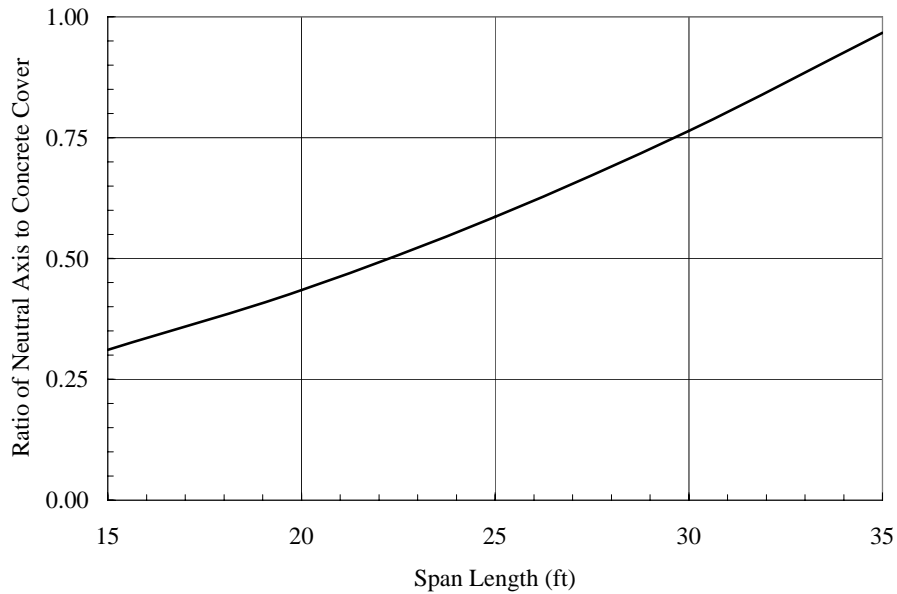


**Figure A.1:** Depth to Neutral Axis Divided by Concrete Cover

The results of these calculations are presented in Table A.1. The depth to the neutral axis,  $c$ , was then compared with the concrete cover.

Figure A.1 graphically shows the trends in Table A.1. This graph shows the ratio of the neutral axis depth,  $c$ , divided by the concrete cover versus the span length. Since this ratio was less than 1 for the range of spans considered, “compression” steel can be neglected in ultimate strength computations because this level of reinforcement was not even in compression. Instead, it was very close to the neutral axis and was in tension.

## APPENDIX B

### MODULE DESCRIPTIONS

The following is an alphabetical listing of all modules developed for the execution of the DESIGN SLAB command.

#### BARDAT.ICE

BARDAT.ice is called from various subroutines during the actual design procedure. This subroutine contains an array with information for all applicable bar sizes, including area and diameter. This subroutine is passed a bar size, and the area and diameter are returned. An additional flag is passed to this subroutine when called, and is set to either 1, 0, or -1. If the flag is set to 1, the next larger bar size than the current bar size and associated properties are returned. If the flag is set to -1, the next smaller bar size than the current bar size and associated properties are returned. If the flag is set to 0, the properties associated with the current bar size are returned.

#### CRCASR.ice

CRCASR.ice is called from CRCSLB.ice and computes the required area of steel to resist the bending moment design envelope. This subroutine first computes the minimum area of steel required to resist temperature and shrinkage effects. Then, the quadratic equation for area of steel required is solved iteratively. Once the area of steel required has converged, the area of steel required for temperature and shrinkage is compared with the area of steel required for flexure, and the maximum of these two values is the required area of steel returned to CRCSLB.ice.

#### CRCCEV.ice

CRCCEV.ice is called from CRCCMN.ice. This subroutine scans the RESULT array



for all active loadings to determine the maximum positive and negative bending moments computed on the section, thus defining the bending moment design envelope.

#### CRCCGC.ice

CRCCGC.ice is called from CRCCGE.ice. This subroutine is passed a node ID and returns the CUT system coordinates of the requested node by searching the array of CUT coordinates computed in CRCCTC.ice.

#### CRCCGE.ice

CRCCGE.ice is called CRCCMN.ice. This subroutine is responsible for building the list of elements along the cut to be used in the calculation of the resultant forces acting on the cut. All elements are checked, and those incident on the cut (the element candidates) are checked according to the selection rules explained in Chapter 4. Once an element has been determined to be included in the computation of force, the element is added to either a list of elements located on the positive Y-CUT side of the cut or to a list of elements located on the negative Y-CUT side of the cut.

#### CRCCGL.ice

CRCCGL.ice is called from CRCCMN.ice and is responsible for finding all nodes on a straight line between the start and end nodes of the cut. This subroutine retrieves the coordinates of the start and end nodes of the cut and defines the bounded region based on this information. Nodes within this bounded region are checked individually for collinearity with the cut line. Once all applicable nodes have been checked, this subroutine sorts all collinear nodes into the correct geometric order in the model.

#### CRCCMN.ice

CRCCMN.ice is the primary algorithm for the DESIGN SLAB command and is called from CRSLAB.cdl once all input data has been processed. This subroutine calls CRCCGL.ice to find all nodes on the cut and populate the cut node list. It calls CRCCTN.ice

to form the transformation to the CUT coordinate system, and then calls CRCCGE.ice to select which elements should be included in the cut definition. The node and element lists are then prepared for the resultant force computation by a call to CRCHEC.ice, and then for each side of the cut, a call is made to STCRES.ice, the primary algorithm of the CALCULATE RESULTANT command. The results of the CALCULATE RESULTANT command are interpreted and the design envelope is determined by calling CRCCEV.ice. CRCSLB.ice is then called in order to design the cross-section to resist the design envelope.

#### CRCCTC.ice

CRCCTC.ice is called from CRCCGE.ice. This subroutine transforms all nodes of all elements incident on the cut line to the CUT coordinate system. This information is then used in the element selection algorithm. Only the coordinates of the nodes of incident elements are transformed to increase the efficiency of solution.

#### CRCCTN.ice

CRCCTN.ice is called from CRCCMN.ice. This subroutine forms the transformation to the CUT coordinate system according to the theory set forth in Chapter 4.

#### CRCHEC.ice

CRCHEC.ice is called from CRCCMN.ice prior to each call to STCRES.ice for the computation of the resultant forces on the section. The purpose of this subroutine is to check that all elements in the element list are of constant thickness and material properties.

#### CRCSLB.ice

CRCSLB.ice is the subroutine containing the main design algorithm for the DESIGN SLAB command. This subroutine interprets the user input to determine the intention of the user and appropriate design method and parameters. The bending moment design envelope is interpreted to determine which surfaces of the slab must be reinforced. Initial design calculations such as material-related parameters are performed, and for each surface, a call

is made to CRCASR.ice to compute the area of steel required. Once the required area of steel has been computed, the appropriate design subroutine is called depending on the parameters specified in the user command. The design subroutine called is either CRSLM1.ice, CRSLM2.ice, CRSLM3.ice, or CRSLM4.ice. After the appropriate design routine returns a design bar size and spacing to CRCSLB.ice, a call is made to CRSULT.ice to compute the ultimate strength of the final design and compare with the design envelope. This subroutine also executes the beam shear check for the cross-section.

#### CRSLAB.cdl

CRSLAB.cdl is the primary CDL routine that processes the DESIGN SLAB command input parameters. First of all, this subroutine processes the cut name, node list, and element list. Design parameters associated with each surface of the slab are then processed, including specific reinforcement sizes and spacing to be used either for the top, bottom, or both faces. Finally, additional optional design parameters, such as reinforcement layer, concrete cover, and the torsional warning threshold, are processed. CRSLAB.cdl is called from DES.cdl.

#### CRSLM1.ice

CRSLM1.ice is called from CRCSLB.ice when the user has specified neither a bar size nor spacing for the cross-section being designed. This subroutine begins design by assuming a #5 bar, determining the number of #5 bars required to provide the required area of steel, and then computing the associated clear and center-to-center spacing. If spacing requirements are violated, the bar size is either increased or decreased and number bars and spacing recomputed until an acceptable design is found. If no acceptable design is found, the user is notified.

#### CRSLM2.ice

CRSLM2.ice is called from CRCSLB.ice when the user has specified a bar size but not

a spacing for the cross-section being designed. This subroutine begins design by determining the number of bars required (of the user-specified bar size) to provide the required area of steel, and then computing the associated clear and center-to-center spacing. If the center-to-center spacing computed is greater than the maximum allowable spacing, the center-to-center spacing is reduced to the maximum allowable spacing. If the minimum clear spacing requirement is violated, the cross-section cannot be designed with the user-specified bar size and the user is notified.

#### CRSLM3.ice

CRSLM3.ice is called from CRCSLB.ice when the user has specified a spacing but not a bar size for the cross-section being designed. The user-specified spacing is first checked against the maximum and minimum spacing requirements. If the spacing is valid, the area of steel required per bar is computed, and the smallest bar size satisfying this steel area is used. If a bar size with large enough area does not exist, the section is not designed and the user is notified.

#### CRSLM4.ice

CRSLM4.ice is called from CRCSLB.ice when the user has specified both a bar size and spacing for the cross-section being designed. When this occurs, the cross-section is simply checked for the user-specified bar size and spacing, and no modifications are made to the bar size or spacing if the section fails.

#### CRSULT.ice

CRSULT.ice is called from CRCSLB.ice. This subroutine provides the final ultimate strength check for the design, regardless of the design method or which properties the user may have constrained. First of all, the actual  $d$ -distance is computed based on the final design bar size, and the total area of steel provided in the cross-section is computed. The depth of the rectangular compression block is computed, along with the depth to the neutral axis to check the strain condition in the reinforcement. Based on the reinforcement strain,

the appropriate strength reduction factor is determined, and the ultimate moment capacity of the section is computed. CRSULT.ice is called separately for the design of the top and bottom surfaces. The numerical results of the ultimate strength check are reported to the user via the GT STRUDL Output Window.

#### DES.cdl

DES.cdl is the first routine called when the DESIGN SLAB command is given. This command is the initially called routine for any GT STRUDL command beginning with the word DESIGN. When the SLAB modifier is present, this subroutine calls CRSLAB.cdl, which processes all information relevant to the DESIGN SLAB command.

## REFERENCES

- [1] ADINI, A. and CLOUGH, R. W., “Analysis of Plate Bending By the Finite Element Method,” 1960. G7337 Report to the National Science Foundation.
- [2] American Concrete Institute, *ACI 318 Building Code Requirements for Structure Concrete and Commentary*, 2002.
- [3] ANDERHEGGEN, E., E. A., “Reinforced-Concrete Dimensioning Based on Element Nodal Forces,” *ASCE Journal of the Structural Division*, vol. 102, pp. 1718–1731, June 1994.
- [4] ARMER, G. S. T., “Discussion of Reference [72],” *Concrete*, vol. 2, pp. 319–320, August 1968.
- [5] BARZEGAR, F. and MADDIPUDI, S., “Generating Reinforcement in FE Modeling of Concrete Structures,” *ASCE Journal of the Structural Division*, vol. 120, pp. 1656–1662, May 1994.
- [6] BASHUR, F. K. and DARWIN, D., “Nonlinear Model for Reinforced Concrete Slabs,” *ASCE Journal of the Structural Division*, vol. 104, pp. 157–170, January 1978.
- [7] BICÁNIC, N., DE BORST, R., MANG, H., and MESCHKE, G., eds., *COMPUTATIONAL MODELING OF CONCRETE STRUCTURES*. Lisse, The Netherlands: A.A. Balkema Publishers, 2003.
- [8] BORKOWSKI, A., “Optimization of Slab Reinforcement by Linear Programming,” *Computer Methods in Applied Mechanics and Engineering*, vol. 12, pp. 1–17, September 1977.
- [9] BROTCHE, J. F. and RUSSELL, J. J., “Flat Plate Structures: Elastic-Plastic Analysis,” *Journal of the American Concrete Institute*, vol. 61, pp. 959–996, August 1964.
- [10] CHEUNG, Y. K., KING, I. P., and ZIENKIEWICZ, O. C., “Slab Bridges with Arbitrary Shape and Support Conditions: A General Method of Analysis Based on Finite Elements,” *Institution of Civil Engineers - Proceedings*, vol. 40, pp. 9–36, May 1968.
- [11] CLOUGH, R., “The Finite Element Method After Twenty-Five Years,” *Computers and Structures*, vol. 12, pp. 361–370, 1980.
- [12] Computer Aided Structural Engineering Center, Georgia Institute of Technology, Atlanta, GA, *GT STRUDL User Reference Manual Abstract of Commands*, 1999. Revision R.
- [13] Computer Aided Structural Engineering Center, Georgia Institute of Technology, Atlanta, GA, *GT STRUDL User Reference Manual Volume 3: Finite Element Analysis, Nonlinear Analysis, and Dynamic Analysis Commands*, 2002. Revision R.

- [14] Computer Aided Structural Engineering Center, Georgia Institute of Technology, Atlanta, GA, *GT STRUDL User Reference Manual Volume 4: Reinforced Concrete Design*, 2002. Revision R.
- [15] Computer Aided Structural Engineering Center, Georgia Institute of Technology, Atlanta, GA, *GT STRUDL User Guide: Getting Started*, 2003. Revision 7.
- [16] Computers and Structures, Incorporated, Berkeley, California, *SAFE - Integrated Analysis and Design of Slabs by The Finite Element Method - User's Manual*, 1998. Version 6.0.
- [17] COOK, R. D. E. A., *CONCEPTS AND APPLICATIONS OF FINITE ELEMENT ANALYSIS*. New York: John Wiley & Sons, Inc., fourth ed., 2002.
- [18] COPE, R. and CLARK, L., *CONCRETE SLABS: Analysis and Design*. London: Elsevier Applied Science Publishers, 1984.
- [19] CORLEY, W. G. and JIRSA, J. O., "Equivalent Frame Analysis for Slab Design," *Journal of the American Concrete Institute*, vol. 67, pp. 875–884, November 1970.
- [20] CUSENS, A. R. and BESSER, I. I., "Elastic Stress Parameters in Simply Supported Skew Plates in Flexure," *Journal of Strain Analysis*, vol. 15, no. 2, pp. 103–111, 1980.
- [21] DAVIES, J. D., "Analysis of Corner Supported Rectangular Slabs," *The Structural Engineer*, vol. 48, pp. 75–82, February 1970.
- [22] DAVIES, J. D., MA, S. P. K., and CHEUNG, Y. K., "Analysis of Corner Supported Skew Slabs," *Building Science*, vol. 3, pp. 81–92, November 1968.
- [23] DE FIGUEIREDO, A. J. M., DA FONSECA, A. M. A., and AZEVEDO, A. F. M., "Analysis and Optimization of Reinforced Concrete Slabs," in *COMPUTER AIDED OPTIMUM DESIGN OF STRUCTURES VI* (HERNANDEZ, S., KASSAB, A. J., and BREBBIA, C. A., eds.), (Southampton, Boston, Massachusetts), WIT Press, 1999.
- [24] DOUGLAS, M. R. and LUNNISS, R. C., "An Application of the Finite Element Technique in Bridge Design," *Concrete*, vol. 4, pp. 197–200, May 1970.
- [25] FAMIYESIN, O. O. R. and HOSSAIN, K. M. A., "Optimized Design Charts for Fully Restrained Slabs by FE Predictions," *ASCE Journal of the Structural Division*, vol. 124, pp. 560–569, May 1998.
- [26] FRENCH, S., KABAILA, A. P., and PULMANO, V. A., "Single Element Panel for Flat Plate Structures," *ASCE Journal of the Structural Division*, vol. 101, pp. 1801–1812, September 1975.
- [27] GAMBLE, W. L. and PARK, R., *REINFORCED CONCRETE SLABS*. New York: John Wiley & Sons, Inc., second ed., 2000.
- [28] GAMBLE, W. L., *Measured and Theoretical Bending Moments in Reinforced Concrete Floor Slabs*. PhD thesis, University of Illinois, Urbana, Illinois, June 1962.
- [29] GENTRY, T. R., "The Use of Elastic Finite Elements in the Design of Reinforced Concrete Flat Plates," Master's thesis, Georgia Institute of Technology, 1986.

- [30] GTICES Systems Laboratory, Atlanta, GA, *GTICES Programmers Reference Guide*, 1991.
- [31] GUPTA, A. K. and SEN, S., “Design of Flexural Reinforcement in Concrete Slabs,” *ASCE Journal of the Structural Division*, vol. 103, pp. 793–804, April 1977.
- [32] HERNANDEZ, S., KASSAB, A. J., and BREBBIA, C. A., eds., *COMPUTER AIDED OPTIMUM DESIGN OF STRUCTURES VI*. Southhampton, Boston, Massachusetts: WIT Press, 1999.
- [33] HILLERBORG, A., *STRIP DESIGN METHOD HANDBOOK*. London, Great Britain: E & FN Spon, 1996.
- [34] HRABOK, M. M., *Stiffened Plate Analysis by the Hybrid Stress Finite Element Method*. PhD thesis, University of Alberta, Edmonton, Alberta, Canada, 1981.
- [35] HRABOK, M. M. and HRUDEY, T. M., “Finite Element Analysis in Design of Floor Systems,” *ASCE Journal of the Structural Division*, vol. 109, pp. 909–929, April 1982.
- [36] HUANG, Y. H. and WANG, S. T., “Finite-Element Analysis of Concrete Slabs and its Implications for Rigid Pavement Design,” *Highway Research Record*, no. 466, pp. 55–69, 1973.
- [37] HUDSON, W. R. and STELZER, C. F., “A Direct Computer Solution for Slabs on Foundation,” *Journal of the American Concrete Institute*, vol. 65, pp. 188–201, March 1968.
- [38] HUGHES, T. J. R. and COHEN, M., “The Heterosis Finite Element for Plate Bending,” *Computers and Structures*, vol. 9, pp. 445–450, 1978.
- [39] HUGHES, T. J. R., TAYLOR, R. L., and KANOKNUKULCHAI, W., “A Simple and Efficient Finite Element for Plate Bending,” *International Journal for Numerical Methods in Engineering*, vol. 11, pp. 1529–1543, 1977.
- [40] ISENBERG, J., ed., *FINITE ELEMENT ANALYSIS OF REINFORCED CONCRETE STRUCTURES II*, (New York, New York), Committee on Finite Element Analysis of Reinforced Concrete Structures, American Society of Civil Engineers, June 1991.
- [41] JIRSA, J. O., SOZEN, M. A., and SIESS, C. P., “Pattern Loadings on Reinforced Concrete Floor Slabs,” *ASCE Journal of the Structural Division*, vol. 95, pp. 1117–1137, June 1969.
- [42] JOFRIET, J. C. and MCNEICE, G. M., “Finite Element Analysis of Reinforced Concrete Slabs,” *ASCE Journal of the Structural Division*, vol. 97, pp. 785–806, March 1971.
- [43] KAHN, L., “Reinforced Concrete Slab Systems.” Course Notes, Georgia Institute of Technology, 2004.
- [44] LAW, F. M., “Design of Irregular Shaped Two-Way Slabs,” *Journal of the American Concrete Institute*, vol. 68, pp. 844–847, November 1971.



- [45] LEWIŃSKI, P. M. and WOJEWÓDZKI, W., “Integrated Finite Element Model for Reinforced Concrete Slabs,” *ASCE Journal of the Structural Division*, vol. 117, pp. 1017–1038, April 1991.
- [46] LIEPINS, A. A. and BELL, G. R., “How To Avoid Common Pitfalls in Structural Analysis by Computer.” ASCE International Convention Exposition, 1992.
- [47] LOGAN, D. L., *A FIRST COURSE IN THE FINITE ELEMENT METHOD*. Pacific Grove, CA: Brooks/Cole, third ed., 2002.
- [48] LOURENÇO, P. B. and FIGUEIRAS, J. A., “Solution for the Design of Reinforced Concrete Plates and Shells,” *ASCE Journal of the Structural Division*, vol. 121, pp. 815–823, May 1995.
- [49] MACGREGOR, J. G., *REINFORCED CONCRETE: Mechanics and Design*. Upper Saddle River, New Jersey: Prentice Hall, third ed., 1997.
- [50] MALHOTRA, V. M., ed., *IMPACT OF COMPUTERS ON THE PRACTICE OF STRUCTURAL ENGINEERING IN CONCRETE*. Detroit, Michigan: American Concrete Institute, 1970. SP-33.
- [51] MCCORMAC, J. C., *DESIGN OF REINFORCED CONCRETE*. New York: John Wiley & Sons, Inc., fifth ed., 2001.
- [52] MELOSH, R. J., “Basis of Derivation of Matrices for the Direct Stiffness Method,” *Journal of the American Institute of Aeronautics and Astronautics*, vol. 1, pp. 1631–1637, 1963.
- [53] MEYER, C. and OKAMURA, H., eds., *FINITE ELEMENT ANALYSIS OF REINFORCED CONCRETE STRUCTURES*, (New York, New York), Committee on Finite Element Analysis of Reinforced Concrete Structures, American Society of Civil Engineers, May 1985.
- [54] MOHR, G. A., “Elastic and Plastic Predictions of Slab Reinforcement Requirements,” *Institute of Engineers, Australia, Civil Engineering Transactions*, vol. CE 21, no. 1, pp. 16–20, 1979.
- [55] NILSON, A. H., ed., *FINITE ELEMENT ANALYSIS OF REINFORCED CONCRETE*. New York, New York: American Society of Civil Engineers, 1982. Committee on Finite Element Analysis of Reinforced Concrete Structures.
- [56] PFAFFINGER, D. D., “Column-Plate Interaction in Flat Slab Structures,” *ASCE Journal of the Structural Division*, vol. 98, pp. 307–326, January 1972.
- [57] PHUVORAVAN, K. and SOTELINO, E. D., “Nonlinear Finite Element for Reinforced Concrete Slabs,” *ASCE Journal of the Structural Division*, vol. 131, pp. 643–649, April 2005.
- [58] Portland Cement Association, Shokie, Illinois, *Concrete Structural Floor Systems and More...*, 2000. CD-ROM Version 1.
- [59] PRICE, W. A., ed., *COMPUTER APPLICATIONS IN CONCRETE TECHNOLOGY*, (Farmington Hills, Michigan), ACI Committee 118 - Use of Computers, American Concrete Institute, 1987. SP-98.

- [60] RAISANEN, DAVID, E. A., “A CASE Project Study of Finite Element Analysis of Concrete Flat Slabs,” 1987. U.S. Army Engineer Waterways Experiment Station - Technical Report ITL-87-2.
- [61] RAM International, Carlsbad, CA, *RAM Concept*, 2003. Version 1.0.
- [62] Research Engineers International, *STAAD.Pro 2004 Technical Reference*, 2004.
- [63] SALEH, L. R. R., “Finite Element Analysis of Shear in Reinforced Concrete Flat Plates,” Master’s thesis, Georgia Institute of Technology, 1987.
- [64] SAWKO, F. and COPE, R. J., “The Analysis of Skew Bridge Decks - a New Finite Element Approach,” *The Structural Engineer*, vol. 47, pp. 215–224, June 1969.
- [65] SEVERN, R. T. and TAYLOR, P. R., “The Finite Element Method for Flexure of Slabs when Stress Distributions are Assumed,” *Proceedings of the Institution of Civil Engineers*, vol. 34, pp. 153–170, 1966.
- [66] SMITH, E. T. and FAULKES, K. A., “Flexural Properties of Flat Plate Floors,” *Institute of Engineers, Australia, Civil Engineering Transactions*, vol. CE 18, no. 2, pp. 140–145, 1976.
- [67] TIMOSHENKO, S. and WOINOWSKY-KRIEGER, S., *THEORY OF PLATES AND SHELLS*. New York: McGraw-Hill Book Company, second ed., 1959.
- [68] TRACY, FRED T., E. A., “User’s Guide for Revised Computer Program to Calculate Shear, Moment and Thrust (CSMT),” 1988. U.S. Army Engineer Waterways Experiment Station - Technical Report ITL-88-4.
- [69] VANDERBILT, D. M., “Equivalent Frame Analysis for Lateral Loads,” *ASCE Journal of the Structural Division*, vol. 105, pp. 1981–1998, October 1979.
- [70] WILL, KENNETH M., E. A., “Procedure for Static Analysis of Gravity Dams Using the Finite Element Method - Phase 1a,” 1987. U.S. Army Engineer Waterways Experiment Station - Technical Report ITL-87-8.
- [71] WILLAM, K. and TANABE, T., eds., *FINITE ELEMENT ANALYSIS OF REINFORCED CONCRETE STRUCTURES*. Farmington Hills, Michigan: American Concrete Institute, 2001. SP-205.
- [72] WOOD, R. H., “The Reinforcement of Slabs in Accordance with a Pre-Determined Field of Moments,” *Concrete*, vol. 2, pp. 69–76, February 1968.
- [73] ZIENKIEWICZ, O. C. and CHEUNG, Y. K., “The Finite Element Method for Analysis of Elastic Isotropic and Orthotropic Slabs,” *Institution of Civil Engineers - Proceedings*, vol. 28, pp. 471–488, August 1964.
- [74] ZWILLINGER, D. E. A., ed., *STANDARD MATHEMATICAL TABLES AND FORMULAE*. Washington, D.C.: Chapman & Hall / CRC Press LLC, 31 ed., 2000.